The Pennsylvania State University

The Graduate School

College of Earth and Mineral Sciences

DEFINING DERECHO INTENSITY AND IMPACTS THROUGH PHYSICAL PROPERTIES, FEMA ASSISTANCE, AND AN EMERGENCY MANAGEMENT IMPACT SCALE AND GIS RESPONSE TOOL

A Dissertation in

Geography

by

Adrienne Katherine Kramer

Submitted in Partial Fulfillment

of the Requirements

for the Degree of

Doctor of Philosophy

May 2018

The dissertation of Adrienne K. Kramer was reviewed and approved* by the following:

Andrew M. Carleton
Professor of Geography
Dissertation Adviser
Chair of Committee

Douglas A. Miller
Research Professor of Geography

Robert G. Crane
Associate Vice Provost for Global Programs and Professor of Geography

Yvette P. Richardson
Associate Dean for Undergraduate Education, College of EMS and Professor of Meteorology

Cynthia A. Brewer
Professor of Geography
Head of the Department of Geography

*Signatures are on file in the Graduate School

Abstract

A derecho is a convectively induced windstorm produced by an extratropical mesoscale convective system (MCS) with straight-line winds exceeding 25ms^{-1}. Fourteen derecho corridors exist in the U.S. The Northern Tier corridor includes derechos that track northwest to southeast from the North Central Plains and Upper Midwest regions through the mid-Atlantic states. This corridor produces more frequent and damaging derechos than those of other U.S. corridors. This dissertation investigates Northern Tier derechos to improve understanding of the factors that influence their intensity, to predict the cost of federal response and recovery activities, and to develop and apply a meteorological impact scale and emergency response GIS tool. Fifty-six summer (JJA) Northern Tier derechos along with their physical atmospheric and land-surface attributes and population characteristics of those impacted by the events are examined to clarify their climatology and impacts. Multiple and geographically weighted regressions, principal component analysis, spatial analysis, and cluster analysis are used to reveal characteristics of derecho intensity and impact such as track length and federal assistance required for response and recovery. Results show that derecho intensity is influenced strongly by the atmospheric and land-surface variables of CAPE, the LLJ, and land use boundaries. Response and recovery funding is related to the area impacted and underlying attributes of the affected populations (e.g., socioeconomic status). A meteorological impact scale classifies the different event impacts and an emergency management GIS response tool is applied and shown to be useful in depicting resource access after a derecho. The research enhances understanding of Northern Tier derechos to

help refine attempts to understand their impacts and improves the ability of emergency managers to prepare for these events.

TABLE OF CONTENTS

List of Figures

List of Tables

Acknowledgments

This dissertation reflects many years of hard work and even more years of dreaming. I encountered many intellectual and personal challenges as I navigated the process of researching and writing this final piece. Thanks to my advisor, Dr. Andrew Carleton, for guiding me and providing meticulous, thoughtful edits to countless drafts of this dissertation and many other papers. Thanks also to my committee members, Drs. Doug Miller, Rob Crane, and Yvette Richardson, who encouraged me to put forth my best work and guided me to realize which of my ideas comprised that work. I would also like to show my appreciation for my mentors at FEMA who were integral in helping me parse through datasets and understand FEMA's geospatial capabilities. The FEMA team gave me the opportunity to learn emergency management practices first-hand and taught me that emergency management is not an exact science, but a constantly evolving effort to support survivors through flexible, innovative processes.

Thanks also to my mother, Kay Tucker, who always put my education first, and did whatever was needed to help me through all levels of schooling, and is one of my greatest cheerleaders. Thanks to Tom Tucker, my father, who was genuinely interested in talking to me about my research, and who is always available to guide me logically through tough decisions. Finally, thanks to my husband, Gottsch Kramer, who did everything he could to make sure I got through every day even when I was taking too much care of my dissertation to take care of myself. I could not have completed this work without the help of these generous people and I am truly honored to call them my family.

CHAPTER 1

INTRODUCTION

Background

A derecho is a widespread, convectively induced straight-line windstorm with winds exceeding 25 ms^{-1} (NOAA SPC, 2004). Differentiated from tornadoes in the late 1800s, these storms cause wind damage in a swath of increasing size from initiation to dissipation (Hinrichs, 1888). Although two types of derechos occur—progressive and serial derechos—progressive derechos are the more intense and consequently more damaging. Progressive derechos are characterized by airflow oriented parallel to the direction of movement of the storm, evident as a single "bow-echo" on radar shaped like a backwards "C" (Johns and Hirt, 1987). Progressive derechos occur across the U.S., but are sectored into corridors based on region of occurrence and direction which they travel. The Northern Tier corridor produces the most frequent and destructive derechos (Bentley and Sparks, 2003; Ashley and Mote, 2005). The high-impact of Northern Tier progressive derechos makes them the subject of this dissertation.

On 29 June 2012 a particularly large and damaging Northern Tier progressive derecho tracked through the midwestern and eastern U.S. It initiated in Iowa and grew progressively larger and more intense as it sped through Illinois, Indiana, Ohio, Kentucky, West Virginia, Virginia, North Carolina, Pennsylvania, New Jersey, Delaware, Maryland, and D.C. The derecho impacted densely populated cities including Chicago, IL, Columbus, OH, and the Baltimore, MD – Washington, DC area. This derecho left a wide swath of damage in its wake and caused fatalities. It was difficult for emergency managers to estimate the resources that would be required to respond to and recover from

the impacts of the 29 June 2012 derecho because emergency operations research had not been conducted on the intensity of derechos, their economic impacts, and how they compare to past events. Although economic losses and societal impacts attributed to other meteorological disasters have been statistically modeled (Boswell *et al.*, 1999; Changnon, 2003; D'Amico *et al.*, 2016), hitherto the economic losses and societal impacts of derechos have not. Also, although other meteorological disasters (e.g., tornadoes, hurricanes, and snowstorms) are well defined and classified (Fujita, 1971; Simpson and Saffir, 1974; Kocin and Uccellini, 2004; Potter, 2007), there were few well-researched Northern Tier derechos against which to compare the apparently anomalous event of 29 June 2012. Therefore, this dissertation seeks to improve the scientific understanding of derechos by determining the meteorological and climatic factors influencing their intensity, modeling the costs of their damage to societies and infrastructure, and developing and applying a derecho impact scale and recommendations to improve the response to their occurrence and to speed recovery from their impacts.

Objectives

To improve understanding of derechos and their impacts, this dissertation has the following three objectives:

1. To classify derechos based on new intensity metrics that can describe their impacts and determine the atmospheric and land surface variables that can be used to predict differences in derecho intensity.
2. To identify and describe the relationships of variables that influence the cost of derecho response and recovery. In particular, the federal

response and recovery costs related to Northern Tier derechos are assessed, which tend to affect multiple states due to their large size and rapid movement.

3. Improve emergency management of derechos by formulating a derecho-specific meteorological impact scale, and developing and applying a GIS response tool that can advise decision-making relevant to post-event allocation of resources such as federal disaster recovery centers that serve survivors.

These objectives are achieved using statistical testing and modeling, machine learning, and geospatial analytics applied to a wide range of meteorological, climatic, and population datasets. The research results attain each of the objectives and have direct application to improving the ability to forecast derechos impacts. The research improves understanding of the multi-faceted issue of disaster response and recovery with respect to under-researched derechos.

Chapter Structures

The second chapter of this dissertation clarifies the factors influencing the intensity of derechos through analysis of their direction, associated rain totals, maximum wind speed, and major and minor axis lengths. Derechos are stratified into subsets of high and low intensity according to these dominant attributes, and are tested for statistical differences in independent variables that potentially explain these intensity differences. The subsets of derechos are mapped and spatially compared and analyzed using geographically weighted regression. In addition, potential relationships between physical

derecho attributes such as CAPE and land use boundaries and these intensity metrics are investigated. This chapter further clarifies what dictates the large variance in derecho intensity and thus sets the stage for analyzing derecho impacts as is done in the subsequent chapters.

The third chapter of this dissertation examines the cost of derechos in terms of federal relief funding by modeling relationships between the key derecho attributes identified in Chapter 2 and characteristics of the populations impacted by derechos. Federal Emergency Management Agency (FEMA) Public Assistance (PA) grants are awarded to assist in the response to and recovery from disasters. The awards given for response and recovery from Northern Tier progressive derechos are statistically modeled to describe the relationship between the cost of derechos and physical attributes of the storms and the socioeconomic attributes of affected populations. Relationships are further analyzed spatially to show the variation in the grant award amounts across the impacted areas. This chapter identifies the variables impacting funding of derecho-related recovery and the statistics help explain how these variables change over the study area.

The fourth chapter of this dissertation clarifies derecho physical and socio-economic impacts through generation of a derecho impact scale and its application to the 56 Northern Tier summer derechos studied in the previous chapters. The impact scale developed quantifies derecho impacts based on the effects on society as well as physical derecho properties. By categorizing derecho events according to their impact, emergency management decision-making ultimately will be improved. An emergency management decision based on previous similar derecho events improves the likelihood of the success of the response and its cost-effectiveness. A GIS tool for use by emergency GIS response

teams to predict resource access and deployment in the wake of a derecho also improves the likely success of the response effort. As a proof-of-concept, I apply the tool to a derecho scenario and demonstrate its utility in derecho-prone areas and as a basis for continued refinement in the future as derecho research continues.

References

Boswell MR, Deyle RE, Smith RA, Baker EJ. 1999. A quantitative method for estimating probable public costs of hurricanes. *Environmental management*, **23**(3): 359-372.

Changnon SD. 2003. Measures of economic impacts of weather extremes: Getting better but far from what is needed—A call for action. *Bulletin of the American Meteorological Society*, **84**(9): 1231-1235.

D'Amico G, Manca R, Corini C, Petroni F, Prattico F. 2016. Tornadoes and related damage costs: statistical modelling with a semi-Markov approach. *Geomatics, Natural Hazards and Risk*, **7**(5): 1600-1609.

Fujita TT. 1971. Proposed characterization of tornadoes and hurricanes by area and intensity. *Satellite and Meteorology Research Paper 91, The University of Chicago*. Chicago, IL.

Kocin PJ, Uccellini LW. 2004. A snowfall impact scale derived from Northeast storm snowfall distributions. *Bulletin of the American Meteorological Society*, **85**(2): 177-194.

Potter S. 2007. Fine-Tuning Fujita: After 35 years, a new scale for rating tornadoes takes effect. *Weatherwise*, **60**(2): 64-71.

Simpson RH, Saffir H. 1974. The hurricane disaster potential scale. *Weatherwise*, **27**(8): 169.

CHAPTER 2

INFLUENCE OF ATMOSPHERIC AND LAND SURFACE CONDITIONS ON NORTHERN TIER STATES DERECHO INTENSITY

Abstract

A derecho is a convectively induced windstorm produced by an extratropical mesoscale convective system (MCS) with straight-line winds exceeding 25ms^{-1}. Fourteen derecho 'corridors' exist in the U.S. The Northern Tier corridor includes derechos that track northwest to southeast from the North Central Plains and Upper Midwest regions through the mid-Atlantic states. This corridor produces the most frequent and damaging derechos of all U.S. derecho corridors (Bentley and Sparks, 2003). This study analyzes the influence of synoptic atmospheric and land-surface variables on Northern Tier derecho intensity. Derecho intensity and physical attributes are classified according to metrics that include storm track direction, rain totals associated with the event, maximum wind speed, and length of the minor and major axes. Data on atmospheric (e.g., CAPE, vertical shear, etc…) and land-surface conditions (soil moisture, land use, etc…) are collected for 56 summer Northern Tier derecho events occurring between 2000 – 2014, and natural breaks are used to separate these derechos into high- and low- intensity subsets. Mean event axes and standard deviation ellipses are mapped to show the event average tracks and the areas typically affected by the high- versus low-intensity derechos. Mann-Whitney Wilcoxon (MWW) tests reveal statistical differences between high- and low-intensity derecho subsets. Derecho major axis track length subsets are found to have statistically significantly different low-level jet (LLJ) influence and CAPE values that are reasonable physically. A multiple regression and geographically weighted regression (GWR) applied

to these data are used to further explore derecho track length. Results show that certain atmospheric variables—notably the 500 hPa height, CAPE, and 300 hPa winds—and land-surface variable dry-wet land use boundaries dominate the differences between derecho intensity as given by their associated rain totals, maximum wind speeds, and major axis length. Conversely, no statistically significant differences are found between derecho physical attributes measured by track direction and minor axis width. The results show that atmospheric and land-surface conditions describe statistical differences between intensities of derechos as described by rain totals, maximum wind speeds, and major axis length.

Keywords: derechos, derecho intensity, intensity metrics, track length, spatial distribution

Introduction

A derecho is a strong, convectively induced windstorm produced by a mesoscale convective system (MCS) with straight-line winds exceeding 25 ms^{-1} (NOAA SPC, 2004). The storms can span over 500 km in width (minor axis length), and can travel up to 2,000 km from their initiation to dissipation locations (major axis length), over approximately 12 – 24 hours. Derechos sustain long paths largely through self-propagation, which occurs through continuous ingestion of warm moist air from the direction of movement (Ashley *et al.*, 2007). The strong winds inflict crippling damage on a variety of landscapes—both rural and urban—and can cause fatalities, mostly from wind-borne debris (Ashley and Mote, 2005). Derechos caused 153 deaths in the U.S. from 1986 to 2003. Compared to fatalities caused by floods, tornadoes, and hurricanes, those from derechos may be underreported due to lack of understanding about this phenomenon among post-storm data collectors and the media (Black and Ashley, 2011). Severe weather-related economic losses are difficult to quantify, but multiple regression modeling suggests that estimates can be made from meteorological, physical, and social characteristics of the storms and impacted populations (Boswell *et al.*, 1999).

Understanding the spatial distribution of these hazards could improve life-saving endeavors and policies. The spatial distributions of derecho injuries show a hot spot located over Lake Michigan and surrounding states (Ashley and Mote, 2005; their Figure 6). These injuries are associated with Northern Tier derecho events (in which derechos develop in North Dakota, South Dakota, Nebraska, Minnesota, Iowa, Missouri, Wisconsin, Illinois, Michigan, Indiana, Ohio, and parts of adjacent states), which are the subject of this research. This chapter aims to enhance the understanding of the physical

variables contributing to potentially damaging and hazardous derecho impacts which are shown to be related to the intensity of a derecho.

Although there are previously documented derecho occurrences and associated fatalities, the storms have been under-researched when compared with other severe weather events such as tornadoes and hurricanes. Hinrichs (1888) first identified derechos in the Great Plains where he noticed wind damage swaths that were much larger than those caused by tornadoes. He termed the storms "derechos," the Spanish word for "straight" (Hinrichs, 1888). Following Hinrichs' observational report, little additional research on derechos was undertaken until the 1980s.

Derecho research was re-visited by researchers classifying downbursts and straight-line wind events into five types (Fujita and Wakimoto, 1981). Aided by satellite remotely sensed visible and infrared imagery, the different intensities of these events were also examined in terms of their associated wind speed and damage in the Northern Tier states comprising initiation and intensification in the North Central Plains and Upper Midwest (Fujita and Wakimoto, 1981). In this dissertation, the Northern Tier refers to derechos that develop in North Dakota, South Dakota, Nebraska, Minnesota, Iowa, Missouri, Wisconsin, Illinois, Michigan, Indiana, Ohio, and parts of adjacent states. Subsequent to Fujita and Wakimoto's (1981) study, the definition of derecho was further clarified and the meteorological conditions associated with derechos were identified including strong instability and occurrence along a stationary front (Johns and Hirt, 1987). These authors set criteria for derecho identification from wind observations that included spatially concentrated wind reports of over 26 ms^{-1}, the spatial and temporal continuity of these reports, and association with a derecho-producing MCS (i.e., DMCS).

In addition, Johns and Hirt (1987) distinguished between derechos occurring with parallel synoptic airflow (i.e., progressive derechos) and those having perpendicular airflow across many bow echoes comprising a squall line (i.e., serial derechos; Johns and Hirt (1987), or squall line windstorms; Corfidi *et al.* (2016)). Progressive derechos, most common in the summer (June-August) in the Northern Tier states, are the focus of this research.

A refined classification of derechos that identified DMCSs and other MCS storm types from satellite and radar data, in conjunction with proximity soundings and storm reports, was given by Jirak *et al.* (2003). Similar methods to theirs are used in the present research to identify derechos from multiple data sources. A characteristic single "bow echo" shape associated with progressive derechos was identified in events occurring in both warm and cool atmospheric environments across all seasons (Johns, 1993). In all seasons, bow echo development tends to occur with anomalously high Convective Available Potential Energy (CAPE), but vertical shear values may vary (Evans and Doswell, 2001). CAPE and shear tend to have minimum thresholds for bow echo formation but not all events are associated with anomalously high CAPE and large vertical shear, and often a low-level stationary front supports bow echo formation (Johns, 1993; Evans and Doswell, 2001; Metz and Bosart, 2010). In atmospheric environments that otherwise support bow echo formation where a stationary front is present, but vertical shear is weak, the atmosphere tends to be highly unstable and thus has anomalously high CAPE and anomalously low Lifted Index (LI) values (Johns, 1993; Weisman, 1993). Warm air advection accompanying a southerly low-level jet (LLJ) is associated with many derecho events and aids in their propagation and enhancement of

rainfall production (Higgins *et al.*, 1987; French and Parker, 2010). High surface temperatures and strong winds aloft at the jet stream level are associated with the strongest derechos (Evans and Doswell, 2001; Coniglio and Stensrud, 2004) A favorable synoptic setup for a derecho will include all these meteorological characteristics, and initiation and propagation will be further aided by surface – atmosphere interactions (Bentley *et al.*, 2000).

Land-surface features such as land-use/land-cover (LULC) boundaries and soil moisture gradients influence convection by changing moisture availability in the planetary boundary layer and the convective fluxes of sensible and latent heat. These LULC gradients and boundaries are common in agricultural areas of the Northern Tier region (i.e., the Corn Belt). The Northern Tier contains mixtures of agriculture, forest, grassland, and urban LULC with varying magnitude horizontal-scale boundaries between LULC types (Segal and Arritt, 1992; Lambin *et al.*, 2001). However, the dominant LULC types of agriculture and forest have boundaries that can influence deep convection and rainfall by adding additional moisture to the atmosphere from evaporation and enhancement of vertical instability due to associated horizontal gradients in roughness length (Anthes, 1984; Pielke and Zheng, 1989; Segal *et al*., 1989). Observational and modeling studies of the Corn Belt have associated its LULC boundaries and gradients with enhanced daytime convective cloud presence, thunderstorm generation under conditions of weak synoptic flow, and occurrence of non-classical mesoscale circulations (NCMCs) (Carleton and O'Neal, 1995; Brown and Arnold, 1998; Carleton *et al.*, 2001; Adegoke *et al.*, 2007; Carleton *et al.*, 2008). NCMCs often occur at surface boundaries. These local to meso-scale surface – atmosphere interactions aid in the development of a

nocturnal LLJ when the synoptic circulation pattern is favorable—typically, incoming low pressure and retreating high pressure—with associated warm-air advection that propagates the movement of DMCSs west-to-east. A nocturnal LLJ is a diurnally varying core of fast winds in the upper planetary boundary layer just below the daytime inversion altitude. It forms in very stable atmospheric conditions as a force imbalance is created when convective mixing ceases at night. The Great Plains LLJ maximizes at night and in the early morning, and is enhanced by other processes that result from the earth's surface sloping downward from west to east (Blackadar, 1957; Bonner, 1968; Shapiro and Fedorovich, 2010).

Detailed classification of derechos followed research on the physical processes that drive these storms. Geographer-climatologists and meteorologists have used criteria derived by Johns and Hirt (1987) with modifications to identify derecho events. A classification of derecho corridors by geographers Bentley and Mote (1998) identified six main corridors in which derechos formed and propagated during the warm and cool seasons of 1986 – 1995. In a subsequent paper, Bentley and Sparks (2003) updated their corridor definitions and added additional derecho corridors to give a total of fourteen. Two corridors, the Southeast and Great Lakes, are dominated by derechos having a west-to-east propagation, as opposed to a predominantly northwest to southeast direction for the Northern Tier. Between 1996 and 2000, the Southeast corridor produced four derechos with moderately long path lengths, whereas the Great Lakes Corridor saw five derechos with shorter tracks. Four derecho corridors—spring-season Southeast, Midwest, Ohio Valley, and Central Plains—produce derechos associated with a southwesterly surface wind. The spring-season 1996-2000 Southeast and Midwest corridors

experienced seven and eight derechos, respectively; the Midwest corridor supported derechos with extensive path lengths. During this period also, ten derechos were initiated in both the Ohio Valley and Central Plains corridors. The Southward Burst corridor, located in the central Great Plains, and the Northern Tier corridor are distinguished by northwesterly flow (i.e., south-eastward propagating) derechos. Although the Southward Burst corridor saw seven derechos in the period 1996-2000, the Northern Tier experienced 21 derechos in the same five years. The Bentley and Sparks (2003) study is foundational to the present research which updates the Northern Tier derecho climatology as one of its first objectives.

In tandem with the geographical studies of derechos, Coniglio and Stensrud (2004) developed a revised set of criteria to identify and create a climatology of derechos based on proximity soundings of atmospheric attributes and wind speed and direction. These events were divided into subsets of derecho intensity based on wind reports, and the Northern Tier region was shown to experience mostly "moderate" and "high-end" derechos (Coniglio and Stensrud, 2004).

Although these climatologies of derechos are comparable, none uses the same criteria to define an event. As noted by Corfidi *et al.* (2016), the wide-ranging definitions used by meteorologists and non-meteorologists, such as geographers and emergency managers, hamper the development of a universal definition of a derecho that can be used by a range of stakeholders to effectively analyze the impacts of the events. Corfidi *et al.* (2016) suggest that such a definition should be standardized objectively based on the dynamics of the storm (e.g., the presence of a cold pool which drives the parent MCS) and on the fact that damage occurs after complete organization of any smaller

thunderstorms into the larger derecho. However, the researchers also acknowledge that more basic research is needed on derecho "ingredients" and public understanding of the terminology before the definition of a derecho can be made as inclusive as possible of the phenomenon and its impacts. Corfidi *et al.* (2016) also suggest that further taxonomic studies will aid in this effort.

Following from the above scientists' derecho definitions distinguishing between those of meteorologists and non-meteorologists, the present paper will be based on geographer-climatologist concepts and methodologies as discussed by Carleton (1999). In this way, the research will describe and classify derecho events by using averages and statistics to determine derecho attributes from many events, as opposed to a single case, and also by emphasizing spatial patterns of derecho intensity and impacts. Accordingly, this research will classify derechos according to intensity-based metrics, distinguish the spatial patterns of derecho intensity, and conduct statistical analyses of the differences between high- and low-intensity derechos to understand why the two distinct populations of events are different. Although meteorological modeling and case studies will aid in refining the definition of a derecho, geographic investigations including identifying statistically significant spatial differences between high- and low-intensity derechos are important.

As an example of a geographic approach to studying derechos, a spatiotemporal analysis of their associated lightning densities (Bentley et al., 2016) showed where and at what stage derecho-associated lightning strikes occur. Maps of lightning strikes and flash densities (i.e., the number of strikes per 16 km^2) show where strikes occurred most frequently and communicated about what time they were most intense (Bentley *et al.*,

2016). However, these maps emphasize only one of the many hazards associated with derechos and DMCSs; other derecho-related impacts include wind-borne debris, flooding, and felled trees (Ashley and Mote, 2005). To aid in preparation efforts and emergency responses, it is vital to study the potential impacts associated with derechos. With increased understanding of the average spatial distribution of derecho intensities and the atmospheric and land-surface variables influencing them, planning for derechos can be improved. Climatologies can be used to strategically prepare resources for deployment and aid in identifying areas historically subject to the impacts of derechos.

Derechos with longer and wider tracks, higher wind speeds, and higher rain totals are likely to cause hazards that have major impacts. Although research on derecho-specific hazards has been limited, the concept that extensive human impacts are more likely with larger, more intense storms are extrapolated from research that investigated severe storms such as hurricanes and tornadoes (Brooks, 2004; Zhai and Jiang, 2014). Thus, greater derecho storm track lengths and widths are related to increased impacts and potentially higher intensity ratings if there were a scale similar to the Saffir-Simpson hurricane scale or the Enhanced Fujita tornado scale (Simpson and Saffir, 1974; Potter 2007). The maximum wind speed in Northern Tier convective high-wind events is related to the number of fatalities, and the fatalities show a spatial distribution similar to the distribution of derechos (Ashley and Mote, 2005; Schoen and Ashley, 2011). Flooding events are also deadly (Ashley and Ashley, 2008a; Ashley and Ashley, 2008b). Accordingly, the present research investigates derecho-associated rainfall and wind speed as storm intensity metrics. In addition, the physical attribute of derecho direction is also

investigated because of its relationship to the other intensity metrics of wind speed and track length.

Therefore, the objective of the present research is to improve understanding of the physical links between derecho hazard intensity metrics (i.e., track length and storm width, rain amounts, and maximum wind speed) and the atmospheric and land-surface variables that influence them. With improved knowledge of these relationships determined through map pattern analysis, derecho group difference testing, and regression modeling it is shown that metrics describing derecho intensity can be used for planning and preparation purposes. Derecho-related hazards can be minimized with appropriate response, and long-term preparation and mitigation accomplished through better understanding the spatial distributions and physical associations of derecho intensity.

Data And Methods

a. Data

Data on derecho occurrence, and atmospheric and land-surface conditions were obtained from conventional observations, and remotely sensed and modeled sources. They were compiled to generate a detailed dataset of 56 derecho events for the period (2000-2014), used to determine the derecho intensity metrics. NOAA Storm Prediction Center (SPC) daily archived storm reports were referenced to identify derecho events that could be confirmed subsequently. Although evidence of the strong winds accompanying derechos and other linear-type storms (e.g., MCS) appears in these reports, the data were not entered into the dataset until confirmation of a derecho was made using supporting

evidence. On a given day, potential events are identified from a west-to-east expanding cluster of SPC wind reports that have a cone-like shape. There are limitations to the SPC wind reports, such as repetition and incorrect reporting (Trapp *et al.*, 2006). To validate the occurrence of a derecho in the SPC wind reports, surface-based remotely sensed data sources were also employed. Specifically, NOAA NWS WSR-88D Level III data were used to identify the typical bow echo shape of a derecho and to confirm that the convective event followed the path depicted in the SPC reports. These radar data were also used to verify temporal continuity of the derecho to ensure that the reports were associated with a continuously propagating single event. In addition, visible and infrared satellite imagery from geostationary platforms were also consulted to further confirm the derecho presence through identification of the high, cold cloud tops that are associated with the convective events.

Criteria for including a derecho in this study require it to have a minor axis over 100 km wide and a major axis (track/path length) of over 400 km (Johns and Hirt, 1987). Although the Johns and Hirt (1987) criteria suggest that derecho wind gusts must be over $26 ms^{-1}$, that threshold was increased to 29 ms^{-1} herein to facilitate comparison to EF0, the lowest scale, tornados on the Enhanced Fujita scale (Potter, 2007). Derechos that initiated in Canada but propagated into the United States were not included in the analysis for data consistency.

Remotely sensed and reanalysis data were used together to identify free-atmosphere and boundary-layer thermodynamic and land-surface variables. Boundary-layer data include specific humidity and the presence or absence of an LLJ at 925 hPa, while free-atmosphere 500 hPa geopotential heights give the wave pattern in the mid-

troposphere, and 300 hPa winds portray the locations of jet streaks. These data comprise part of the NCEP North American Regional Reanalysis (NARR) (Mesinger *et al.*, 2006). (In)stability indices including CAPE and convective inhibition (CIN) were also extracted from NCEP NARR, and proximity soundings were obtained from the University of Wyoming archive (http://weather.uwyo.edu/upperair/sounding.html).

Land-surface variables of LULC and normalized difference vegetation index (NDVI) were retrieved to represent variations in Earth surface properties of vegetation and soil moisture that have been previously shown to influence boundary layer processes involved in convection, and to interact with stationary fronts. These data are acquired on different time scales to represent the "cycle" that occurs with respect to each type of land-surface property. For example, NDVI changes with the progression of the seasons (i.e., phenology), whereas human land-use change occurs over longer—multi-annual and decadal—time periods. Land-use boundaries, such as those between forest and agriculture were identified from the Landsat-derived National Land Cover Database (NLCD). This dataset stratifies LULC type based on automated classification of remotely sensed imagery and data derived by the Multi-Resolution Land Characteristics Consortium (MRLC) team, a multi-agency group, and is updated every five years (Homer *et al.*, 2001; Homer *et al.*, 2015). Data on phenology-related land-cover variables were extracted from weekly AVHRR-derived NDVI.

Globally averaged near-surface air temperature data were available as yearly averages in the NCDC Global Historical Climatology Network-Monthly (GHCN-M) dataset (Lawrimore *et al.*, 2011). In addition, near-surface air temperature averages and anomalies were extracted from the U.S. Climate Divisional Dataset (Karl and Koss,

1984; Vose *et al.*, 2014) for the U.S. and the Corn Belt region to reflect changes in LULC and NDVI data (photosynthesis and respiration). The Corn Belt region data were averaged across the climatological summer (JJA) to align with the period of study for derechos. These data, along with the atmospheric and land-surface data comprise a suite of atmospheric and land surface variables potentially related to explaining intensity of Northern Tier derechos.

b. Methods of Analysis

After identifying and verifying derechos to include in this study, intensity metrics were formulated and measured for each event. The intensity metrics include track direction, rain totals associated with the event, maximum wind speed, and major and minor axis lengths. They were chosen because they help distinguish derechos of different intensity and hazard potential according to a number of explanatory variables such as CAPE, 300 hPa shear, and near-surface air temperature, shown in previous severe-weather research (Brooks, 2004; Ashley and Ashley, 2008a; Ashley and Ashley, 2008b; Zhai and Jiang, 2014). The present study will further clarify how the above potential explanatory variables may influence derecho intensities based on the intensity metrics.

To facilitate investigation of the differences between high- and low-intensity derechos, and determine the reasons for such differences, the 56 events compiled for the study period were subset into groups based on within-group similarity. The natural breaks method, which minimizes the within-group variance and maximizes the between-group variance, was used to determine the subset groups. Natural breaks is an iterative test that repeats calculations of the sum of squared deviations of the mean to group events with

the lowest variance (Jenks, 1963; Jenks, 1967). The data are not necessarily normally distributed and the groups can have sample sizes of less than 30 events. Thus, analysis of what differences of physical variables requires nonparametric statistics to describe high- versus low-intensity derechos.

Accordingly, the Mann-Whitney-Wilcoxon (MWW) test was employed to test differences between high- and low- intensity derechos for each of the five metrics of intensity (i.e., storm track direction, rain totals associated with the event, maximum wind speed, major and minor axis lengths). Output statistics with statistically significant p-values ($p < 0.05$) represent significant difference between variables associated with high- and low-intensity derechos (Wilcoxon, 1945; Mann and Whitney, 1947).

When the MWW test statistics revealed a statistically significant difference between the derecho groups distinguished on the basis of intensity that was not explained by a simple physical mechanism known to influence the intensity metric, additional analysis of the data was required to understand how the independent atmospheric and land-surface variables influenced the intensity variable. To further disclose the possible underlying physical reasons revealed by the MWW tests, a multiple regression and geographically weighted regression (GWR) were run on the atmospheric and land-surface data found to be relevant to the differences identified by the MWW tests. These tests clarify the high- versus low- intensity derecho differences and reveal the spatial variation of the influence as discussed below.

Multiple regression estimates the coefficient values of explanatory variables (e.g., CAPE) describing an intensity metric. It minimizes the sum of the squared residuals to describe the influence of the explanatory variables on the intensity metric (Charlton *et al.*,

2009; Scott and Janikas, 2010). The explanatory variables used in the model are tested for autocorrelation and multicollinearity so as to eliminate redundancy in the model (i.e., use of multiple variables that are correlated and thus have the same influence on the model and likely a similar/redundant physical influence).

To determine the spatial dependence of each of the explanatory variables in the regression model, a GWR is used. The GWR reveals where the explanatory variables influence the derecho intensity metric that is being examined (Brunsdon *et al.*, 1996; Brunsdon *et al.*, 1998; Fotheringham *et al.*, 2002). A Moran's I test was run on the regression residuals to ensure they are not spatially autocorrelated which would bias the GWR. If autocorrelation is found, the model inputs were revised. An adaptive bandwidth is used to accommodate the non-uniform spatial distribution of the underlying data (the derecho information) by finding an optimized number of nearest neighbors on which to base the regression. Generating this model has been shown in previous work to improve spatial interpretation of the multiple regression results and produces mapped surfaces that can be used to estimate locational influences of natural phenomena (Lv and Zhou, 2016; Kumari *et al.*, 2017). The mapped model result can also be compared to the observations from the derecho events to depict how well the model predicted the magnitude of the particular intensity metric across space.

Results and Discussion

Fifty-six derecho events are identified in the 15 summer seasons 2000-2014 (Table 2-1). When two derechos occurred on the same day, the first is identified with an 'A' and the second with a 'B' (Table 2-1). The derechos are mapped from initiation to

dissipation to show the tracks of propagation (Figure 2-1). Derecho major axis/track lengths vary, but generally they propagate northwest to southeast, agreeing with past work (Bentley and Sparks, 2003) and many track over the Corn Belt. Tracks average 902.8 km in length. Spatial analysis of the derechos' initiation (first sign of convection), intensification (the stage at which convection is organized into a coherent bow-echo shape), and dissipation (the stage at which the derecho is no longer an organized storm) latitudes and longitudes yields ellipses that denote one standard deviation of Northern Tier derecho tracks (Figure 2-2). The ellipses reveal that the storms tend to initiate in the Upper Midwest and North Central Plains, intensify just southeast of their initiation locations, and dissipate across a wider area, also agreeing with past findings (Bentley and Sparks, 2003). The ellipses' increasing size from initiation to dissipation mirror the increasing size as a derecho propagates through the stages of development. Although derechos tend to initiate, intensify, and dissipate within these ellipse boundaries, they do not all share the same intensities (i.e., storm track direction, rain amount associated with the event, maximum wind speed, minor axis length, and major axis length) as will be further discussed below.

The results show that using natural breaks to categorize the derechos into two groups for each metric sufficiently described the differences between high- and low-intensity derechos. Other methods to divide the derechos into subsets were tested, including manual classification and cluster analysis, but these did not separate events as logically as natural breaks. The two groups are distinctly different and have a reasonable number of derechos to differentiate statistically. Groups had close to 30 events each requiring non-parametric analysis, while maintaining a relatively high sample size.

Through separating the derechos using natural breaks, two subsets of storm track direction were identified; one subset contained 24 westerly events and the other contained 32 northwesterly events. Westerly events had a mean track direction of 275.29° and northwesterly events had a mean track direction of 300.15°. Rain totals associated with the derechos were stratified into subsets of 29 low-rain total events (mean = 26.72 mm) and 27 high-rain total events (mean = 60.19 mm). The subset for low maximum wind speed has 19 events designated as having lower reported wind speeds (mean = 35.52 m/s) while the subset for high maximum wind speed has 37 events having higher reported wind speeds (mean = 43.97 m/s). Subsets were generated for derechos with a small minor axis (14 events, mean = 159.01 km) and those with a larger minor axis (42 events, mean = 356.6 km). Events were subset based on major axis size, or track length, into 25 short events with a mean major axis of 615.79 km and 31 long events with a mean major axis of 1,134.26 km.

To show the differences in geographic distribution of high- and low-intensity derechos, mean derecho axes and standard deviation ellipses are mapped (Figures 2-3 – 2-7). Mean event axes show the average track of derechos and the one standard deviation ellipses show the area covered by 68% of derechos. The maps are discussed followed by a discussion of the results of statistical analyses. Figure 2-3 shows the mean event axes (top) and standard deviation ellipses (bottom) for westerly (grey) and northwesterly (black) derechos. Westerly derechos have longer tracks on average, but there is minimal difference between the typical areas covered by these events as shown by the similarity in the ellipses in Figure 2-3, bottom. Mean event axes of the high- and low-rain derecho subsets show that derechos associated with higher rain totals tend to track farther south

(Figure 2-4, top), and standard deviation ellipses indicate that high rain events cover a horizontal area over Iowa through Ohio (Figure 2-4, bottom). The mean event axes for events in the high and low-maximum wind speed subsets show that derechos with higher maximum wind speeds average a higher latitude track (Figure 2-5, top). Although the higher maximum wind speed events tend to have tracks that are further north of the lower maximum wind speed events, the latter tend to have a larger domain in which 68% of the derechos occur (Figure 2-5, bottom). Mean event axes for small versus large minor axis derechos show that events with larger minor axes occur north of derechos having smaller minor axes, and the area in which 68% of events occur has the same pattern (Figure 2-6). Mean event axes of long and short-track derechos show that longer derechos initiate farther west and dissipate farther east and have a slightly lower angle than short derechos (Figure 2-7, top). The standard deviation ellipses for long and short-track derechos show that long derechos occur over a smaller area than small derechos (Figure 2-7, bottom).

The MWW tests reveal the statistical differences between the high-intensity and low-intensity derecho subsets discussed above and shown in Figures 2-3 – 2-7. Differences between the high-intensity and low-intensity groups subset using other methods such as manual classification did not reveal any additional statistically significant differences that could be explained physically. No statistically significant differences in any of the meteorological variables in the dataset were found between northwesterly and westerly derechos or between derechos with small and large minor axes. This suggests that the derecho subsets in these two metrics are not significantly different, and are not a good indicator of intensity and are merely physical attributes of derechos. Apparent differences in the rain totals associated with high versus low intensity

derechos revealed that derechos with higher rain totals had a statistically significantly lower ($U = 529.5$, $p = 0.01603$) 500 hPa geopotential mean height (5,800 m vs. 5,840 m) over the whole event. Differences between derechos having higher maximum wind speeds (43.97 m/s) versus lower maximum wind speeds (35.52 m/s) were associated with 300 hPa jet streak presence (which was present in 63% of high maximum wind speed events and only 35% of low maximum wind speed events; $U = 450$, $p = 0.04892$) and differences in dissipation location (average of 40.5°N in high maximum wind speed derechos and 38.7°N in low maximum wind speed events; $U = 491$, $p = 0.01575$).

Statistically significant differences between derechos having long versus short major axes were found ($U = 523$, $p = 0.02542$). Derechos having longer major axes are associated with more westerly tracks (average = 279.5°) contrasted with derechos having shorter major axes (average = 288.5°). This is potentially related to the influence of wind direction aloft and according synoptic setup. Derechos having longer major axes also are 2.5 times as likely ($U = 516.5$, $p = 0.03256$) to cross a dry-to-wet land-surface boundary, defined as a transition from dry-to-wet land-use types, near its intensification. That is, a longer derecho is more likely to cross from an urban center to an irrigated area, for example, which could add moisture to the derecho system. In addition, longer-track/major axis derechos are associated with higher 925 hPa specific humidity than derechos having shorter track or major axis ($U = 261.5$, $p = 0.03324$); averaging, respectively, 13.5 g/kg versus 13 g/kg. Longer axis/track derechos may be associated with higher 925 hPa specific humidity than shorter axis/track derechos because the increased moisture available aids the propagation of the derecho. These statistically significant differences between derechos having long versus short major axes are likely to

be physically complex so further investigation is undertaken below to help explain the associated mechanisms.

Multiple regression and GWR were conducted to further explore the variables impacting derecho major axis length. Multiple regression revealed that 925 hPa specific humidity, CAPE, and the time of day when the derecho intensified together influence the major axis length (Table 2-2). A Moran's I test confirmed that the residuals of the statistical model were not spatially autocorrelated, and thus are likely to be independent, further validating the regression results. Specific humidity at 925 hPa shows a strong, positive relationship with major axis length ($p = 0.000001$). The CAPE has a statistically significant positive relationship with major axis length ($p = 0.02572$), while the diurnal time of event intensification shows a highly significant negative relationship with major axis length ($p = 0.00025$). Together, the atmospheric specific humidity at 925 hPa, CAPE, and time of event explained around two-thirds of the variance in major axis length ($R^2 = 0.679$). The model indicates that an increase in specific humidity at 925 hPa and CAPE together predict a longer derecho major axis. In addition, the earlier a derecho occurs during the day, the longer its major axis will be. This finding indicates that the diurnal processes of derecho generation such as strong daytime surface heating and a nighttime strong LLJ likely work together to help sustain derecho propagation and lengthen the major axis, and thus produce a more intense derecho. This possibility is further tested using a GWR, below.

To better understand the spatial influences of 925 hPa specific humidity, CAPE, and time of day on major axis length, a GWR was conducted. The spatial variation of the influence of the coefficients revealed by the GWR improved the model's effectiveness

(R^2 = 0.788 versus 0.699). Figure 2-8 shows the spatial variation of the specific humidity at 925 hPa concentration coefficient across the study area for the model. The map shows that the 925 hPa specific humidity coefficient has the greatest influence on derecho track length over the central area of study and is reduced outward across the Corn Belt. This pattern of influence on derecho track length resembles that of an LLJ advecting warm, moist air from the Gulf of Mexico. The 925 hPa specific humidity coefficient has the lowest values in the northwestern part of the study area that lies outside the average influence of the LLJ.

Figure 2-9 shows the CAPE - derecho major axis length coefficients across the study region. CAPE has the strongest relationship with major axis length in the west and northwest parts of the study region, decreasing south and eastward. This pattern is essentially opposite that of the 925 hPa specific humidity-derecho major axis length coefficient, and suggests that CAPE has a greater influence on major axis length where the LLJ is not as influential**.** The time of the event coefficient in the GWR also has a pattern that is the same as that of a strong LLJ (Figure 2-10). Time is likely another representation of the importance of an LLJ in determining major axis length as this feature also tends to be strongest at night.

The GWR reveals where the model is either over-predicting or under-predicting derecho major axis length for the 56 observed derechos in the dataset (Figure 2-11). The observed and predicted data have a correlation coefficient of P = 0.9104, showing that the predicted major axis lengths are highly correlated with the observed major axis lengths of derechos. Areas where the model over-predicts, it estimates longer major axis lengths than those that were observed. Conversely, areas of under-prediction occur where the

model under-predicts the major axis lengths compared to those that were observed. The model over-predicts derecho major axis lengths across eastern Minnesota, Wisconsin, and western Michigan which may be related to the strong influence of the CAPE regression coefficient in this area (Figure 2-9). In these events, instability may be high, but other factors necessary for derecho propagation may not be prime to sustain the storm for a long track length. The GWR model under-predicts derecho major axis lengths in northern Iowa which is on the edge of the area of highest influence of both the 925 hPa specific humidity coefficient and the time of event coefficient. The under-prediction may be caused by this area frequently experiencing conditions that are prime for development of long derechos, but being just outside of these areas of highest influence of the model coefficients.

Conclusions

This research investigates the intensity of Northern Tier states' derechos for a 56-event derecho database spanning the period 2000-2014. The derechos initiate, intensify, and dissipate over increasingly large areas. The derecho database was subset into two independent intensity groups for each of the following metrics that describe event intensity: storm direction, associated rain totals, maximum wind speed, and the minor and major axes. Modeled reanalysis, observed, and remotely sensed data were employed to identify the differences in derecho variables for the high versus low intensity derechos according to their direction, rain totals, maximum wind speed, and minor and major axes. The high- versus low- intensity derechos were mapped according to the five intensity metrics to identify their spatial differences. Mean event axes show the average tracks for

derechos in each intensity subset, while mapped standard deviation ellipses showed the area influenced by 68% of derechos.

To determine the statistical significance of the differences between the high- and low- intensity derecho subsets for each intensity metric, MWW tests were run. The results showed that no statistically significant physically reasonable differences existed between the high- and low-intensity groups of derechos in the physical attributes of direction of movement and minor axis categories. However, the 500 hPa height was significantly lower in derechos that had the higher rain totals, and upper-tropospheric jet streaks were more likely to accompany derechos having higher maximum near-surface wind speeds. Most interestingly, derechos with longer major axes were associated with a more zonal direction, the crossing of a dry-to-wet land use boundary, and higher specific humidity at 925 hPa indicating the influence of surface features.

Further investigation into the variables influencing derecho major axis length employed multiple regression and GWR. Although the regressions run on four of the intensity metrics (i.e., storm direction, rain totals, maximum wind speed, minor axis length) revealed no statistically significant relationships, that run on major axis length showed positive and statistically significant relationships with 925 hPa specific humidity and CAPE (i.e., greater specific humidity at 925 hPa and higher instability accompanying longer track lengths). Also, a negative and statistically significant relationship was found for the diurnal time of the derecho and derecho major axis length. A GWR clarified how the variables in this model (925 hPa specific humidity, CAPE, and time of event) were important across the study area (Figures 2-8 – 2-10). Specific humidity at 925 hPa and time of day reflected LLJ influence and had a strong role in the central Midwest. CAPE

was more influential in the western part of the study area. The GWR predicts derecho major axis lengths well ($R^2 = 0.788$) across the study area, with some areas of minor over-prediction and under-prediction (Figure 2-11).

Although the derecho direction and storm minor axis length are not differentiated by statistically significant differences in atmospheric and land-surface characteristics tested herein, they still have impacts on society, which are considered in the following two chapters. Significant differences in derecho intensity based on their associated rain totals and maximum wind speeds are found to be physically related to the atmospheric variables of 500 hPa height, upper-tropospheric jet streak presence, and dissipation location. Differences in major axis lengths that describe derecho intensity are related to specific humidity at 925 hPa, CAPE, and time of day of derecho intensification. In the following chapters, the five intensity metrics are used to assess derecho societal impacts and to develop a derecho impact scale similar to those applied to hurricanes, tornadoes, and snowstorms.

References

Adegoke JO, Pielke R, Carleton AM. 2007. Observational and modeling studies of the impacts of agriculture-related land use change on planetary boundary layer processes in the central U.S. *Agricultural and Forest Meteorology*, **142**: 203–215. doi:10.1016/j.agrformet.2006.07.013

Anthes RA. 1984. Enhancement of Convective Precipitation by Mesoscale Variations in Vegetative Covering in Semiarid Regions. *Journal of Climate and Applied Meteorology*, **23**(4): 541–554.

Ashley ST, Ashley WS. 2008a. Flood fatalities in the United States. *Journal of Applied Meteorology and Climatology*, **47**(3): 805-818.

Ashley ST, Ashley WS. 2008b. The storm morphology of deadly flooding events in the United States. *International Journal of Climatology*, **28**(4): 493-503.

Ashley WS, Mote TL. 2005. Derecho Hazards in the United States. *Bulletin of the American Meteorological Society*, **86**(11): 1577–1592. doi:10.1175/BAMS-86-11-1577

Ashley WS, Mote L, Bentley ML. 2007. The extensive episode of derecho-producing convective systems in the United States during May and June 1998: A multi-scale analysis and review. *Meteorological Applications*, **14**: 227–244. doi:10.1002/met

Bentley ML, Franks JR, Suranovic KR, Barbachem B, Cannon D, Cooper SR. 2016. Lightning characteristics of derecho producing mesoscale convective systems. *Meteorology and Atmospheric Physics*, **128**(3): 303-314.

Bentley ML, Mote TL. 1998. A Climatology of Derecho-Producing Mesoscale Convective Systems in the Central and Eastern United States, 1986 – 95. Part I :

Temporal and Spatial Distribution. *Bulletin of the American Meteorological Society*, **79**(11): 2527–2540.

Bentley ML, Mote TL, Byrd, SF. 2000. A Synoptic Climatology of Derecho Producing Mesoscale Convective Systems in the North-Central Plains. *International Journal of Climatology*, **20**: 1329–1349.

Bentley ML, Sparks JA. 2003. A 15 yr climatology of derecho-producing mesoscale convective systems over the central and eastern United States. *Climate Research*, **24**: 129–139.

Black AW, Ashley WS. 2011. The Relationship between Tornadic and Nontornadic Convective Wind Fatalities and Warnings. *Weather, Climate, and Society*, **3**(1): 31–47. doi:10.1175/2010WCAS1094.1

Blackadar AK. 1957. Boundary layer wind maxima and their significance for the growth of nocturnal inversions. *Bulletin of the American Meteorological Society*, 283-290.

Bonner WD. 1968. Climatology of the low level jet. *Mon. Wea. Rev*, **96**(12): 833-850.

Boswell MR, Deyle RE, Smith RA, Baker EJ. 1999. A quantitative method for estimating probable public costs of hurricanes. *Environmental management*, **23**(3): 359-372.

Brooks HE. 2004. On the relationship of tornado path length and width to intensity. *Weather and Forecasting*, **19**(2): 310-319.

Brown ME, Arnold DL. 1998. Land-surface-atmosphere interactions associated with deep convection in Illinois. *International Journal of Climatology*, **18**: 1637–1653.

Brunsdon C, Fotheringham AS, Charlton ME. 1996. Geographically weighted regression: a method for exploring spatial nonstationarity. *Geographical analysis*, **28**(4): 281-298.

Brunsdon C, Fotheringham S, Charlton M. 1998. Geographically weighted regression. *Journal of the Royal Statistical Society: Series D (The Statistician)*, **47**(3): 431-443.

Carleton AM. 1999. Methodology in climatology. *Annals of the Association of American Geographers*, **89**(4): 713-735.

Carleton AM, Adegoke JO, Allard J, Arnold DL, Travis DJ. 2001. Summer season land cover - convective cloud associations for the Midwest U.S. "Corn Belt." *Geophysical Research Letters*, **28**(9): 1679–1682.

Carleton AM, Arnold DL, Travis DJ, Curran S, Adegoke JO. 2008. Synoptic circulation and land surface influences on convection in the Midwest U.S. "corn belt" during the summers of 1999 and 2000. Part II: Role of vegetation boundaries. *Journal of Climate*, **21**: 3617–3641. doi:10.1175/2007JCLI1578.1

Carleton AM, O'Neal M. 1995. Satellite-derived land surface climate 'signal' for the Midwest USA. *International Journal of Remote Sensing*, **16**(16): 3195-3202.

Charlton M, Fotheringham S, Brunsdon C. 2009. Geographically weighted regression. *White paper. National Centre for Geocomputation. National University of Ireland Maynooth*.

Coniglio MC, Stensrud DJ. 2004. Interpreting the Climatology of Derechos. *Weather and Forecasting*, **19**: 595–605.

Corfidi SF, Coniglio MC, Cohen AE, Mead CM. 2016. A proposed revision to the definition of "Derecho." *Bulletin of the American Meteorological Society*, **97**(6): 935–939.

Evans JS, Doswell CA. 2001. Examination of Derecho Environments Using Proximity Soundings. *Weather and Forecasting*, **16**: 329–342.

Fotheringham AS, Brunsdon C, Charlton M. 2003. *Geographically weighted regression: the analysis of spatially varying relationships*. John Wiley & Sons.

Francis JA, Vavrus SJ. 2012. Evidence linking Arctic amplification to extreme weather in mid‐latitudes. *Geophysical Research Letters*, **39**(6).

French AJ, Parker MD. 2010. The response of simulated nocturnal convective systems to a developing low-level jet. *Journal of the Atmospheric Sciences*, **67**(10): 3384-3408.

Fujita TT, Wakimoto RM. 1981. Five Scales of Airflow Associated with a Series of Downbursts on 16 July 1980. *Monthly Weather Review*, **109**: 1483–1456.

Higgins RW, Yao Y, Yarosh ES, Janowiak JE, Mo KC. 1997. Influence of the Great Plains Low- Level Jet on Summertime Precipitation and Moisture Transport over the Central United States. *Journal of Climate*, **10**: 481–507.

Hinrichs G. 1888. Tornadoes and derechos. *American Meteorological Journal,* **5**: 341-349.

Homer CG, Dewitz JA, Yang L, Jin S, Danielson P, Xian G, ... & Megown K. 2015. Completion of the 2011 National Land Cover Database for the conterminous United States-Representing a decade of land cover change information. *Photogrammetric Engineering and Remote Sensing*, **81**(5): 345-354.

Homer C, Huang C, Yang L, Wylie B, Coan M. 2004. Development of a 2001 national land-cover database for the United States. *Photogrammetric Engineering & Remote Sensing*, **70**(7): 829-840.

Jenks GF. 1963. Generalization in statistical mapping. *Annals of the Association of American Geographers*, **53**(1): 15-26.

Jenks GF. 1967. The data model concept in statistical mapping. *International yearbook of cartography*, **7**(1): 186-190.

Jirak IL, Cotton WR, McAnelly RL. 2003. Satellite and Radar Survey of Mesoscale Convective System Development. *Monthly Weather Review*, **131**: 2428–2449.

Johns RH. 1993. Meteorological Conditions Associated with Bow Echo Development in Convective Storms. *Weather and Forecasting*, **8**: 294–299.

Johns RH, Hirt WD. 1987. Derechos: Widespread Convectively Induced Windstorms. *Weather and Forecasting*, **2**: 32–49.

Karl T, Koss WJ. 1984. *Regional and national monthly, seasonal, and annual temperature weighted by area, 1895-1983*. National Climatic Data Center.

Kumari M, Singh CK, Bakimchandra O, Basistha A. 2017. Geographically weighted regression based quantification of rainfall–topography relationship and rainfall gradient in Central Himalayas. *International Journal of Climatology*, **37**: 1299–1309.

Lambin EF, Turner BL, Geist HJ, Agbola SB, Angelsen A, Bruce JW, ... & Xu J. 2001. The causes of land-use and land-cover change: moving beyond the myths. *Global environmental change*, **11**(4): 261–269.

Lawrimore JH, Menne MJ, Gleason BE, Williams CN, Wuertz DB, Vose RS, Rennie J. 2011. An overview of the Global Historical Climatology Network monthly mean temperature data set, version 3. *Journal of Geophysical Research: Atmospheres*, **116**(D19).

Lv A, Zhou L. 2016. A Rainfall Model Based on a Geographically Weighted Regression Algorithm for Rainfall Estimations over the Arid Qaidam Basin in China. *Remote Sensing*, **8**(4): 311.

Mann HB, Whitney DR. 1947. On a test of whether one of two random variables is stochastically larger than the other. *The annals of mathematical statistics*, 50-60.

Mesinger F, DiMego G, Kalnay E, Mitchell K, Shafran PC, Ebisuzaki W, ... & Ek MB. 2006. North American regional reanalysis. *Bulletin of the American Meteorological Society*, **87**(3): 343-360.

Metz ND, Bosart LF. 2010. Derecho and MCS Development, Evolution, and Multiscale Interactions during 3–5 July 2003. *Monthly Weather Review*, **138**(8): 3048–3070. doi:10.1175/2010MWR3218.1

NOAA/NWS Storm Prediction Center. Retrieved from http://www.spc.noaa.gov/

Pielke RA, Zeng X. 1989. Influence on severe storm development of irrigated land. *National Weather Digest*, **14**(2): 16–17.

Potter S. 2007. Fine-Tuning Fujita. *Weatherwise*, **60**(2): 64-71.

Schoen JM, Ashley WS. 2011. A climatology of fatal convective wind events by storm type. *Weather and forecasting*, **26**(1): 109-121.

Scott LM, Janikas MV. 2010. Spatial statistics in ArcGIS. In *Handbook of applied spatial analysis* (pp. 27-41). Springer Berlin Heidelberg.

Segal M, Arritt RW. 1992. Nonclassical Mesoscale Circulations Caused by Surface Sensible Heat-Flux Gradients. *Bulletin of the American Meteorological Society*, **73**(10): 1593–1604.

Segal M, Garratt JR, Kallos G, Pielke RA. 1989. The Impact of Wet Soil and Canopy Temperatures on Daytime Boundary–Layer Growth. *Journal of the Atmospheric Sciences*. doi:10.1175/1520-0469(1989)046<3673:TIOWSA>2.0.CO;2

Shapiro A, Fedorovich E. 2010. Analytical description of a nocturnal low-level jet. *Quarterly Journal of the Royal Meteorological Society*, **136**(650): 1255-1262.

Simpson RH, Saffir H. 1974. The hurricane disaster potential scale. *Weatherwise*, **27**(8): 169.

Trapp RJ, Wheatley DM, Atkins NT, Przybylinski RW, Wolf R. 2006. Buyer beware: Some words of caution on the use of severe wind reports in postevent assessment and research. *Weather and forecasting*, **21**(3): 408-415.

Vose RS, Applequist S, Squires M, Durre I, Menne MJ, Williams Jr CN, ... & Arndt D. 2014. Improved historical temperature and precipitation time series for US climate divisions. *Journal of Applied Meteorology and Climatology*, **53**(5): 1232-1251.

Weisman ML. 1993. The genesis of severe, long-lived bow echoes. *Journal of the atmospheric sciences*, **50**(4): 645-670.

Wilcoxon F. 1945. Individual comparisons by ranking methods. *Biometrics bulletin*, **1**(6): 80-83.

Zhai AR, Jiang JH. 2014. Dependence of US hurricane economic loss on maximum wind speed and storm size. *Environmental Research Letters*, **9**(6): 064019.

Tables and Figures

Table 2-1. Derecho events identified in this study listed chronologically with associated event numbers.

Derecho Event Number	Derecho Date
1	6/1/2000
2	6/25/2000
3	8/6/2000
4	8/9/2000 A
5	8/9/2000 B
6	6/11/2001
7	7/8/2001
8	8/9/2001
9	6/11/2002
10	7/27/2002
11	7/2/2003
12	7/4/2003
13	7/7/2003
14	8/26/2003
15	6/14/2004
16	7/13/2004
17	8/3/2004
18	6/8/2005
19	6/20/2005
20	7/23/2005
21	7/25/2005
22	7/13/2006
23	7/21/2006
24	8/9/2007
25	8/11/2007
26	8/12/2007
27	6/3/2008
28	6/4/2008
29	6/8/2008
30	7/20/2008
31	7/27/2008
32	7/31/2008
33	8/4/2008
34	6/18/2009
35	6/19/2009
36	8/4/2009
37	6/1/2010
38	6/18/2010
39	6/19/2010
40	6/23/2010

41	8/4/2010
42	6/18/2011
43	6/26/2011
44	7/10/2011
45	7/11/2011
46	7/30/2011
47	8/19/2011
48	6/29/2012
49	7/24/2012
50	7/26/2012
51	8/4/2012
52	8/16/2012
53	6/13/2013 A
54	6/13/2013 B
55	6/24/2013
56	6/30/2014

Table 2-2. This table shows variables related to major axis length identified in a multiple regression. Coefficients are the regression coefficients and p-values are shown for each variable.

Variable	Coefficient	p-value
925 hPa specific humidity	82.810	0.000001
CAPE	0.072	0.02572
Event time	-0.247	0.00025

Figure 2-1. Northern Tier derecho tracks from initiation to intensification.

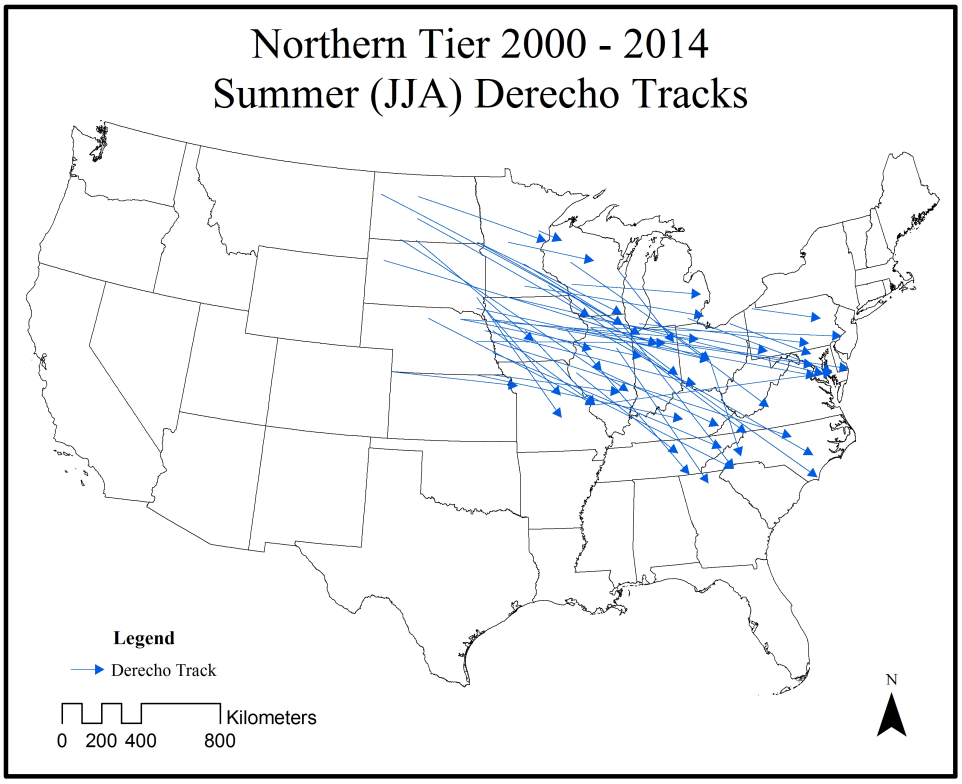

Figure 2-2. One-standard deviation ellipses for Northern Tier derecho initiation, intensification, and dissipation locations.

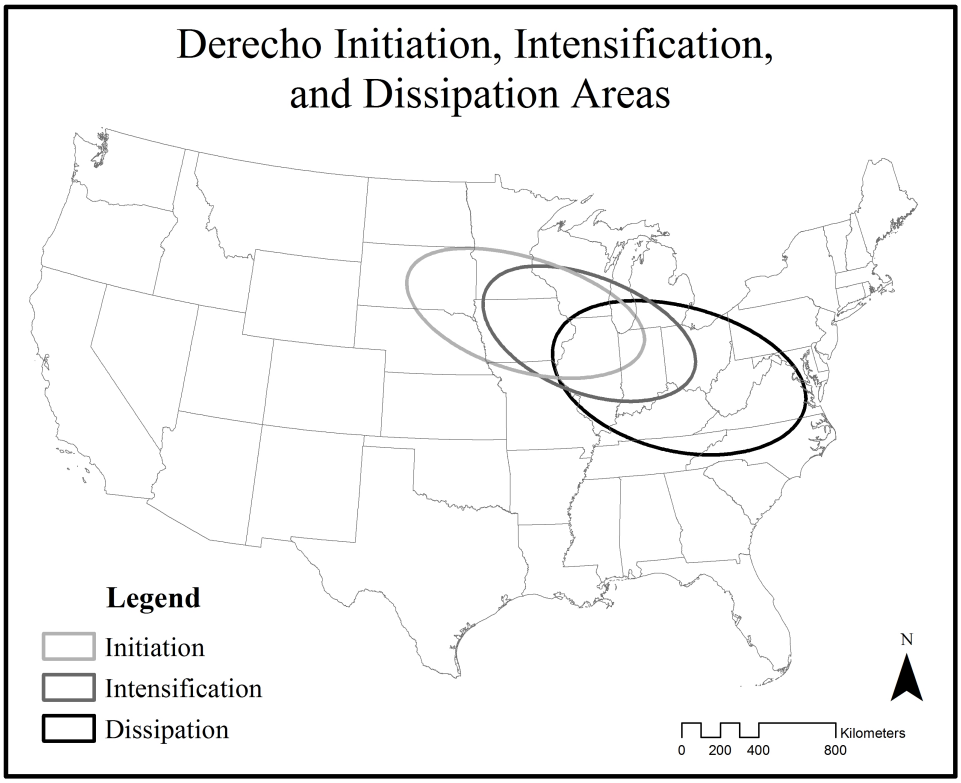

Figure 2-3. Mean derecho axes (top) and one-standard deviation ellipses (bottom) for derechos in the two direction intensity metric subsets (westerly and northwesterly).

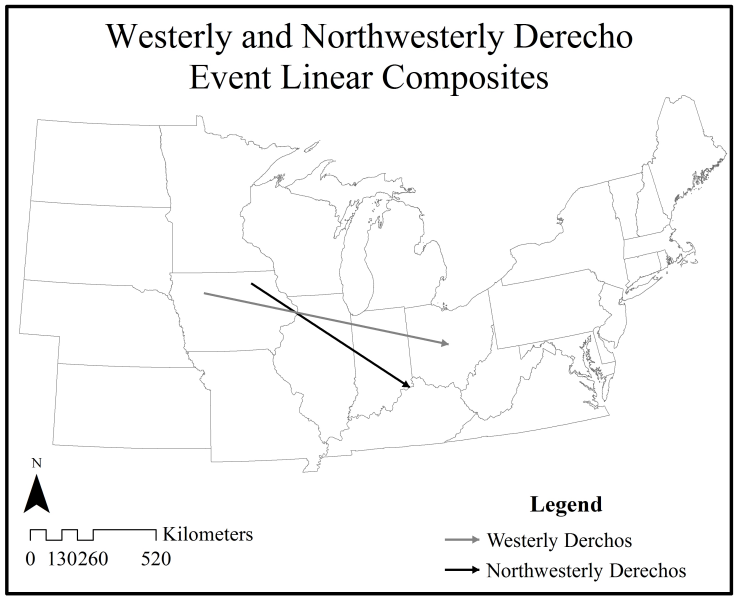

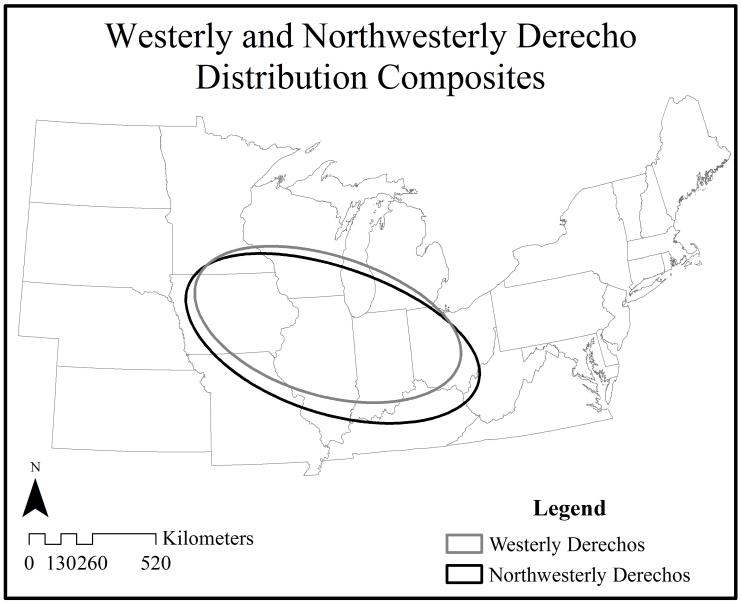

Figure 2-4. Mean derecho axes (top) and standard deviation ellipses (bottom) for derechos in rain totals intensity metric subsets (low-rain and high-rain).

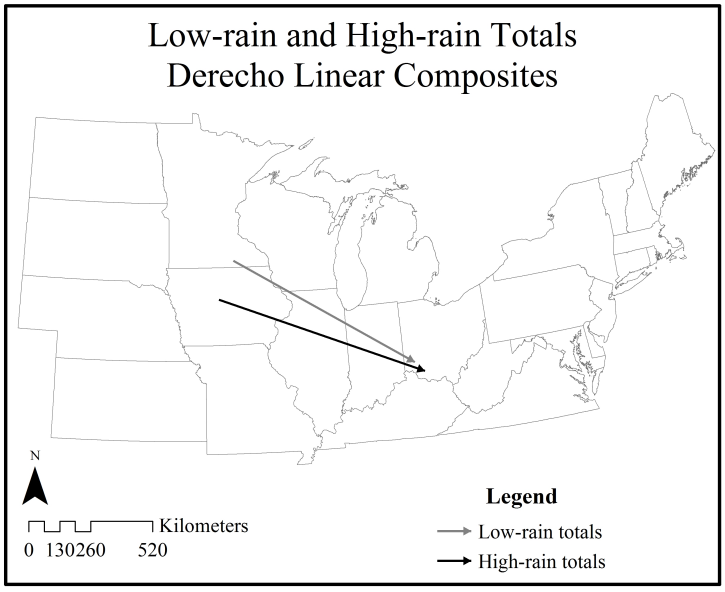

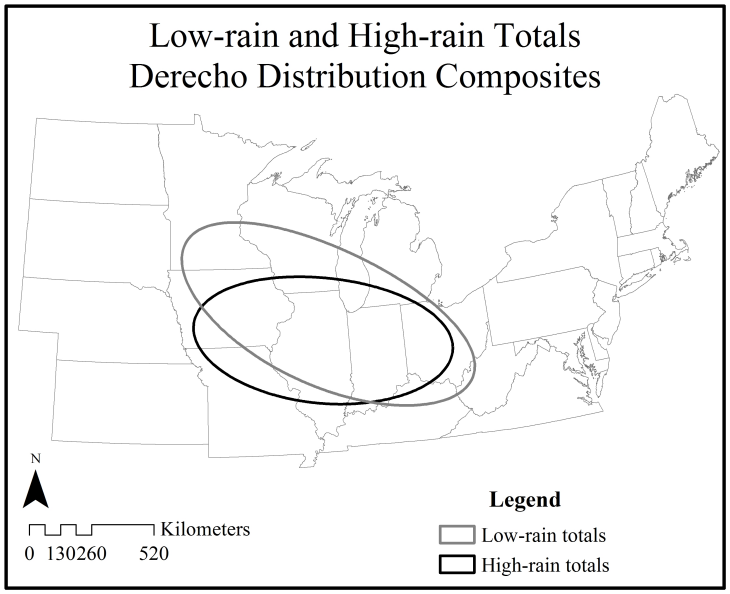

Figure 2-5. Mean derecho axes (top) and one-standard deviation ellipses (bottom) for derechos in maximum wind speed intensity metric subsets (low maximum wind speed versus high maximum wind speed).

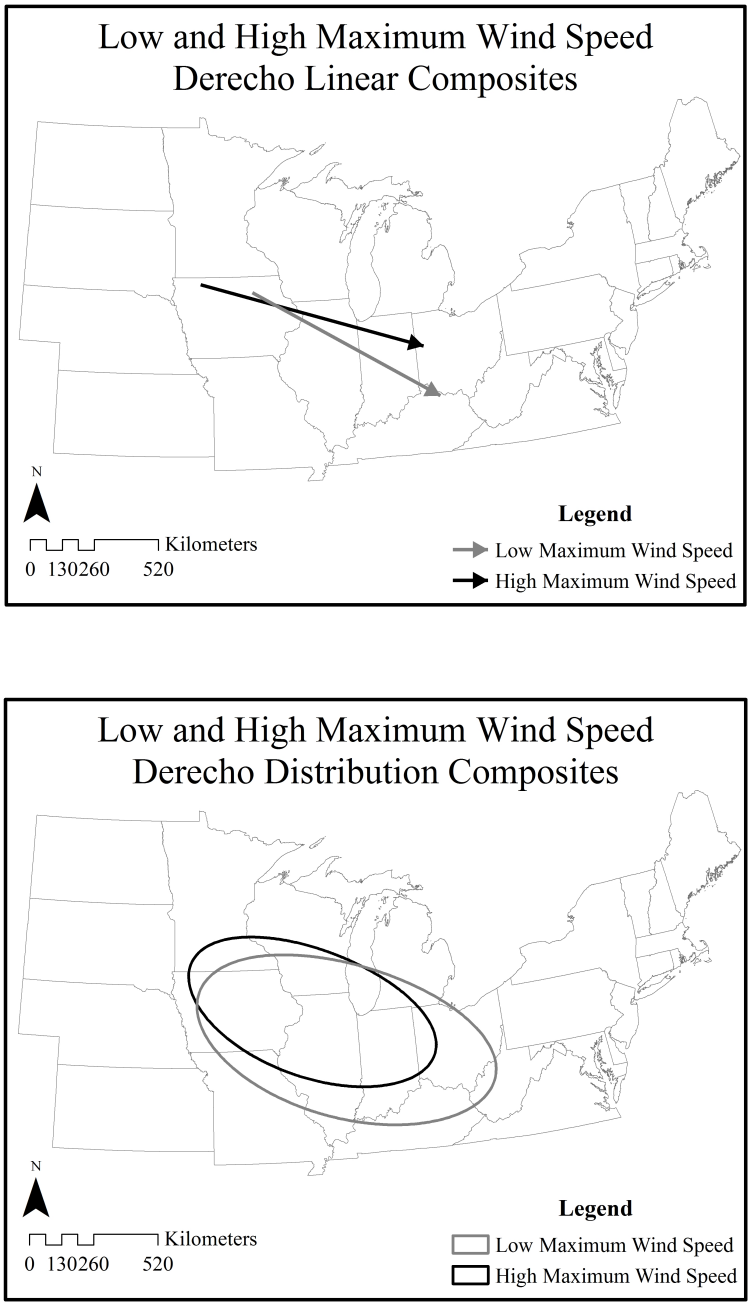

Figure 2-6. Mean derecho axes (arrows) and one standard deviation ellipses (ellipses) for derechos in minor axis length intensity metric subsets (small and large).

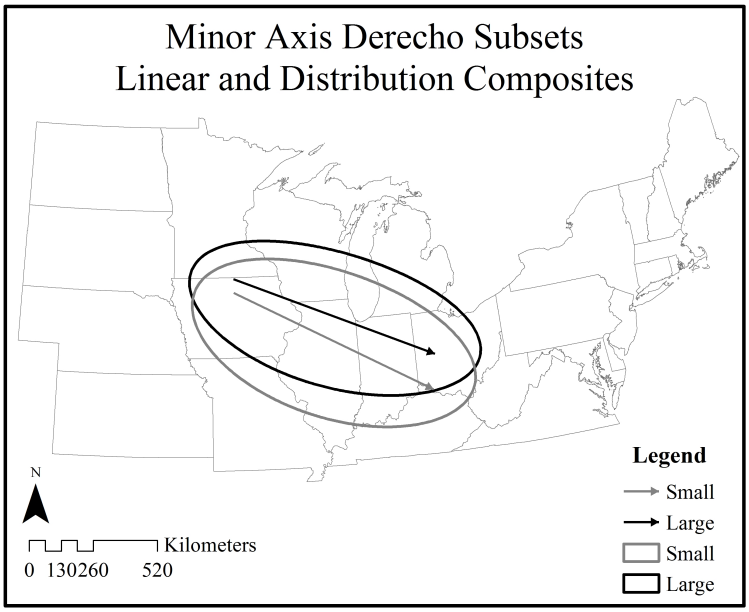

Figure 2-7. Mean derecho axes (top) and one standard deviation ellipses (bottom) for derechos in major axis length intensity metric subsets.

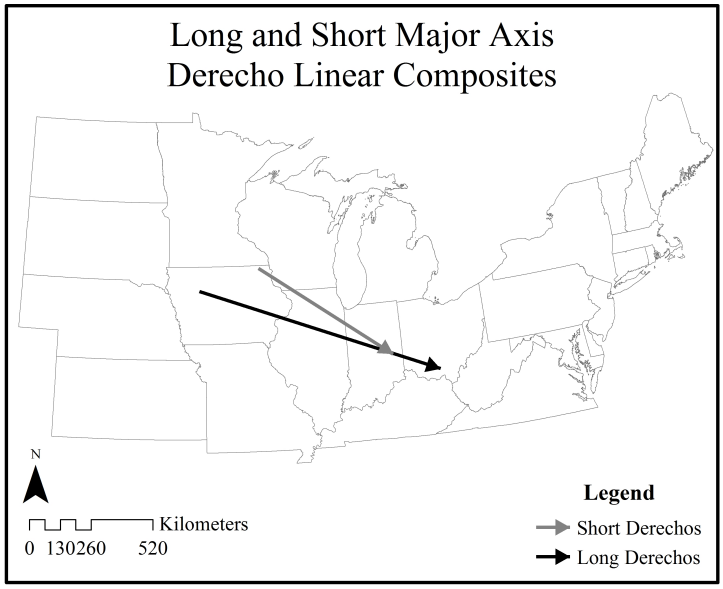

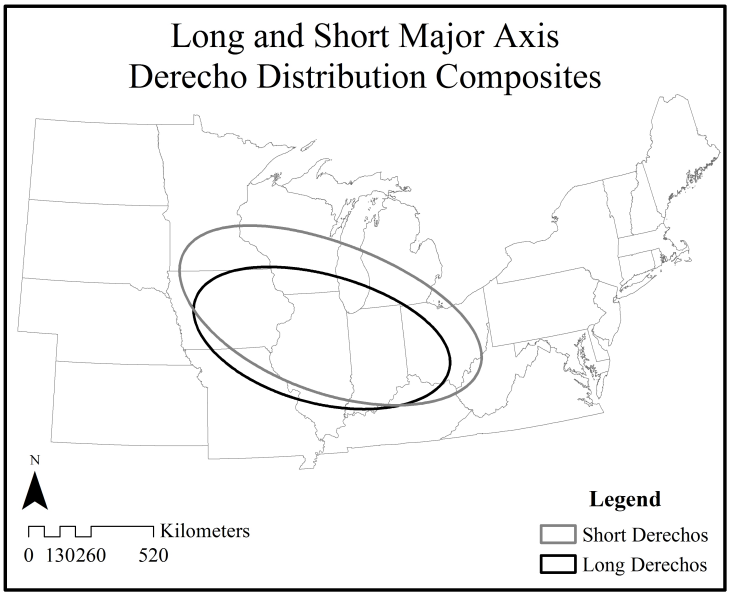

Figure 2-8. 925 hPa specific humidity – major axis length GWR coefficient values

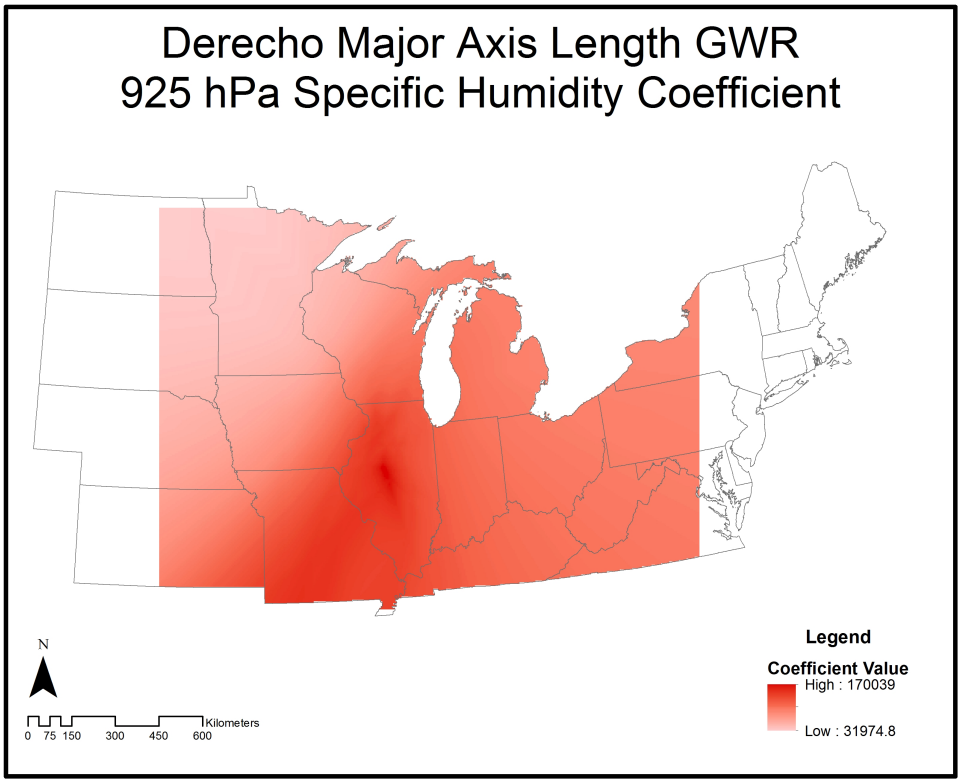

Figure 2-9. CAPE – major axis length GWR coefficient values.

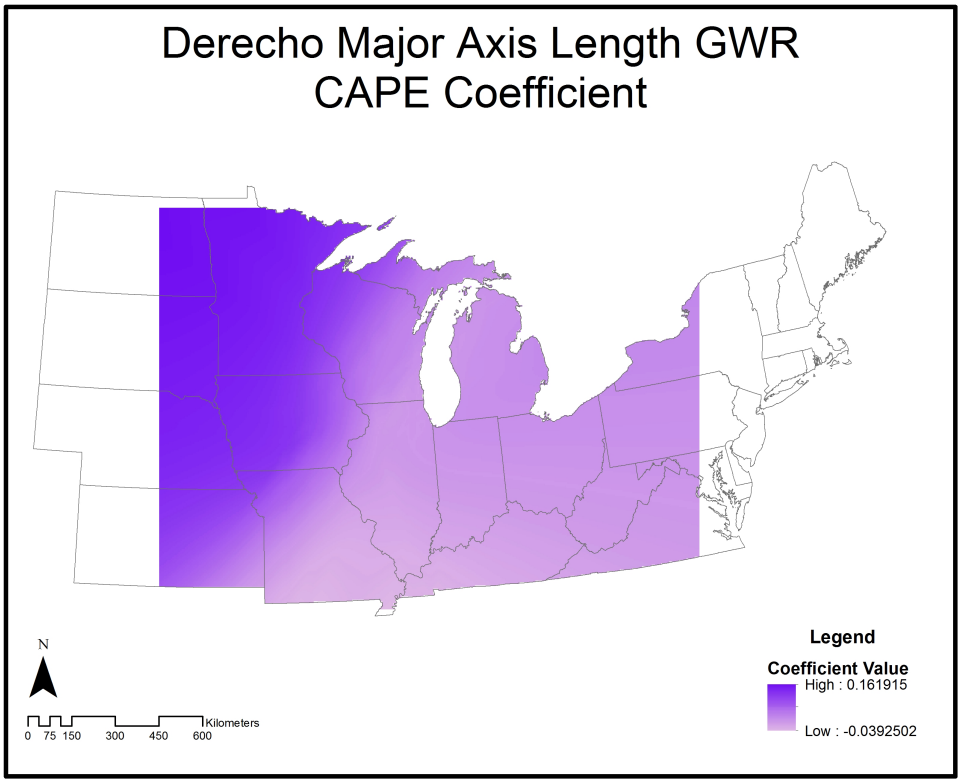

Figure 2-10. Event time – major axis length GWR coefficient values.

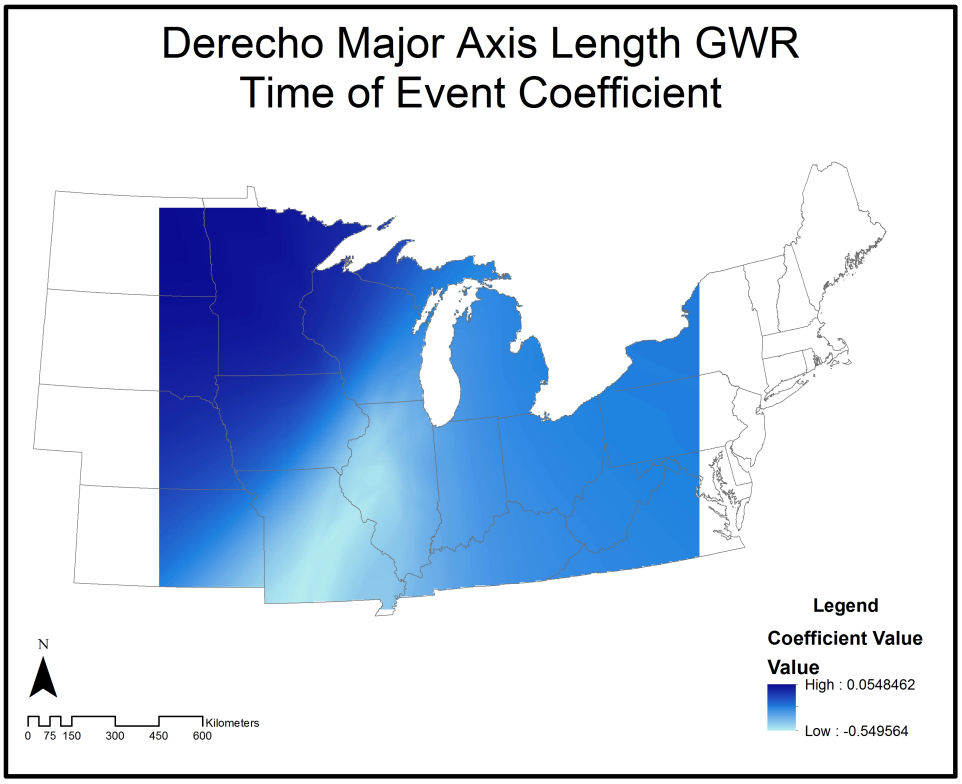

Figure 2-11. Major axis lengths observed from the 56 derechos analyzed (top) and as predicted by the GWR (bottom).

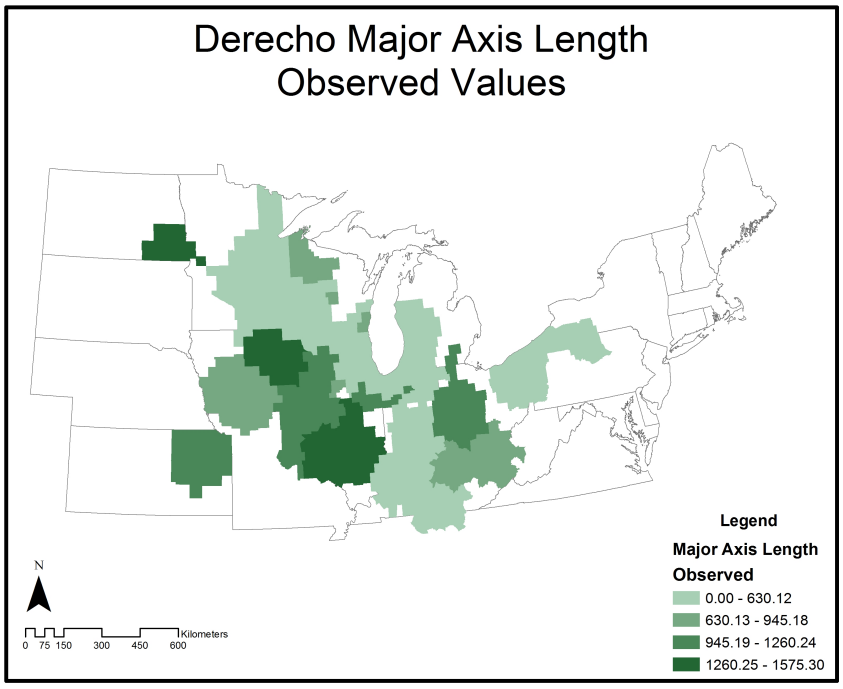

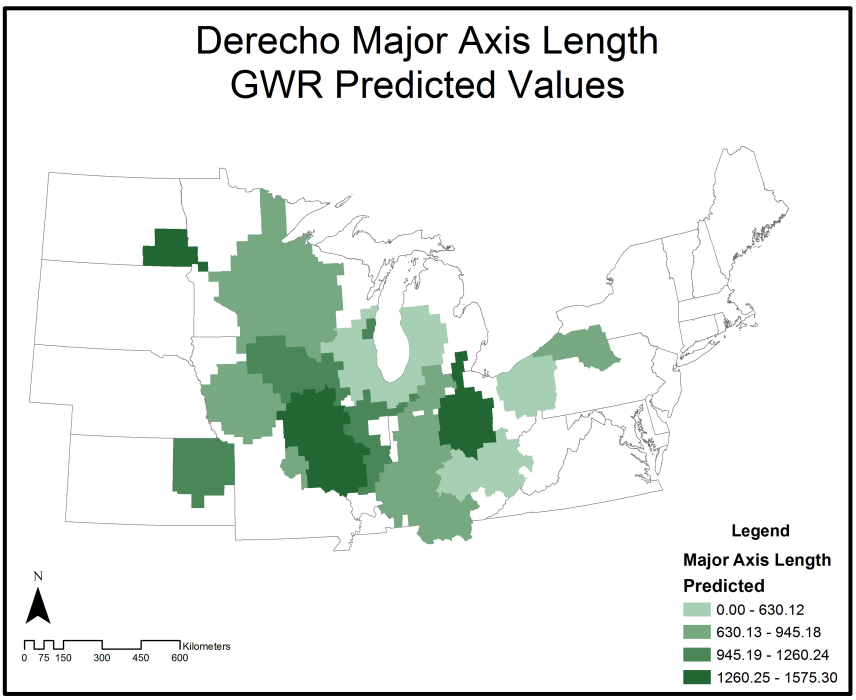

CHAPTER 3

STATISTICAL MODELING OF NORTHERN TIER STATES DERECHO-RELATED FEMA PUBLIC ASSISTANCE GRANT AWARDS

Abstract

A derecho is a convectively induced windstorm produced by an extratropical mesoscale convective system (MCS) with winds that exceed 25 ms^{-1}. Fourteen derecho "corridors" exist in the U.S. The Northern Tier corridor includes derechos that track northwest to southeast from the North Central Plains and Upper Midwest regions through the mid-Atlantic states. This corridor produces more frequent and damaging derechos than other U.S. corridors. Derecho impacts often overwhelm local and regional emergency management organizations. Under the Stafford Act (1998), federal assistance can be provided to the affected counties and states through the Federal Emergency Management Agency (FEMA) to assist with response and recovery. The present research investigates the physical and social factors that determine FEMA grant amounts awarded to aid response and recovery efforts related to Northern Tier derechos. A backward stepwise regression and geographically weighted regression (GWR) are used to model the relationship between explanatory variables such as derecho size and impacted population socioeconomic status and total FEMA grant awards. A Varimax-rotated Principal Component Analysis (PCA) is employed to further parse the factors explaining the variance in FEMA grants. Results show that the areal coverage of the derecho and the social vulnerability of the impacted populations influence FEMA grant award amounts. Overall, social vulnerability and exposure to hazards primarily determine grant amounts,

but more specific social vulnerability factors, such as population age and the number of mobile homes in a local area, affect cost variations.

Keywords: Northern Tier states, derechos, FEMA, FEMA PA grants, damage cost

Introduction

a. FEMA Grants

The U.S. Federal Emergency Management Agency (FEMA) was established to manage national disasters (Publication 1, 2016). FEMA's mission is to support survivors and first responders to maintain and bolster disaster preparation, protection, response, recovery, and mitigation (Publication 1, 2016). The Robert T. Stafford Disaster Relief and Emergency Assistance Act of 1988 enables FEMA to fulfill this mission by providing economic assistance and coincident support to states impacted by disasters (Publication 1; Public Law 100-707). Under this law, FEMA can provide grants for response and recovery efforts. FEMA disaster assistance can be given to individuals, counties, and states, and can continue for weeks to years. Although FEMA offers support for individual citizens in the form of Individual Assistance (IA) grants (CFR 44 Chapter 1 § 206.131 – 206.199), the focus of the present research is on assistance to local communities which is covered by the Public Assistance (PA) program.

The PA program awards grants to local governments to assist with response and recovery costs. This program provides government grants to repair and improve publicly owned infrastructure and facilities (CFR 44 Chapter 1 § 206.200 – 206.339). For example, the repair of public dams, bridges, community centers, and water treatment facilities are fundable through PA grants. Funding is categorized into seven groups (A – G), as follows: debris removal, emergency protective measures, roads and bridges, water control facilities, public buildings and contents, public utilities, and parks, recreational,

and other facilities. For FEMA to release funding for these types of work, a Presidential emergency or major disaster declaration must be made.

Emergency declarations allow for funding of categories A and B, whereas major disaster declarations allow for funding of all categories (A-G). Emergency declarations are made by the President usually in conjunction with the Governor(s) of the affected state(s), and typically occur when there is an approaching disaster for which the need for federal assistance is anticipated, or immediately following a disaster (CFR 44 Chapter 1 § 206.61 – 206.100). The purpose of an emergency declaration is to address the immediate needs of the affected places by saving lives, protecting property, and ensuring safety. Only PA categories A and B and limited categories of IA can be funded through an emergency declaration. The federal share of the disaster recovery cost is 75% leaving 25% to be paid by the state. The state usually pays a share of the 25% and the affected county another share, thus reducing the economic stress on local governments. However, these shares vary state-to-state.

Major disaster declarations, on the other hand, provide funding for a wider range of recovery efforts (CFR 44 Chapter 1 § 206.1 – 206.60). These declarations are requested by the Governor(s) of the impacted state(s) within 30 days of the event and are declared or denied by the President. The time immediately following the disaster is used to estimate losses and create a budget for recovery through preliminary damage assessments (PDAs). Although the state is eligible to receive funding through all PA categories (A-G) after a major disaster declaration is made, PDAs, the formal major disaster declaration request, and FEMA recommendations determine which IA and PA categories will be awarded grants for recovery from a disaster. In addition, with a major

disaster declaration, the state receives hazard mitigation support which allows it to address vulnerabilities across the state and enhance its resilience. Federal funding of recovery ranges from 75% to 90% and the remaining cost is left to the state to cover.

Following the closure of all event-related funding projects, data on FEMA grant funding is published to the FEMA National Emergency Management Information System (NEMIS). FEMA disaster declarations that are associated with a derecho are classified as straight-line wind events. NEMIS data on each event includes the number of states and counties impacted, PA and IA grant approval status, the amount of emergency funding awarded, the amount of permanent funding awarded, and the total amount of funding awarded. Money is considered awarded once it has been fully paid by FEMA and there are no outstanding costs associated with the disaster declaration.

Through emergency and major disaster declarations, FEMA helps states respond to and recover from disasters by providing funding through IA, PA, and Hazard Mitigation grant awards. Measuring the cost of recovery through these grant programs can be difficult. Hazard mitigation grants cover an entire state which may not be representative of a storm's impact. IA grants are associated with personally identifiable information (PII). Although the fine spatial resolution of these data may make it ideal for understanding individual losses, major damage to infrastructure (bridges, roads, etc.) is not accounted for, and regulations surrounding the use of PII make it difficult to access, extract, and analyze without violating privacy policies. In addition, insurance policies and individual choice play a role in IA grants. Some individuals may decide to rebuild their homes fully and stay in hotels while doing so—thus requesting high grant awards—while others may stay with family members and have home repairs fully covered by their

insurance. The wide variations in IA grant requests are difficult to quantify over such a large region as the Northern Tier states. Thus, PA grant data comprise the most comprehensive, accessible, and spatially appropriate FEMA grant program to analyze for determining costs of a disaster and community recovery.

b. Statistical Modeling Of Severe Weather-Related Economic Losses

Many studies aim to estimate the economic cost of severe weather events. Although it is difficult to identify storm loss data that are used consistently across studies, insurance records and FEMA's grant program records are frequently used to study severe weather-related losses (Changnon, 2003; Gall *et al.*, 2009). Records of FEMA's PA grant programs are well-maintained and open source. With improved methods of data retention, normalization to relate yearly cost data based on inflation, and modeling, the datasets are improving and becoming more available for use in emergency management research (Changnon, 2003; Noble, 2004; Downton and Pielke, 2005; Gaddis *et al.*, 2007; Smith and Katz, 2013). Often, research on disaster losses is driven by the insurance industry (Changnon *et al.*, 1999). Insurers and researchers are interested in identifying potential losses associated with particular types of storms, climate variability and change, and population distribution (Kunkel *et al*., 1999; Changnon *et al.*, 2001). For example, high-density housing in coastal areas and Midwest-region crops are vital to the health of the U.S. economy, but are also vulnerable to the impacts of severe weather events. Thus, the regional focus has been on coastal areas that are subject to flooding and hurricane damage which may be intensified through climate change, and the Midwest which sees frequent severe weather events in the warm season (Changnon, 1972; Pielke and

Landsea, 1998; Changnon *et al.*, 1999; Gall *et al.*, 2011; Felsenstein and Lichter, 2014). Often, the disasters that cause economic losses cover wide areas and cross political boundaries. Comparing the events year-to-year can be difficult because loss estimates are given in dollar amounts that fluctuate, and population density and distributions change. Thus, researchers have devised methods to analyze storm loss data regionally and globally to understand economic losses across spatiotemporal scales (Neumayer and Barthel, 2011; Mohleji and Pielke, 2014). These studies, however, acknowledge that this is a difficult task that requires further study particularly emphasizing variation of affected populations across study areas. Investigation of the NWS flood loss database revealed that loss estimates are improved when multiple disasters of the same type are aggregated and studied (Downton *et al.*, 2005). More research on many disasters of the same type is needed to examine the local variations in economic losses associated with a specific type of storm (here, derechos).

c. Influence Of Social Vulnerability On Economic Losses

When modeling economic losses due to severe weather events it is inherently important to understand the storm characteristics, but it is also necessary to incorporate knowledge on the affected population. Social vulnerability refers to a population's ability to respond to, recover from, and adjust to disasters (Cutter *et al.*, 2003; Cutter and Finch, 2008; Flanagan *et al.*, 2011). Research shows that demographic factors such as social vulnerability are correlated with losses related to severe weather and extremes (Changnon, 2003; Schultz and Elliott, 2012). Evidence from severe weather events in the 1990s shows that changes that increased social vulnerability led to increased severe

weather-related economic losses in that decade (Changnon and Changnon, 1999; Schultz and Elliott, 2012). Other work investigated disaster-specific impacts incorporating social vulnerability. Felsenstein and Lichter (2014) show the strong influence of social vulnerability on economic losses related to flooding. Hurricane Katrina affected vulnerable populations more severely than those that were less vulnerable. These amplified impacts lasted throughout the storm and into the lengthy response and recovery phases (Masozera *et al.*, 2007). Burton (2010) addresses the idea that social vulnerability either enhances or diminishes the impacts of a hurricane on a community by modeling hurricane-related economic losses. His work calls for more integration of social vulnerability variables into economic loss modeling and notes that while results shown in studies like that by Masozera *et al.* (2007) are important, often their results are not incorporated into statistical models. Changnon (2003) also cites the importance of including social vulnerability when assessing economic impacts of disasters and building statistical models. Recently, work has emphasized forward projecting economic loss while incorporating social vulnerability. Future losses have been suggested to increase because of the combination of social vulnerability factors (Preston, 2013) and climate change (Visser *et al.*, 2014). Discussing climate change and future losses reinforces the importance of considering social vulnerability in economic loss studies. For example, social vulnerability of coastal populations increases with sea-level rise. In addition, climate change-social vulnerability research shows that it is important to continue studying loss and to refine statistical models to assist with this task. Severe weather response and recovery costs are related to the needs and social vulnerability

characteristics of the impacted population and are thus also an emphasis of the present research.

d. The Importance of Studying Derechos In The Context of Economic Loss and Social Vulnerability

Derechos can track over large areas covering close to half of the U.S. (2,000 km) and can be as wide as 500 km (NOAA SPC, 2004). The storms have associated winds reaching tropical storm to hurricane-force and can cause widespread damage across urban and rural landscapes. Derechos also are often accompanied by heavy rain and lightning (Bentley *et al.*, 2016). Although the public may not understand derechos as well as they do hurricanes and tornadoes, they can be just as damaging (Black and Ashley, 2011; Corfidi *et al.*, 2016). Table 3-1 shows the number of fatalities caused by derechos compared to those caused by hurricanes and low-category tornadoes in the period 1986 – 2003 (Ashley and Mote, 2005; adapted from their Table 3). Although derechos occur less frequently than F0 and F1 tornadoes, they caused more fatalities during this period. In addition, derechos caused over three billion dollars in damage from 1986 – 2003 (Ashley and Mote, 2005). Some derechos ranked comparatively in insurance losses among the costliest of hurricanes (Table 3-2) (Ashley and Mote, 2005; adapted from their Table 5). As is demonstrated by derecho impacts, it is appropriate to study derecho-associated economic losses using FEMA response and recovery cost data.

Background

Although hurricane economic loss estimates, like those associated with floods, have been modeled in previous research, very few investigations into derecho economic loss modeling exist. The present research aims to quantify derecho losses through the analysis of PA grant awards, and identify the variables that determine those losses. Further, few studies look at the geographic goodness of fit, or local effectiveness, of model results. Thus, these questions are addressed in the present research which statistically models FEMA PA grant award amounts associated with derecho event damage. In addition, overall goodness of fit, or model effectiveness, is tested along with local goodness of fit, or model effectiveness at a point in space, to determine where, geographically, the model performs best and where, geographically, it needs improvement. Thus, this research enhances understanding of derecho-related economic losses regionally and locally, and improves knowledge on derecho-related FEMA PA grant awards.

Floods can cause widespread economic and social devastation. Flooding events are often studied with respect to their associated economic costs. They are also studied because they occur frequently across the U.S. and can have economic impacts on different populations across space and time which can be analyzed through statistical modeling (Dutta *et al.*, 2003; Zhu *et al.*, 2007; Smith and Katz, 2013). Flood losses are so common that flood insurance is federally regulated by the National Flood Insurance Program (NFIP) through the Federal Insurance and Mitigation Administration (FIMA). FEMA's severe storm hazards impacts tool, the Hazards U.S. Multi-Hazard (HAZUS-MH) is capable of modeling potential damage from multiple types of severe weather. It is frequently used to model flood losses and damage caused by flooding. Statistical

evaluations show that HAZUS-MH can aid in predicting the types and number of resources required for response efforts across the U.S. (Scawthorn *et al.*, 2006a; Scawthorn *et al.*, 2006b). Location-specific case studies by flood loss models are also used to identify and refine variables that determine loss (Dutta *et al.*, 2003; Zhu *et al.*, 2007). Case studies cover smaller regional and local areas, and studies examining flood insurance purchasing address flood loss at individual and community levels (Browne and Hoyte, 2000). Flooding occurs at many spatiotemporal scales, and thus many studies explore flood economic losses (Kunkel *et al.*, 1999; Pielke and Downton, 2000). In an effort to compare flood losses across time, normalizing the loss data with respect to inflation is also a topic of interest to researchers (Noble, 2004; Pielke *et al.*, 2002). Although floods are a frequently researched topic, less common but still large-scale (in damage and size) derechos are not studied as specifically. In addition, flood loss modeling tends to be undertaken at a finer resolution than is appropriate for derecho events.

Akin to the economic losses associated with floods, hurricane economic losses due to extreme winds and storm surge are investigated using similar approaches. Derechos have hazards similar to those of hurricanes such as high winds and flooding. Hurricanes are large-scale events that impact broad populations and cause major infrastructure destruction and financial devastation. As with floods, attempts are made to normalize the economic impacts of hurricanes over time based on inflation for improved analysis (Pielke and Landsea, 1998; Pielke *et al.*, 2008). Similarly, statistical models are constructed to predict hurricane-related economic losses (Watson and Johnson, 2004; Malmstadt *et al.*, 2009; Pan, 2014). Although these models have improved over time,

there is a call for continued research on better defining the economic losses from hurricanes. Derechos are under-researched in this area. HAZUS-MH has been used to estimate potential losses from a hypothetical hurricane showing that while local variations are important, regional models can aid understanding of hurricane economic losses (Pan, 2011). Boswell *et al.* (1999) examined PA grant awards associated with hurricanes and used multiple regression to generate a model to predict PA cost. They then estimated public costs for hurricanes in each of the Saffir-Simpson categories using various statistical models (Boswell *et al.*, 1999). Likewise, this research uses a backward stepwise regression to generate a similar model for derechos.

Although derecho-related economic losses have not been thoroughly investigated, the FEMA PA grant program and FEMA response operations have been previously examined by researchers studying local and federal emergency response to derechos. For example, relationships between FEMA disaster declarations and blizzard tracks have been analyzed. Although qualitative relationships were evident, backward stepwise regressions revealed that a single equation could not predict FEMA declarations from blizzard tracks (Atkinson, 2010). Other studies look at FEMA response and recovery operations immediately following various storm types through PDAs and debris removal, which are activities that require coordinating community involvement and FEMA support. The studies reveal that little research has been conducted on the effectiveness and impact of these initial stages of FEMA support. (Fetter, 2010; Fleming, 2012). Downton and Pielke (2005) investigated FEMA loss data and found that the over- and under-predictions evident in the county-level information were improved upon when the data were spatially aggregated and then analyzed. These authors suggest that using the

data over regional areas and longer time periods yield more statistically significant results (Downton and Pielke, 2005). A similar approach is undertaken in the present research which investigates PA funding of derecho events.

Data and Methods

a. Data

The data used in this study include storm reports, satellite and remotely sensed imagery, local near-surface air temperatures, FEMA grant award amounts, and social vulnerability measures of populations by Census tract. These data are used to identify derechos and their synoptic climatological properties, associate FEMA grant award amounts with derecho events, and identify socioeconomic factors of impacted populations such as housing types and family makeup. The data comprise a suite of variables that can be tested statistically to reveal relationships between derecho events and FEMA funding of response and recovery efforts, and make comparisons to other disaster types.

High-wind reports for the climatological summer (June, July, and August) period of 2000 to 2014 are available from NOAA Storm Prediction Center (SPC). They were inspected for spatial and temporal continuity of wind reports exceeding 25 m/s to identify potential derecho events. However, previous research shows that SPC wind reports can be flawed due to observer and reporting errors (Trapp *et al.*, 2006). Following Trapp *et al*. (2006), derecho identification from SPC wind reports was verified using NOAA NWS WSR-88D Level III radar reflectivity data. In the presence of a derecho, this imagery displays evidence of sustained convection organized quasi-linearly—often in a "bow-

echo", or backward-C shape that progresses along a long path—to support the SPC wind data. Satellite visible and infrared imagery are also used to confirm derecho development and progression by determining if high, cold-top clouds are present. In addition, National Centers for Environmental Protection (NCEP) North American Regional Reanalysis (NARR) three-hourly reanalysis model output (Mesinger *et al.*, 2006) and University of Wyoming 12-hour vertical profiles provide data on atmospheric properties of the confirmed derechos such as Convective Available Potential Energy (CAPE) and vertical wind shear. Other important variables obtained through inspection of radar images include the major axis length (in km) and dissipation latitude of the storm centroid. The dissipation latitude is that at which the storm weakens enough to no longer maintain organized convection. Local near-surface temperature data were acquired using the U.S. Climate Divisional Dataset (Karl and Koss, 1984; Vose *et al.*, 2014).

The social vulnerability data for this analysis comprise measurements of socioeconomics, household composition and disability, minority status and language, and housing and transportation. They are extracted from the 2014 Centers for Disease Control and Prevention Agency for Toxic Substances and Disease Registry (CDC/ATSDR) Geospatial Research, Analysis & Services Program (GRASP) Social Vulnerability Index (SVI). This index provides the disaster management-specific vulnerability rankings and metrics for U.S. Census tracts (Flanagan *et al.*, 2011). Each of the four categories in the SVI mentioned above contains data on two to five related social vulnerability sub-factors. The Socioeconomics category encompasses the number of individuals below the poverty line, the number of unemployed individuals, the per capita income, and percentage of people over 25 who do not have a high school diploma. The Household Composition and

Disability category includes the number of people over 65 years old, the number of people 17 and younger, the number of people with a disability, and the number of single-parent households with children. The Minority Status and Language category includes the estimate of all non-White people and the number of people over five years-old who speak English "less than well." The Housing and Transportation category includes housing in structures with more than 10 units, number of mobile homes, the number of households that have more people than rooms in their dwellings, the number of households without a personal vehicle, and the number of people institutionalized (Flanagan *et al.*, 2011). Every Census tract is given a percentile score in each of these sub-factors and summary categories. An overall social vulnerability ranking is included as a percentile (Flanagan *et al.*, 2011). The disaster-specific SVI is used widely by FEMA to analyze program effectiveness in post-event scenarios and potential impacts following disaster events. Its use in the present research maintains consistency with FEMA's analyses and encourages FEMA's acceptance of the results while helping to explain the variance in the disaster losses.

To analyze the statistical relationship of FEMA funding with derecho impacts and social vulnerability variables, FEMA disaster declaration data were used. The NEMIS data, accessed using OpenFEMA, was cross-referenced with derecho event dates to identify if the derecho prompted a FEMA disaster declaration and subsequent release of funding. Although the declarations can be coincident with the event, often the damage assessments, application, and subsequent presidential approval of a disaster requiring FEMA assistance take several weeks (Publication 1). Thus, this analysis addresses all

funded projects, including those that were applied for in the weeks following a derecho, but not those in which FEMA funding was applied for but denied.

b. Methods

A backward stepwise regression is used to generate a linear model that predicts FEMA PA grant award amounts based on the explanatory variables of social vulnerability and storm properties. Backward stepwise regression has been used in climatological research, social vulnerability studies, and disaster research (Ninyerola *et al.*, 2000; Ebert *et al.*, 2009; Burton, 2010). The regression produces an equation that describes how the independent variables of population, storm attributes (e.g., size), and social vulnerability affect FEMA PA grant award amounts. The backward stepwise approach tests all the potential independent variables to determine a combination of variables needed to produce the most statistically significant model fit to the data. The statistically significant model fit shows that the equation that describes the overall trends in the PA data relative to the explanatory variables is likely to accurately estimate results at the 95% confidence level. This regression technique also eliminates problems of multicollinearity and redundancy in explanatory variables, which means that variables can be considered to be independent of one another and not representative of the same information. Backward stepwise regression results can be confirmed and expanded upon by conducting a geographically weighted regression (GWR) to show the model's spatial variation by creating geographically relevant regression coefficients that can be plotted on a map.

A GWR is used in this research to further clarify regression results across the study area in terms of regression coefficients and model goodness of fit and identify spatial relationships between explanatory variables and FEMA PA grant awards (Ninyerola, 2000; Ebert *et al.*, 2009; Lv and Zhou, 2016; Kumari *et al.*, 2017). The GWR depicts the relationships between the explanatory variables and the FEMA PA grants by mapping the regression coefficients across the study area to show their relative influence and by mapping the R^2 to show local goodness of fit (Brunsdon *et al.*, 1996; Brunsdon *et al.*, 1998; Fotheringham *et al.*, 2002). GWR has been used to validate and further define simple regressions in disaster-related work (Ebert *et al.*, 2009; Burton, 2010). For this analysis, the GWR shows where the regression coefficients are highest and lowest and thus have the most influence on the FEMA PA grant award amounts. An adaptive bandwidth is used to accommodate spatial non-conformity of the underlying FEMA PA grant award data by referencing a varying number of nearest neighbors best suited to each location to generate the regression. The adaptive bandwidth method finds an optimized number of nearest neighbors on which to base the coefficient surface as opposed to a fixed number or fixed radius that may be unrepresentative of the data because of the varying spatial distribution of the derechos. Especially given the region of interest, which has many physical and social variations across space, the adaptive bandwidth approach is highly effective. In addition, the GWR also permits local evaluation of goodness of fit which is defined as the location-respective R^2 for the model, which is important to the research to show that the influence of the explanatory variables and how the model varies over space. To ensure GWR residuals are not spatially autocorrelated, and thus the model is not biased, a Moran's I test is conducted (Goodchild, 1986). Should the residuals be

autocorrelated, the model would not be representative of an independent process and would be discarded.

To further clarify inter-variable relationships and their statistical significance identified by the backward stepwise backward stepwise regression and the GWR, a Varimax-rotated principal components analysis (PCA) is subsequently used to describe the variance of explanatory variables in the derecho-related dataset. The Varimax rotation ensures the PCA has a simple structure where the component loadings show clustering of the loading variables allowing for easily interpretable results (Richman, 1986; White *et al.*, 1991).

Results

Results from the backward stepwise regression, GWR, and PCA are explained in this section that is followed by a subsequent discussion of their implications in the Discussion section.

a. Predicting Grant Award Amounts from Explanatory Variables

Results of the backward stepwise regression show that FEMA PA grant award amounts are directly related to the population impacted by the derecho. The model revealed that two variables significantly predict FEMA PA grant award amounts – the number of counties impacted and overall percentile SVI ranking, at a significance level of $p < 1*10^{-7}$. This model has a high adjusted R^2 of 0.9202, meaning that it successfully predicts grant award amounts based on the number of impacted counties and overall percentile SVI ranking at a rate of 92%.

The standardized residuals of the model are normally distributed and not spatially autocorrelated, thus showing the backward stepwise regression model is not biased because any error is a result of a random process and there is not another equation that could better fit the data (Figure 3-1). The size of the storm relates positively to the number of counties impacted; a larger storm will likely impact more counties as it tracks over a larger area and thus increases the total FEMA PA grant award amounts. In addition, the social vulnerability of the impacted Census tracts positively correlates with the FEMA grant award amounts. The influence of social vulnerability is less than that of the number of counties impacted. Thus, it is likely that the social vulnerability moderates the variation of the data on a finer geographic scale, or is a more locally important component. Further spatial and statistical analyses are therefore undertaken to reveal how the localized influence of SVI helps to shape the model.

b. Spatial Variations of Grant Award Regression Coefficients Related to Derechos

Depicting the relationship shown in the backward stepwise regression through a GWR shows where each of the regression coefficients discussed below are most influential. Both variables (i.e., the number of impacted counties and the overall percentile SVI ranking) that significantly predicted the FEMA PA grant award amounts in the backward stepwise regression also significantly predicted the grant awards when mapped. The GWR improved the model's fit, such that the independent variables of number of impacted counties and overall percentile SVI ranking significantly predict the dependent variable of FEMA PA grant award amount with an adjusted R^2 of 0.974. Coefficient surfaces that show the change in coefficient values across the study area

produced in the GWR show spatial variations in the influence of the independent variables (number of impacted counties and overall percentile SVI ranking) on the dependent variable (PA grant award amounts) across space (Figure 3-2a – 3-2c).

The map of regression coefficient values for the number of counties (Figure 3-2a) shows a high-to-low gradient of the coefficient values from west to east across the region. The coefficient is highest in northeastern Wisconsin and southwestern Virginia. It is lowest in the southeastern portion of the study area with the exception of the high values in Virginia. Figure 3-2b shows the mapped regression coefficient values for the overall percentile SVI ranking. The coefficient is highest at the intersection of the border of Minnesota, Iowa, and Wisconsin. Immediately west of this area the overall percentile SVI ranking regression coefficient is low meaning that the influence of the SVI coefficient is lower in this area. It is also low in the eastern part of the study region. This coefficient value field has a map pattern similar to that of the intercept field which shows the field of intercept values in the equation (Figure 3-2c), however there is more variation in the intercept field. The intercept field is highest and lowest in similar locations to the overall percentile SVI ranking regression coefficient. This pattern implies that the number of counties coefficient drives the relationship to the dependent variable. However, the spatial variation of the SVI shows that the ranking will guide the model in areas where it is highest (e.g., at the border of Minnesota, Iowa, and Wisconsin).

The mapped standardized residuals of the GWR (Figure 3-3) show that the model predicts most FEMA PA grant award amounts to within two standard deviations, with the majority of the study region falling within one standard deviation. Areas that are over-predicted are in southern Wisconsin, northern Illinois, and northwestern Iowa. The model

under-predicts FEMA PA grant award amounts south of Lake Michigan, at the intersection of the borders of Iowa, Wisconsin, and Illinois, and in western Iowa meaning that grants will likely be higher in these areas than the model shows. The standardized residuals are randomly distributed and not statistically significant (not shown) verifying that the model is not biased, and therefore that the equation explains the variation of the data adequately and without duplicate inputs. The mapped standardized residuals are not spatially autocorrelated as determined by a Moran's I test (Figure 3-4), implying that they are randomly distributed and independent ($z = -1.361$, $p = 0.173$).

The local R^2 values—depicting the locations where the model is most effective at predicting PA grant awards—vary in a similar way to the standardized residuals across the study area (Figure 3-5). The majority of the study area has an $R^2 > 0.787$, with the southern portion of the region having the highest R^2 values (mostly exceeding 0.910). This result shows that the model locally predicts PA grant award amounts correctly at a rate between 78.7% and 91% in these areas. The model does not perform as well in northern Indiana and southern Michigan, where local R^2 values are less than 0.5. These locations may be influenced by other variables that are less important across the study area generally, but have a high local importance. The model is a reasonably good fit with moderate to high R^2 values and predicts the FEMA PA grant amounts well across the study region in connection with derechos.

c. Further Clarifying the Variance of FEMA PA Grant Award Amounts

The Varimax-rotated PCA further clarifies the results of the backward stepwise regression and GWR by revealing principal components loaded by independent variables

that describe the dependent variable, FEMA PA grant award amounts. The scree test (Cattell, 1996) determines the number of principal components that collectively explain the greatest amount of variance in the dataset. The scree plot (Figure 3-6) shows the variances of the individual components from the PCA run on the FEMA PA grant award amount data. The graph shows ten components that are potentially useful in explaining the variance in the dataset. Components on the tail of the graph where the slope flattens out should be eliminated because they do not explain a sufficient amount of the variance (Cattell, 1996). The first five components have steep slopes; accordingly, these components are used to describe the variance in the FEMA PA grant award amounts data. The first five rotated principal components explain 99% of the variation in FEMA grant award amounts. The rotated component names, the variables that load heavily onto each rotated component, and the percent of variance explained by each rotated component, are shown in Table 3-3.

Accordingly, local temperature is heavily loaded onto the Temperature rotated component, suggesting that while the measured social vulnerability characteristics are important factors in the overall grant award amount, local environmental factors can have an antecedent influence. Antecedent factors may influence vulnerability on different temporal scales. Persistent flooding, for example, could occur over weeks, whereas a short, pronounced heat wave could occur in a few days before a derecho and both could increase vulnerability. The Temperature rotated component explains 25% of the variance in the data. Physically, this association could be because higher temperatures are associated with higher energy (e.g., CAPE) and potentially larger storms that impact more counties. Socially, impacted communities are at a greater risk when pre-event

temperatures are higher than when they are lower (e.g., Watts and Kalkstein, 2004; Harlan *et al.*, 2006).

The second rotated component, Living Conditions, is loaded by Minority Status, Household Composition, and Mobile Home Units. The Living Conditions component explains 22% of the variance in the grant award amounts and shows that areas with more minorities, more vulnerable residents, and more mobile homes are associated with higher grant award amounts following derecho events.

The third rotated component, Size, is heavily loaded by the Major Axis of the derecho. This rotated component explains 19% of the variance in the grant award amounts. The result that longer derecho path lengths are associated with higher grant award amounts is logical because longer-lived derechos are likely to impact more people and communities which would require increased grant funding for recovery. In addition, derechos with longer path lengths also tend to be more intense storms with higher winds and, accordingly, greater potential for damage, as shown in the first chapter of this dissertation. The Size component reflects the number of impacted counties coefficient identified as significant in the backward stepwise regression analysis.

The fourth rotated component, Exposure, is loaded by variables that show that both the physical attributes of the derecho such as dissipation latitude and the social vulnerability of the impacted population are statistically significant in determining grant award amount. The Exposure rotated component explains 17% of the variance. It is loaded by dissipation latitude of the derecho and the percentage of people living below the poverty line. The loading of this component shows that grant award amounts are statistically likely to be higher when the dissipation latitude is lower. This relationship

has two possible explanations. First, these derechos could have longer path lengths because they dissipate further south. In this situation, the exposure is higher and there is a similar relationship to that shown in the Size rotated component. Another explanation is that the derechos that impact the lower latitudes are also impacting more vulnerable populations. This rotated component likely addresses both of these possible explanations. However, the Exposure rotated component is also loaded heavily by percentage below the poverty line showing that poorer communities receive higher grant award amounts, and thus indicating that those derechos that dissipate at lower latitudes are likely impacting more vulnerable populations.

The fifth rotated component, Socioeconomics, is loaded heavily by socioeconomic status variables from the SVI. The Socioeconomic rotated component explains 17% of the variation in the data. The Socioeconomic rotated component is heavily loaded by the overall SVI ranking, which is inclusive of all sub-category variables identified in the CDC SVI: Socioeconomic Status, Household Composition and Disability, Minority Status and Language, and Housing and Transportation. Thus, this rotated component represents the overall impact of the socioeconomic factors on FEMA PA grant award amounts.

Discussion

This research demonstrates that FEMA PA grant award amounts for straight-line wind damage accompanying Northern Tier states' derechos can be predicted to a high degree of confidence (i.e., statistical significance) through spatial modeling of a number of atmospheric and socio-economic variables. The results, above, confirm that FEMA PA

grant award amounts are closely tied to the number of counties impacted by a derecho and the socioeconomic status of these affected counties (explains 92% of the variance, backward stepwise regression model). This significant association is logical because when a derecho impacts many counties more infrastructure is destroyed and more local governments and counties become involved with response and recovery efforts. Likewise, more counties apply for federal assistance in the form of FEMA PA grants and more are likely to be awarded the necessary funding. The socioeconomic status of the affected population is also important because more socially vulnerable counties will require greater financial assistance from FEMA PA grants for recovery and rebuilding of public resources. Moreover, the community infrastructure may be more easily damaged due to antecedent state of disrepair or insufficient antecedent care in poorer communities. The PCA indicates that the socioeconomic status of communities explain 17% of the FEMA PA grant award variation. This result reinforces that it is necessary to account for social vulnerability when investigating meteorological disaster-related losses. It would be advisable to conduct similar research to analyze the spatial and statistical relationships between FEMA PA grant award amounts and social vulnerability for other storm types.

The multiple regression model is improved by introducing a spatial component; the goodness of fit of the GWR model, which increases the R^2 to 97%, means that introducing local variations of the grant award amounts and explanatory variables increases the model's ability to predict the FEMA PA grant award amounts. From the maps of GWR coefficients, the fact that the "number of counties" term has a higher coefficient where long-tracking derechos are likely to form means that more counties will be impacted by a derecho tracking from the northwest of the study area to the southeast;

therefore, more funding will be requested. The socioeconomic coefficient will have a larger influence on the dependent variable (FEMA PA grant award amounts) in areas where the number of counties term is lower. The implication of this result is that when fewer counties request FEMA grants and they are awarded amounts similar to those awarded to many counties, those fewer counties are likely to be highly socially vulnerable. Furthermore, if many counties are awarded low FEMA PA grant amounts they are likely to be less socially vulnerable. The results of the Varimax-rotated PCA showing that five factors explain most of the variance in the FEMA PA grant award amounts (i.e., temperature, living conditions, size of event, exposure, and socioeconomics) are reasonable because they support the idea that the areal impact of a derecho and the socioeconomics of those impacted by a derecho can predict the FEMA PA grant award amounts resulting from a derecho event. These analyses agree that the number of people impacted by a derecho and their social vulnerability are directly related to and can be a predictor of FEMA PA grant award amounts.

Conclusions

This research investigated the statistical relationships between FEMA PA grant award amounts given in response to derechos and potential explanatory variables such as social vulnerability. The number of counties that were impacted by the derecho and the overall percentile SVI ranking were shown to be directly and significantly related to the FEMA PA grant award amounts. These two variables fit the grant award amount data well with an adjusted $R^2 = 0.9202$ (backward stepwise regression). A GWR examined the data spatially and the model fit increased to an adjusted $R^2 = 0.974$, meaning that taking

spatial variations into account improved the model. Regression coefficient spatial surfaces show the number of counties term is highest in the north central and southeast parts of the study area and the social vulnerability term is highest near the boundaries of Wisconsin, Minnesota, and Iowa. In addition, the spatial variation of the success of the model in predicting the FEMA PA grant award amounts over space (standardized residuals and local R^2 fields) indicate the model performs well across the study region except in southern Michigan and northern Indiana. A Varimax-rotated PCA identified combinations of variables that explain the variance in the data. Five components in descending order of importance—temperature, living conditions of the impacted populations, derecho major axis, population exposure, and socioeconomic status of the affected population—explain most of the variation in the FEMA PA grant award amounts. These results show that FEMA PA grant award amounts for derechos can be well-predicted using information on the number of counties impacted and social vulnerability of the affected populations, with additional variance explained by mitigating physical and social factors such as temperature and mobile home housing. Temperature plays a dominant role in the PCA and it is likely related to higher temperatures being associated with larger storms which thus impact a broader area (and likely more counties).

This work provides a basis for analyzing derecho impacts and FEMA PA grant awards for derecho events. Future work can be done to further explore what types of damage result from derechos and how much funding is allocated to different categories of recovery. Further investigation into these topics will improve FEMA's ability to respond to derechos and predict potential funding requirements. These results could be used in

conjunction with a climatological study on derecho frequency and intensity to determine what months and years may require the most FEMA PA grant awards to serve communities impacted by damaging derechos on a year-to-year basis.

References

Ashley WS, Mote TL. 2005. Derecho Hazards in the United States. *Bulletin of the American Meteorological Society*, **86**(11): 1577–1592. doi:10.1175/BAMS-86-11-1577Atkinson CJ. 2010. *Spatial and Temporal Analysis of Extreme Midwestern Blizzard Storm Tracks and Subsequent Federal Disaster Declarations* (Doctoral dissertation, University of Kansas).

Bentley ML, Franks JR, Suranovic KR, Barbachem B, Cannon D, Cooper SR. 2016. Lightning characteristics of derecho producing mesoscale convective systems. *Meteorology and Atmospheric Physics*, **128**(3): 303-314.

Black AW, Ashley WS. 2011. The Relationship between Tornadic and Nontornadic Convective Wind Fatalities and Warnings. *Weather, Climate, and Society*, **3**(1): 31–47. doi:10.1175/2010WCAS1094.1

Boswell MR, Deyle RE, Smith RA, Baker EJ. 1999. A quantitative method for estimating probable public costs of hurricanes. *Environmental management*, **23**(3): 359-372.

Browne MJ, Hoyt RE. 2000. The demand for flood insurance: empirical evidence. *Journal of risk and uncertainty*, **20**(3): 291-306.

Brunsdon C, Fotheringham AS, Charlton ME. 1996. Geographically weighted regression: a method for exploring spatial nonstationarity. *Geographical analysis*, **28**(4): 281-298.

Brunsdon C, Fotheringham S, Charlton M. 1998. Geographically weighted regression. *Journal of the Royal Statistical Society: Series D (The Statistician)*, **47**(3): 431-443.

Burton CG. 2010. Social vulnerability and hurricane impact modeling. *Natural Hazards Review*, **11**(2): 58-68.

Cattell, RB. 1966. The scree test for the number of factors. *Multivariate Behavioral Research*, **1**(2): 245-276.

Changnon SA. 1972. Examples of economic losses, from hail in the United States. *Journal of Applied Meteorology*, **11**(7): 1128-1137.

Changnon SA, Changnon D. 1998. Record-high losses for weather disasters in the United States during the 1990s: How excessive and why?. *Natural Hazards*, **18**(3): 287-300.

Changnon SA, Changnon JM, Hewings GJ. 2001. Losses caused by weather and climate extremes: A national index for the United States. *Physical Geography*, **22**(1): 1-27.

Changnon SA, Fosse ER, Lecomte EL. 1999. Interactions between the atmospheric sciences and insurers in the United States. In *Weather and Climate Extremes*, **42**: 51-67.

Changnon SD. 2003. Measures of economic impacts of weather extremes: Getting better but far from what is needed—A call for action. *Bulletin of the American Meteorological Society*, **84**(9): 1231-1235.

CFR 44 Part 206 Subpart A – K. 2011. Code of Federal Regulations 44: Emergency Management and Assistance. CFR 44 § 206.1 – § 206.389.

Corfidi SF, Coniglio MC, Cohen AE, Mead CM. 2016. A proposed revision to the definition of "Derecho." *Bulletin of the American Meteorological Society*, **97**(6): 935–939.

Cutter SL, Boruff BJ, Shirley WL. 2003. Social vulnerability to environmental hazards. *Social science quarterly*, **84**(2): 242-261.

Cutter SL, Finch C. 2008. Temporal and spatial changes in social vulnerability to natural hazards. *Proceedings of the National Academy of Sciences,* **105**(7): 2301-2306.

Downton MW, Miller JZB, Pielke Jr RA. 2005. Reanalysis of US National Weather Service flood loss database. *Natural Hazards Review*, **6**(1): 13-22.

Downton MW, Pielke RA. 2005. How accurate are disaster loss data? The case of US flood damage. *Natural Hazards*, **35**(2): 211-228.

Dutta D, Herath S, Musiake K. 2003. A mathematical model for flood loss estimation. *Journal of hydrology*, **277**(1): 24-49.

Ebert A, Kerle N, Stein A. 2009. Urban social vulnerability assessment with physical proxies and spatial metrics derived from air-and spaceborne imagery and GIS data. *Natural hazards*, **48**(2): 275-294.

Federal Emergency Management Agency. 2016. *Publication 1*.

Felsenstein D, Lichter M. 2014. Social and economic vulnerability of coastal communities to sea-level rise and extreme flooding. *Natural hazards*, **71**(1): 463-491.

Fetter GM. 2010. *Improving Post-Disaster Recovery: Decision Support for Debris Disposal Operations* (Doctoral dissertation, Virginia Polytechnic Institute and State University).

Flanagan BE, Gregory EW, Hallisey EJ, Heitgerd JL, Lewis B. 2011. A social vulnerability index for disaster management. *Journal of Homeland Security and Emergency Management*, **8**(1).

Fleming MC. 2014. *Exploratory Study of Preliminary Damage Assessments in Northern Illinois* (Doctoral dissertation, Oklahoma State University).

Fotheringham AS, Brunsdon C, Charlton M. 2002. *Geographically weighted regression: the analysis of spatially varying relationships*. John Wiley & Sons.

Gaddis EB, Miles B, Morse S, Lewis D. 2007. Full-cost accounting of coastal disasters in the United States: Implications for planning and preparedness. *Ecological Economics*, **63**(2): 307-318.

Gall M, Borden KA, Cutter SL. 2009. When do losses count? Six fallacies of natural hazards loss data. *Bulletin of the American Meteorological Society*, **90**(6): 799-809.

Goodchild MF. 1986. *Spatial autocorrelation* (Vol. 47). Geo Books.

Harlan SL, Brazel AJ, Prashad L, Stefanov WL, Larsen L. 2006. Neighborhood microclimates and vulnerability to heat stress. *Social science & medicine*, **63**(11): 2847-2863.

Karl T, Koss WJ. 1984. *Regional and national monthly, seasonal, and annual temperature weighted by area, 1895-1983*. National Climatic Data Center.

Kumari M, Singh CK, Bakimchandra O, Basistha A. 2017. Geographically weighted regression based quantification of rainfall–topography relationship and rainfall gradient in Central Himalayas. *International Journal of Climatology*, **37**: 1299–1309.

Kunkel KE, Pielke Jr RA, Changnon SA. 1999. Temporal fluctuations in weather and climate extremes that cause economic and human health impacts: A review. *Bulletin of the American Meteorological Society*, **80**(6): 1077-1098.

Lv A, Zhou L. 2016. A Rainfall Model Based on a Geographically Weighted Regression Algorithm for Rainfall Estimations over the Arid Qaidam Basin in China. *Remote Sensing*, **8**(4): 311.

Malmstadt J, Scheitlin K, Elsner J. 2009. Florida hurricanes and damage costs. *Southeastern Geographer*, **49**(2): 108-131.

Masozera M, Bailey M, Kerchner C. 2007. Distribution of impacts of natural disasters across income groups: A case study of New Orleans. *Ecological Economics*, **63**(2): 299-306.

Mesinger F, DiMego G, Kalnay E, Mitchell K, Shafran PC, Ebisuzaki W, ... & Ek MB. 2006. North American regional reanalysis. *Bulletin of the American Meteorological Society*, **87**(3): 343-360.

Mohleji S, Pielke Jr R. 2014. Reconciliation of trends in global and regional economic losses from weather events: 1980–2008. *Natural Hazards Review*, **15**(4): 04014009.

Neumayer E, Barthel F. 2011. Normalizing economic loss from natural disasters: a global analysis. *Global Environmental Change*, **21**(1): 13-24.

Ninyerola M, Pons X, Roure JM. 2000. A methodological approach of climatological modelling of air temperature and precipitation through GIS techniques. *International Journal of Climatology*, **20**(14): 1823-1841.

NOAA/NWS Storm Prediction Center. Retrieved from http://www.spc.noaa.gov/

Noble E. 2004. An improved technique for understanding damage from floods. SOARS: Significant Opportunities for Atmospheric Research.

Pan Q. 2011. Economic losses from a hypothetical hurricane event in the Houston-Galveston area. *Natural Hazards Review*, **12**(3): 146-155.

Pan Q. 2014. Estimating the economic losses of Hurricane Ike in the Greater Houston Region. *Natural Hazards Review*, **16**(1): 05014003.

Pielke Jr RA, Downton MW. 2000. Precipitation and damaging floods: trends in the United States, 1932–97. *Journal of Climate*, **13**(20): 3625-3637.

Pielke RA, Downton MW, Miller JB. 2002. *Flood damage in the United States, 1926-2000: a reanalysis of National Weather Service estimates*. Boulder, CO: University Corporation for Atmospheric Research.

Pielke Jr RA, Gratz J, Landsea CW, Collins D, Saunders MA, Musulin R. 2008. Normalized hurricane damage in the United States: 1900–2005. *Natural Hazards Review*, **9**(1): 29-42.

Pielke Jr RA, Landsea CW. 1998. Normalized hurricane damages in the United States: 1925–95. *Weather and Forecasting*, **13**(3): 621-631.

Preston BL. 2013. Local path dependence of US socioeconomic exposure to climate extremes and the vulnerability commitment. *Global Environmental Change*, **23**(4): 719-732.

Richman, MB. 1986. Rotation of Principal Components. *International Journal of Climatology*, **6**: 293-335.

Scawthorn C, Blais N, Seligson H, Tate E, Mifflin E, Thomas W, ... & Jones C. 2006a. HAZUS-MH flood loss estimation methodology. I: Overview and flood hazard characterization. *Natural Hazards Review*, **7**(2): 60-71.

Scawthorn C, Flores P, Blais N, Seligson H, Tate E, Chang S, ... & Lawrence M. 2006b. HAZUS-MH flood loss estimation methodology. II. Damage and loss assessment. *Natural Hazards Review*, **7**(2): 72-81.

Schultz J, Elliott JR. 2013. Natural disasters and local demographic change in the United States. *Population and Environment*, **34**(3): 293-312.

Smith AB, Katz RW. 2013. US billion-dollar weather and climate disasters: data sources, trends, accuracy and biases. *Natural hazards*, **67**(2): 387-410.

Trapp RJ, Wheatley DM, Atkins NT, Przybylinski RW, Wolf R. 2006. Buyer beware: Some words of caution on the use of severe wind reports in postevent assessment and research. *Weather and forecasting*, **21**(3): 408-415.

Visser H, Petersen AC, Ligtvoet W. 2014. On the relation between weather-related disaster impacts, vulnerability and climate change. *Climatic Change*, **125**(3-4): 461-477.

Vose RS, Applequist S, Squires M, Durre I, Menne MJ, Williams Jr CN, ... & Arndt D. 2014. Improved historical temperature and precipitation time series for US climate divisions. *Journal of Applied Meteorology and Climatology*, **53**(5): 1232-1251.

Watson Jr CC, Johnson ME. 2004. Hurricane loss estimation models: Opportunities for improving the state of the art. *Bulletin of the American Meteorological Society*, **85**(11): 1713-1726.

Watts JD, Kalkstein LS. 2004. The development of a warm-weather relative stress index for environmental applications. *Journal of Applied Meteorology*, **43**(3): 503-513.

White D, Richman M, Yarnal B. 1991. Climate regionalization and rotation of principal components. *International Journal of Climatology*, **11**(1): 1-25.

Zhu Q, Chen X, Yang H, Huang Z. 2007. A mathematical model for flood loss estimation based on grid [J]. *Engineering Journal of Wuhan University*, **6**: 009.

Tables And Figures

Table 3-1. Number of deaths caused by derechos, hurricanes, and F0 and F1 tornadoes. Modified from Ashley and Mote (2005), their Table 3.

Year	*Derechos*	*Hurricanes*	*F0 and F1 tornadoes*
1986	6	8	0
1987	8	0	2
1988	0	4	3
1989	13	37	9
1990	7	0	2
1991	6	15	8
1992	2	23	3
1993	2	3	6
1994	6	8	2
1995	18	23	3
1996	11	48	3
1997	13	2	7
1998	21	5	2
1999	14	60	6
2000	10	1	1
2001	9	0	5
2002	6	0	6
2003	1	17	3
Total	*153*	*254*	*71*

Table 3-2. Costliest hurricanes and derechos 1986 – 2003. (Adapted from Ashley and Mote (2005), their Table 5).

Storm	Cost (in millions)	Year
Andrew	18,985	1992
Hugo	3,993	1989
Opal	2,411	1995
Floyd	2,117	1999
Fran	1,803	1996
Isabel	1,685	2003
Georges	1,264	1998
Bob	766	1991
Lili	437	2002
May 31 derecho	432	1998
Erin	431	1995
Bonnie	394	1998
September 7 derechos	252	1998
June 4 – 6 derechos	191	1998
May 4 derecho	180	1989
February 16 derecho	176	2001
April 26 derecho	162	1999
Bertha	152	1996
March 9 derechos	137	2002
Irene	108	1999

Table 3-3. Varimax-rotated PCA rotated principal components, loadings, and percent variance explained.

Rotated Component	Loading Variables	Variance Explained
Temperature	Local Temperature	25%
Living Conditions	Minority Status, Household Composition, Mobile Home Units	22%
Size	Derecho Major Axis Length	19%
Exposure	Derecho Dissipation Latitude, Percent Living Below Poverty Line	17%
Socioeconomics	SVI Socioeconomic Theme, Overall SVI Ranking	17%

Figure 3-1. Histogram of standardized residuals from the backward stepwise regression analysis. The graph shows a normal distribution of the standardized residuals implying the model is not biased; therefore, that the data are independent.

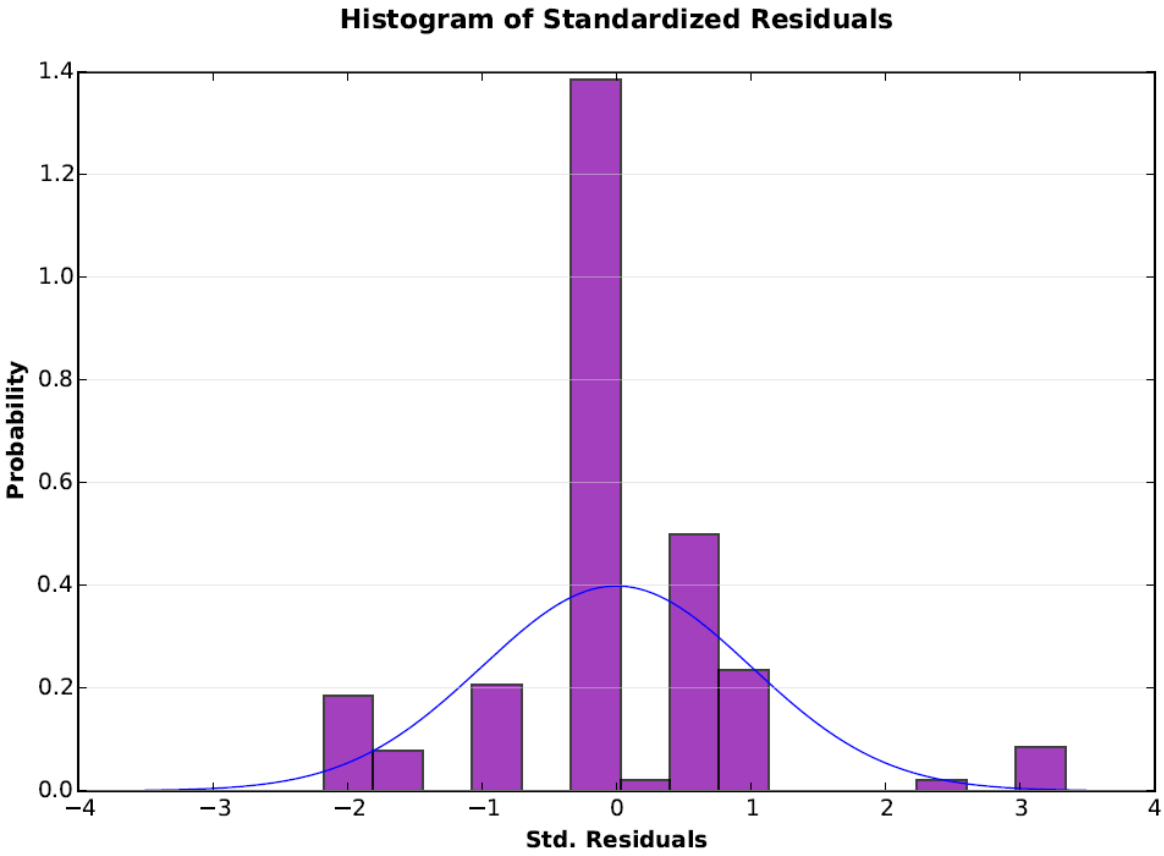

Figure 3-2a. Mapped GWR coefficients for the "number of impacted counties" term.

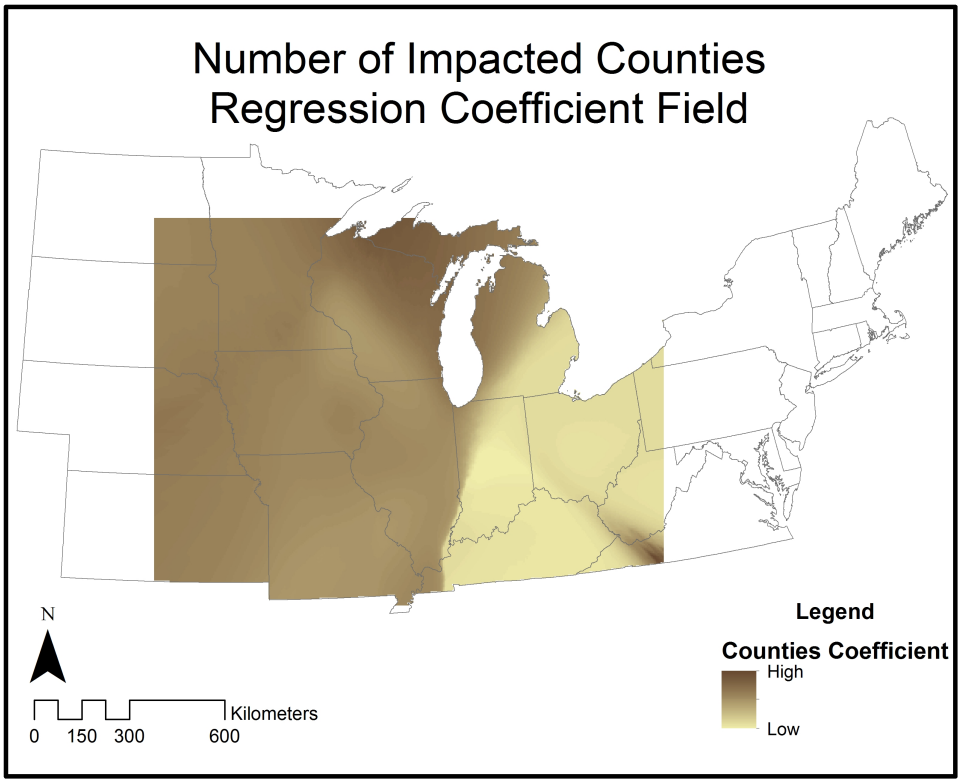

Figure 3-2b. Mapped GWR coefficients for the overall percentile SVI ranking term.

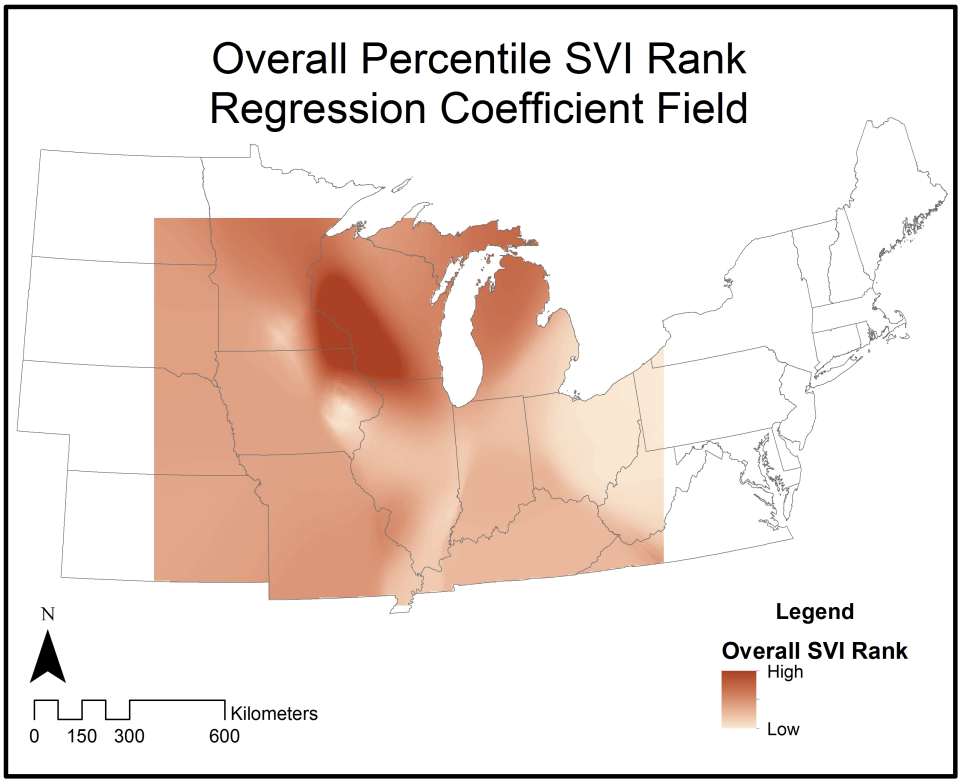

Figure 3-2c. Mapped GWR intercept values.

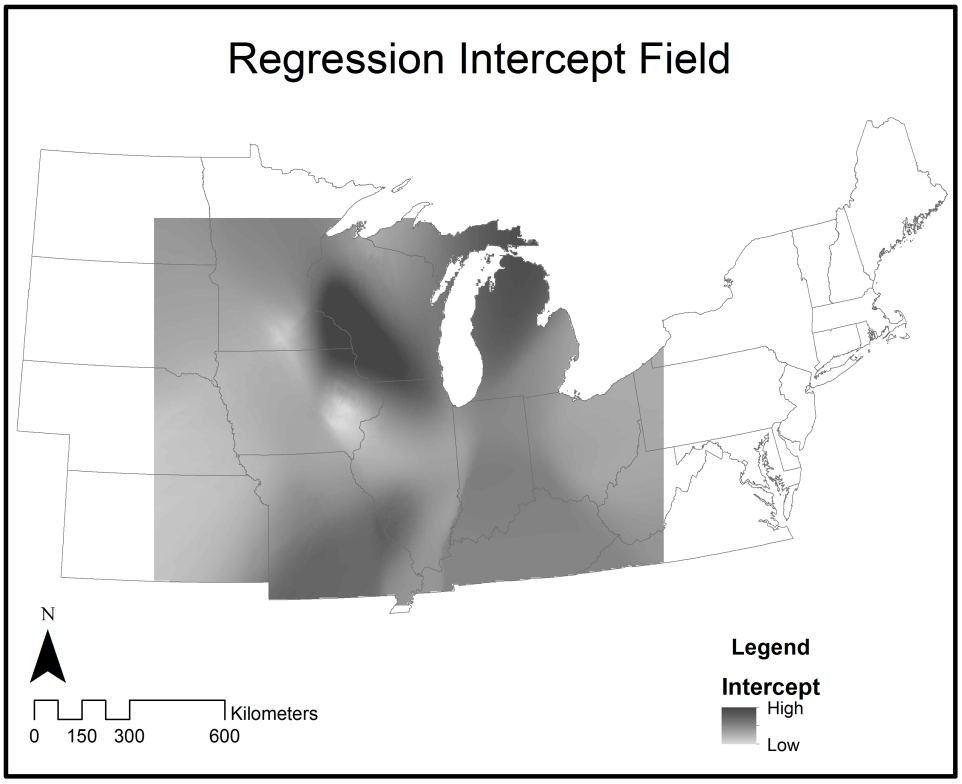

Figure 3-3. GWR standardized residuals mapped across the study area show that the model generally fits well, with some areas of over-prediction (red) and some areas of under-prediction (blue). Each blue and red category represents one standard deviation from the center (yellow).

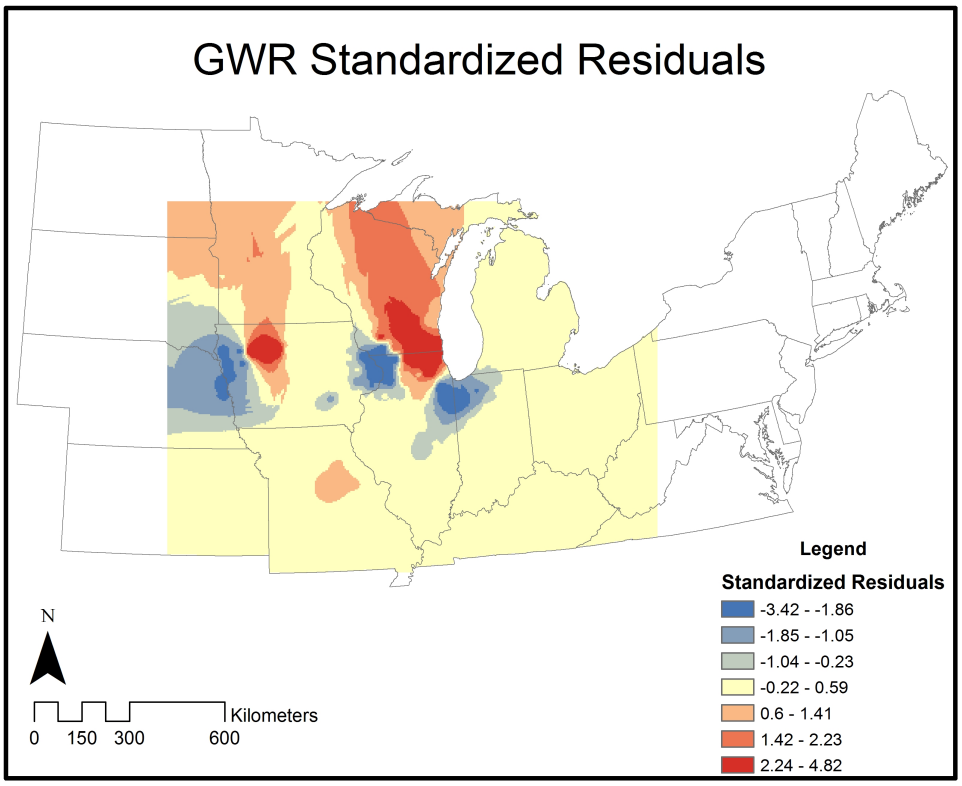

Figure 3-4. Results of Moran's I test on the backward stepwise regression residuals. The results show that the data are random and thus not spatially autocorrelated; therefore, the model is not biased with collinear inputs.

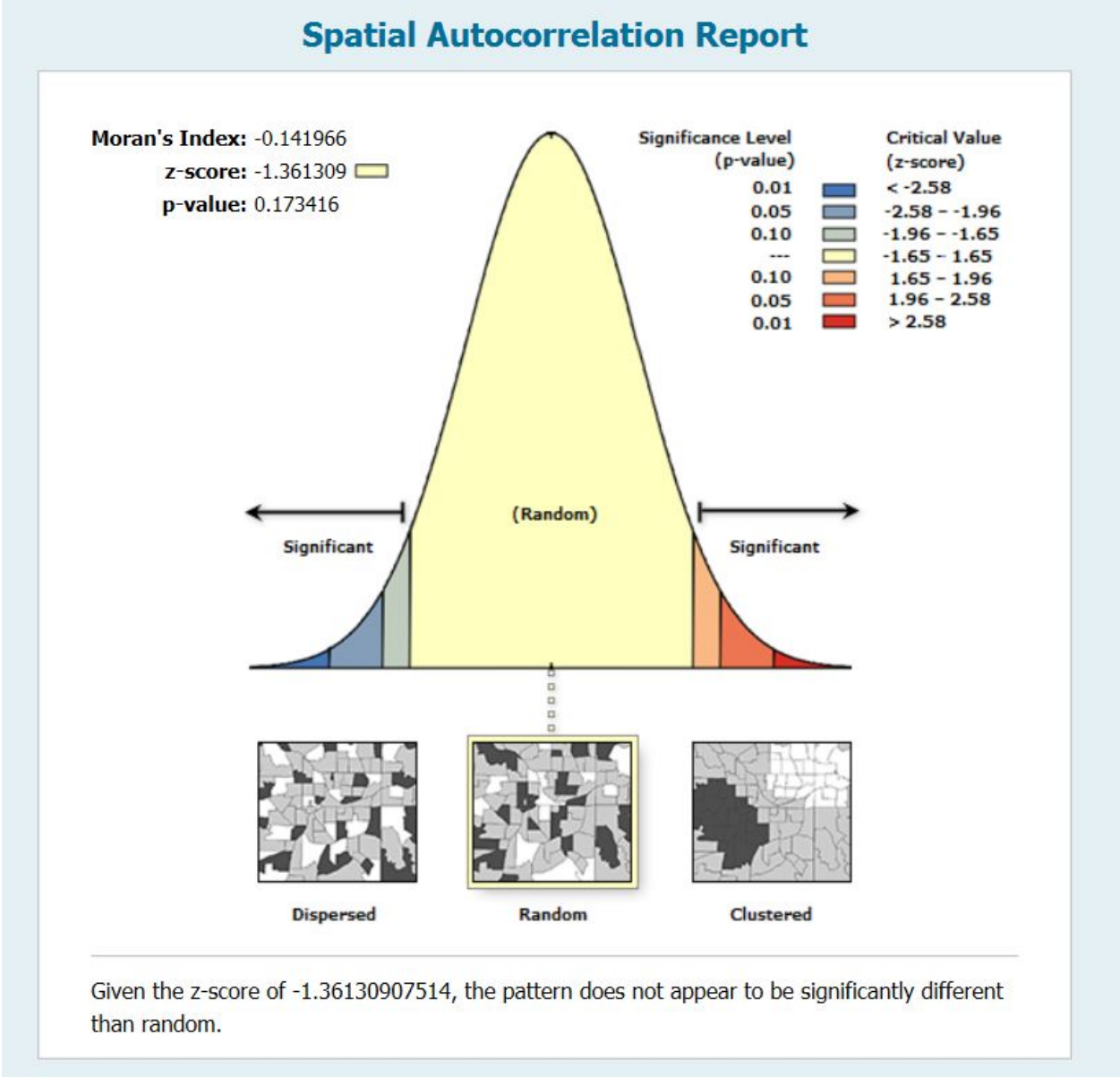

Figure 3-5. Mapped local R^2 values from the GWR model.

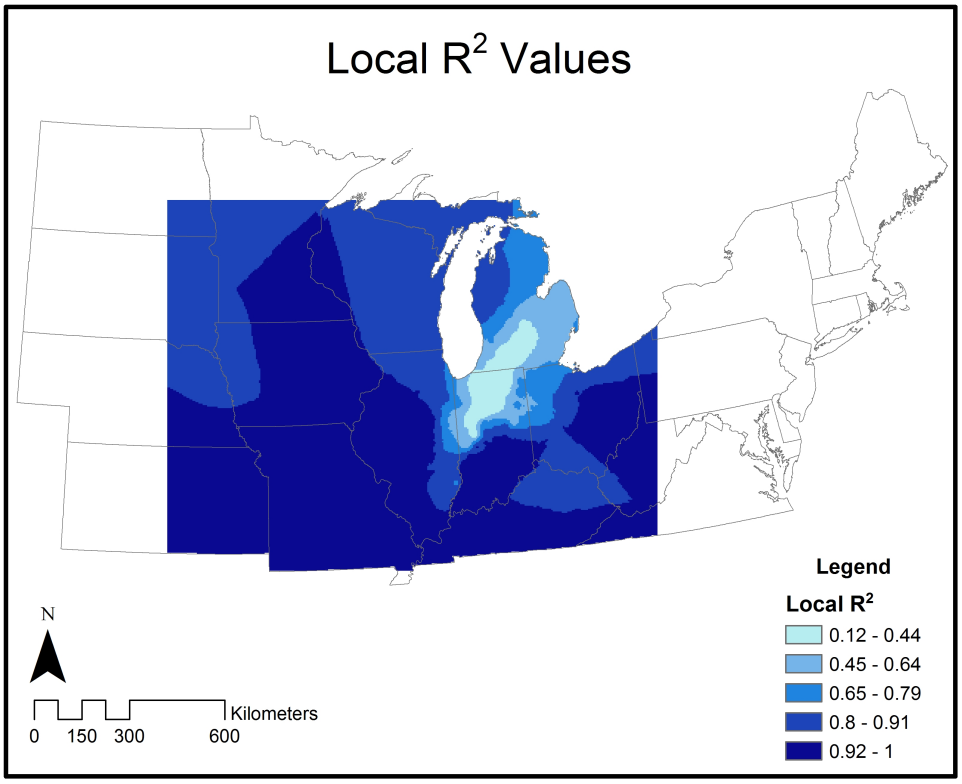

Figure 3-6. Screeplot showing explained variances by rotated PCA component (refer text).

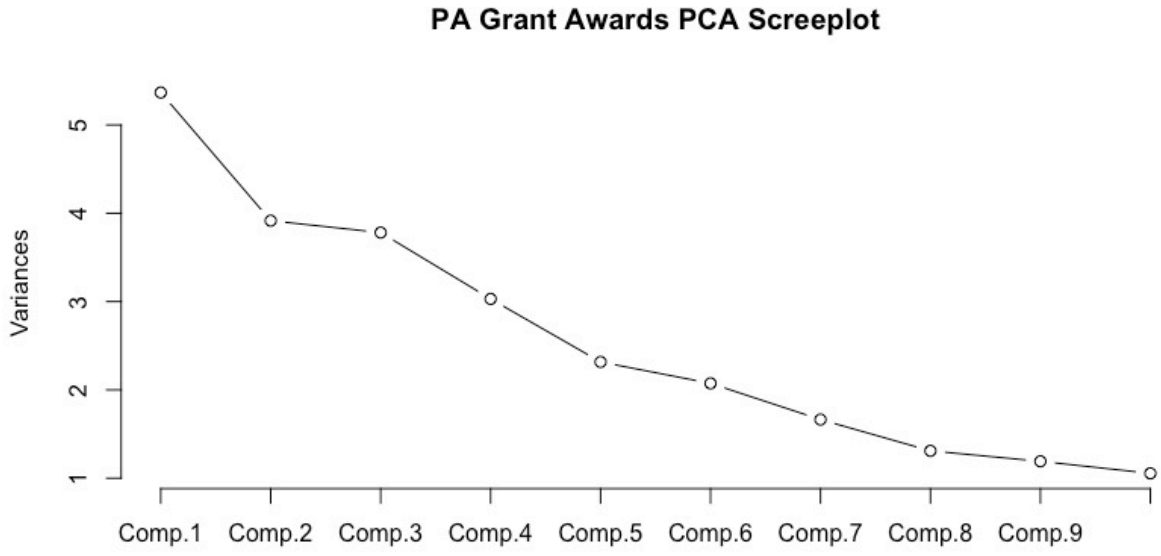

CHAPTER 4

IMPROVING EMERGENCY MANAGEMENT RESPONSE TO DERECHOS VIA THE CREATION AND APPLICATION OF A DERECHO IMPACT SCALE AND GIS TOOL

Abstract

This chapter addresses the emergency management responses to derechos through the generation of a derecho impact scale and a recommended process for a GIS tool that visualizes emergency management resource access. Many types of severe weather events have been categorized in terms of their intensity; two widely used examples of such meteorological impact scales are those for tornadoes—the Enhanced Fujita scale—and hurricanes, the Saffir-Simpson scale. However, these impact scales do not account for the storm direct impacts on populations and do not address certain physical aspects of the storms they categorize, such as size (which is a determining factor in the number of people it impacts). Conversely, the Northeast Snowfall Impact Scale (NESIS) includes both the physical characteristics and human impacts of Northeast snowstorms. Thus, the present research uses NESIS as a model to develop a derecho impact scale for Northern Tier States derecho events called the Derecho Wind-Area-Society (DEWARS) Impact Scale. To further facilitate the emergency management responses to derechos, a GIS tool is developed that aids decision-making by effectively and efficiently mapping emergency management resource access immediately following the storm. As demonstrated in a case study, incorporating the DEWARS impact scale in this GIS tool is recommended for use by FEMA.

Keywords: derecho, impact scale, derecho categories, population impacts, DEWARS impact scale.

Introduction and Background

The present research aims to aid the emergency management responses to Northern Tier States summer derecho events. This chapter expands on the research presented earlier in this dissertation by presenting an impact-based derecho scale for Northern Tier summer derechos designed to inform emergency management decisions. An emergency management GIS tool that will aid derecho emergency response activities is also developed and applied to a case study. A framework for developing this tool is also presented based on calls for this type of decision-support tool in the emergency management literature (Meade and Abbott, 2003; Morss and Ralph, 2007). This chapter is organized as follows: The first section provides a review of the literature relevant to severe weather event impact scales and the importance of integrating social and physical variables in emergency management decision support systems (DSSs). Next is a discussion of the data and methods used to create the derecho impact scale. Following, the results of applying the impact scale to Northern Tier derecho events are discussed. Then, the GIS emergency management tool that can be used alongside the impact scale is described. Finally, a conclusion that summarizes the work is presented.

a. Meteorological Impact Scales and Categorization of Severe Weather Events

Emergency managers use disaster impact scales to aid in real-time emergency management decision-making. However, these impact scales have been developed by meteorologists and engineers. Meteorological impact scales such as the Enhanced Fujita (EF) tornado scale (Fujita, 1971) and the Saffir-Simpson hurricane scale (Simpson and Saffir, 1974; Saffir, 1977) empower decision-makers by providing a description of the

impacts of tornadoes and hurricanes and grouping events of similar magnitude into categories based on the potential of the storm to cause damage to different types of structures. By enabling comparisons to previous severe weather events in the same category, impact scales can inform senior leaders' decisions on distributing emergency resources and allocating recovery funding (Xu and Brown, 2008; Li and Jin, 2010; Tate *et al.*, 2010). Although general in scope, these scales permit quick evaluation of potential storm impacts and facilitate effective responses by providing emergency managers a relative impact of the disaster. Often, emergency managers must make critical decisions in real time based on limited information and complex meteorological data which can be difficult to reconcile and interpret owing to lack of understanding of meteorological processes (Pielke and Carbone, 2002; Baumgart *et al.*, 2006; White and Turoff, 2012). Thus, reduction and amalgamation of these data in order to improve understanding of forecasts is commonplace in emergency response situations. Emergency managers use tools such as general principles and guiding frameworks to guide decision-making based on complex information and situations (Meade and Abbott, 2003; Morss *et al.*, 2008). Using impact scales to inform decisions provides a general understanding of the range of societal impacts from which estimates of required emergency support can be made.

Categorizing the impacts of severe storms on society has been undertaken extensively since sailors started monitoring wind speeds affecting their ships. Accordingly, the Beaufort scale was developed based on rudimentary experiments that related wind speeds to their effects on ship sails (Meaden *et al.*, 2007). Tornado impact scales were first developed in the late 1800s when Hazen (1890) suggested a tornado scale based on economic losses. Although this early tornado impact scale focused on

human impacts, few meteorological impact scales developed since have incorporated the human component. Fujita (1971) created a tornado impact scale that relied on damage assessments to estimate wind speeds. Post-event damage assessments are required to categorize a storm on the Fujita scale and it was subsequently suggested that its categories needed further refinement (Forbes and Wakimoto, 1983; Doswell and Burgess, 1988; Doswell, 2003; Edwards *et al.*, 2013). Meaden (1975) proposed a tornado impact scale called the TORRO scale or T-Scale that ranked tornadoes based only on wind speed, but it is disfavored in comparison to Fujita's scale. The Beaufort scale, Fujita scale, and T-Scale can be used to rate tornado intensity, but each impact scale emphasizes wind speed and does not address economic losses or human impacts (Meaden *et al.*, 2007). The EF scale updates the Fujita scale to make it more relevant to current U.S. structures and more easily related to specific types of damage to newer building materials (Potter, 2007; Doswell *et al.*, 2009). Tornado frequencies, path widths, and seasonal variations have been associated with specific EF scale categories in studies that show high numbers of small tornadoes in low EF rankings and low frequencies of large tornadoes in high EF rankings (Fujita, 1973; Brooks and Doswell, 2001; Dotzek *et al.*, 2003; Brooks, 2004; Feuerstein *et al.*, 2005; Edwards *et al.*, 2013). Currently, the EF scale is the standard tornado impact scale for emergency managers even though research shows emergency managers have difficulty interpreting wind speed data to inform their decisions (Baumgart *et al.*, 2006).

Like tornadoes, hurricanes also have been categorized based on their meteorological impacts. The Saffir-Simpson scale assesses a hurricane's potential impact based on sustained wind speeds and was implemented to advise officials on the damage a

hurricane could cause (Simpson and Saffir, 1974; Saffir, 1977). Categorizing hurricanes has enabled researchers to further investigate hurricane hazards and clarify the wind impacts of hurricanes on both human and physical landscapes (Dvorak, 1975; Sallenger, 2000; Webster *et al.*, 2005; Senkbeil and Sheridan, 2006; Irish *et al.*, 2008; Irish and Resio, 2009). However, the Saffir-Simpson scale has been criticized for its discrete ranges of wind speed associated with each intensity category, its highest category containing too many events to represent the relative infrequency of these high-intensity hurricanes, and its lack of accounting for differences in rainfall rates and storm surge height and its inland extent (Mahendran, 1998; Kantha, 2006). Alternative scales have been created to describe hurricane impacts on populations and coastlines that address some of the shortcomings with the Saffir-Simpson scale. Kantha (2006) recommended adding metrics, or standards for evaluating storm intensity, to the Saffir-Simpson scale that incorporate hurricane rainfall, flood damage, and storm surge height. Likewise, Jordan and Clayson (2008) found including surge height improves the hurricane impact scale. Likewise, Irish and Resio (2009) suggested a hydrodynamically based impact scale for hurricanes that includes storm surge height and physical attributes related to hydrodynamics of the storm such as regional bathymetry. In addition, many of these alternative scales attempt to take into account that the number and frequency of high-ranking hurricanes are projected to increase under climate change (Emmanuel, 2005; Webster *et al.*, 2005). With increasing number and frequency, hurricane categorization that incorporates all potential impacts is critical to successful emergency response. Powell and Reinhold (2007) propose an impact scale that estimates hurricane destruction potential on human environments through modeling and comparing storm-associated

energy. Other researchers emphasize the need to have different scales for hurricanes that make landfall as opposed to those that remain at sea or those that may make landfall in places that are particularly vulnerable in terms of coastal development and population density (Sallenger, 2000; Senkbeil and Sheridan, 2006). Although many researchers argue for modifications of the Saffir-Simpson scale to improve its application to disaster management, emergency managers use it as the standard hurricane impact scale. Thus, lessons learned from developing and refining hurricane impacts scales can be applied to the development of a derecho impact scale.

Although it would be convenient to copy the EF scale and Saffir-Simpson scale processes to create a derecho impact scale, there are insufficient derecho damage assessments to support this method. In addition, these scales have been criticized for not accounting for important variables that relate to human impacts such as the density of the population impacted and the population's vulnerability to meteorological disasters (Kantha, 2006; Potter 2007). Moreover, research shows it is challenging for emergency managers to use severe weather wind speeds to inform their decisions because it is not usual practice for them to convert wind speeds into human impacts which may include flooded homes and downed power lines. Thus, the present study seeks to show that derechos can be categorized using an impact scale that incorporates their wind speed, but that also emphasizes their size (i.e., the total area over which they track from initiation to dissipation) and influence on societies of various sizes and vulnerabilities. The scale will also follow the Magnitude-Frequency relationship that holds that severe weather events that have uncharacteristically large impacts and occur less frequently and those that have lesser impacts and occur more frequently.

Development of a derecho impact scale can incorporate certain characteristics of another severe weather event that impacts human and physical landscapes, the snowstorm. Call (2005) argues that snowstorms must be analyzed in the context of their effects on daily life interruptions. Snowstorm impacts on transportation, fatalities, and business and education operations have been categorized regionally (i.e., across several states) and locally (i.e., in towns and cities) using classification scales similar to the EF and Saffir-Simpson scales (Zielinski, 2002). Cluster analysis has driven the categorization of storms that have wide impacts, and researchers show that similar events can be grouped by their meteorological properties into a five-category impact scale (Dolan and Davis, 1992). Additional research has incorporated the presence and vulnerability of affected populations, climatological normals, and antecedent weather events into a description of a snowstorm's physical and social impacts (Hart and Grumm, 2001; Cerruti and Decker, 2011; Mayes Boustead *et al.*, 2015). The ranking of Northeast snowstorms according to their severity that has served as a model for ranking snowstorms in other regions is the Northeast snowfall impact scale (NESIS). NESIS incorporates both storm extent and human effects, defined as the population affected by the storm at different intensities (Kocin and Uccellini, 2004; Squires and Lawrimore, 2006; Squires *et al.*, 2014). The NESIS equation is:

$$\text{NESIS} = \sum_{n}^{X} [n(\frac{A_n}{A_{\text{mean}}} + \frac{P_n}{P_{\text{mean}}})],$$

where n is snow accumulation over an area, A_n represents the area where snow accumulations are greater than n, and A_{mean} is the mean area of snow accumulation above 10 inches in a 30-event sample. P_n represents the total population living in areas with snow accumulation and P_{mean} refers to the average population size computed from a 30-

event sample living within areas of snow accumulation greater than 10 inches (Kocin and Uccellini, 2004). The framework used to develop the NESIS serves as a model for the present research which takes into account storm and population attributes. The impact scale defined by the NESIS equation and subsequent classification scheme put forth by Kocin and Uccellini (2004) identifies variables that are needed to define impacts of snowstorms that closely align with those that are also needed to analyze the impact of derechos. Thus, to improve the emergency management of derechos, this research develops a derecho impact scale similar to the NESIS and analyzes classification methods to statistically find groups that appropriately categorize the human impacts of derechos.

b. Integrating Physical and Social Variables in a GIS to Aid Emergency Management Decision Support

Geographic Information Systems (GISs) are used in meteorological applications and emergency management procedures, and include both planning and response. Although the use of mapping products and tools is commonplace in these fields, there is little cross-disciplinary research, development, and implementation of GIS technology (Riad *et al.*, 1999; Meade and Abbott, 2003). Moreover, emergency management could be improved with deeper integration of meteorological concepts and social vulnerability, or the ability of a population to respond to, recover from, and adjust to a disaster (Morrow, 1999; Riad *et al.*, 1999; Cutter *et al.*, 2003; Cutter and Finch, 2008; Flanagan *et al.*, 2011), in their DSSs (Subramaniam and Kerpedjiev, 1998; Golden and Adams, 2000; Meade and Abbott, 2003; Morss *et al.*, 2008). Tools that incorporate weather data and decision support methodologies are underdeveloped, not used broadly, and many are out

of date (Subramaniam and Kerpedjiev, 1998; Golden and Adams, 2000; Han and Liu, 2008; Zhao *et al.*, 2009). Researchers and government agencies call for further DSS development, enhanced meteorological data and forecasts, and improved cross-disciplinary applications (Meade and Abbott, 2003; Morss *et al.*, 2008). Advancement toward simplifying meteorological outputs for interpretation by emergency managers will greatly improve emergency response capabilities, and aid life-saving efforts (Morss and Ralph, 2007).

As indicated above, social vulnerability also needs to be accounted for in conceptual models that aid emergency management decisions. Based on interviews, Morss and Ralph (2007) observed that emergency managers tend to use local knowledge of social vulnerability, however it is situational and based on individual perceptions. Social vulnerability research is vast and the scope of the present research does not permit a detailed comparison of social vulnerability indices. However, some general comments are appropriate. Social vulnerability varies across space and time, but can be defined using indices that depict the resilience of a population, or their ability to recover from, and adaptive capacity, or the ability of a population to adjust to, a disaster (Cutter *et al.*, 2003; Smit and Wandel, 2006; Cutter and Finch, 2008; Fekete *et al.*, 2010; Flanagan *et al.*, 2011). These factors are particularly important to consider within the context of climate change because populations will face new and different intensities and frequencies of hazards and disasters (Smit and Wandel, 2006; McLaughlin and Dietz, 2008). Social vulnerability indices and markers (e.g., number of mobile home units, population age) should be used with real-time meteorological data for emergency managers to improve the effectiveness of their operations (Cutter *et al*., 2003; Cutter and

Finch, 2008; Morss *et al.*, 2008, Morss *et al.*, 2011). The nexus of these fields—meteorology, social vulnerability, and emergency management—is a relatively new interdisciplinary area in which further research and GIS development could directly improve emergency planning and response, an aim of this study. Another aim of the present research is to develop and apply an emergency management GIS tool that visualizes access to emergency management resources such as first responders and disaster recovery centers.

Meteorological forecasts, data, and research have greatly developed since the 1970s (Golden and Adams, 2000), however integration of these data and techniques such as probabilistic (as opposed to static deterministic) warnings into usable DSSs has lagged (Meade and Abbott, 2003). Regardless, situational awareness of and planning for potential meteorological disasters is a daily activity at the U.S. federal, state, and local levels. In the wake of a meteorological disaster, monetary and operational losses are difficult to measure, particularly when the definition of disaster impacts is unclear (Changnon, 2003; Doswell *et al.*, 2006). Social vulnerability is a confounding factor in identifying loss and recovery needs including funding amounts that takes into account the at risk population and socioeconomic status of communities (Riebsame *et al.*, 1986; Changnon, 2003; IPCC, 2013). Moreover, research shows that climate change will likely enhance severe weather intensity and frequency (IPCC, 2013). Although scientists generally agree on the role of climate change in amplifying severe weather frequency and intensity, uncertainty varies with severe weather type. Climate change impacts on severe weather will differentially impact communities across spatial and temporal scales (Kunkel *et al.*, 1999; Greenough *et al.*, 2001; Choi and Fisher, 2003). This spatiotemporal

variability compounds difficulties of analyzing socioeconomic loss that are pertinent to improving emergency management responses to severe weather disasters. Using a GIS would likely improve understanding of the geographic variations of severe weather impacts.

The social vulnerability of populations is often omitted from meteorological research and is not always used in emergency management response operations. Often it is not a lack of information that leads to mismanagement, but too much information in a format that is too detailed for interpretation by non-meteorologists (Liu *et al.*, 1996; Baumgart *et al.*, 2006, White and Turoff, 2012). Qualitative research has been done to understand the community-based component of preparing for meteorological disasters (Penning-Roswell and Wilson, 2006; Kapucu, 2008). Although these studies emphasize the importance of community awareness, they similarly highlight the necessity of comprehensible meteorological information for appropriate preparation.

The integration of updated meteorological products with emergency management decision structures, the frameworks that guide emergency management decisions, will improve emergency responses. Currently, emergency management operating procedures and policies are not consistently updated to incorporate meteorological advancements. Pielke and Carbone (2002) highlight that emergency management decision-makers do not use meteorological information productively because they often do not understand forecasts. Likewise, Morss *et al.* (2008) argue that forecasts are not effective without considering the impacts of the forecasted weather on society. The synthesis of meteorological data, information on the socioeconomic contexts of affected populations, and emergency management decision structures are required for effective severe weather

disaster response and planning. Although the desire to collaborate is emphasized by government research agenda advisors, there are very few funded projects that incorporate social vulnerability and DSSs like GIS map products (Meade and Abbott, 2003).

It is expected that climate change will continue to change the intensity and frequency of severe weather events (IPCC, 2013). The social vulnerability literature, however, is still lagging on identifying the most appropriate approach to analyzing vulnerability to meteorological disasters with respect to climate change because variables like urban development and adaptive capacity are fluid (Thomalla *et al.*, 2006; Fussel, 2007; Ionescu *et al.*, 2009). The exposure of a population to hazards is often left out of analyses of vulnerability and emergency response (Comfort *et al.*, 1999). Confounding these difficulties is the inherent disagreement as to how vulnerability research should be conducted and interpreted, as often, studies fail to take into account the scale of a population (i.e., local vs. national) and how important specific vulnerability markers may be within that population (Hinkel, 2011).

The three distinct research areas discussed above (meteorology, emergency management, and vulnerability) require collaboration by researchers at this nexus and collaboration with GIS developers (Demuth *et al.*, 2007; Morss *et al.*, 2008). The tool presented in this paper aims to marry meteorology, emergency management, and vulnerability in a DSS that supports emergency management decision-making after a derecho.

Data

The derecho dataset used in the previous chapters is also used herein. That dataset contains 56 summer-season (JJA) Northern Tier States events for the period 2000-2014, identified using NOAA Storm Prediction Center (SPC) high wind reports, in conjunction with remotely sensed imagery including NOAA NWS WSR-88D Level III radar images and visible and infrared satellite imagery. Derecho size was obtained through overlaying the radar and satellite images in a GIS and extracting the area that the storm affected, from initiation to dissipation. For purposes of describing derecho impact, data is also included on derecho physical properties, attributes of the impacted populations, and the derecho intensity metrics as discussed in the first chapter of this dissertation. Physical atmospheric properties of derecho environments such as Convective Available Potential Energy (CAPE), surface air temperature, and 300 hPa shear are obtained from National Centers for Environmental Prediction (NCEP) North American Regional Reanalysis (NARR) 3-hourly modeled data (Mesinger *et al.*, 2006). The SPC high wind reports, radar and satellite imagery, and physical atmospheric properties for Northern Tier summer derechos are used in GIS format for analysis with respect to Census American Community Survey (ACS) population data by Census tract.

ACS data are referenced for total population and population density, as well as in the social vulnerability index. These data are obtained for the geospatial and statistical analyses to be described below. The social vulnerability data are collected from the 2014 Centers for Disease Control and Prevention Agency for Toxic Substances and Disease Registry (CDC/ATSDR) Geospatial Research, Analysis & Services Program (GRASP) Social Vulnerability Index (SVI). Those data include a social vulnerability ranking, and indices that represent social vulnerability based on four summary categories including:

Socioeconomic Status, Household Composition and Disability, Minority Status and Language, and Housing and Transportation (Flanagan *et al.*, 2011). These categories incorporate vulnerability-related metrics including number of people below the poverty line, number of mobile homes, and number of children and elderly. The CDC SVI is designed particularly for emergency management use because it develops vulnerability metrics based on disaster risk and hazards, and is thus chosen for this investigation. Derecho impact metrics derived and analyzed in the first chapter of this dissertation are also used in the present research. These metrics include major axis length, minor axis length, rain rate, maximum wind speed and wind direction. Federal Emergency Management Agency (FEMA) Public Assistance (PA) grant award amount data are also used as an indicator of storm impact. All of these data have geographic attributes that can be spatially analyzed within a GIS, and include raw data that can be analyzed using traditional non-geospatial statistical methods such as multiple regression and cluster analyses. These methods are described below.

Methods

Regression and clustering methods are used to investigate associations among variables under consideration for a derecho impact scale. Relationships are analyzed between storm impact and physical atmospheric characteristics, including wind speed, which has been used in other meteorological disaster impact scales such as the EF Scale and Saffir-Simpson scale (see above). Derecho impacts and attributes of the impacted populations such as population density are also analyzed. Simple linear and multiple regressions identify relationships between derecho impacts and physical atmospheric

characteristics such as wind speed, pressure, and CAPE and population density and social vulnerability. Many combinations of variables are tested to determine their association to derecho impacts. Random forest regressions, a decision tree-based regression technique, are run to identify if any non-linear patterns exist that could describe and categorize derecho impacts. The random forest method is also used to rank the importance of independent variables such as wind speed, population density, and social vulnerability in explaining derecho impact. These regression techniques expose if a linear or non-linear relationship exists between explanatory variables such as wind speed and social vulnerability and derecho impact (Ho, 1998; Breiman, 2001; Liaw and Wiener, 2002; Criminisi *et al.*, 2012). Many combinations of variables are tested using regressions to identify if they collectively describe derecho impact.

Clustering methods are also used to generate derecho impact scales by grouping similar derechos into groups of three to five according to their associated meteorological and social variables. Through hierarchical clustering, *k*-means, and Self Organizing Maps (SOMs), the multidimensional derecho attributes are reduced to a more manageable set of clusters of similar events. The cluster members are then compared to derecho impacts by testing their statistical relationships to the intensity metrics discussed in the second chapter (maximum wind speed, associated rain totals, and minor and major axis/track length) to determine if the clusters accurately reflect derecho groups with similar intensities. Clusters of derecho events are created by reducing the entire multidimensional dataset of meteorological and social variables into groups using hierarchical and non-hierarchical methods such as hierarchical and *k*-means clustering. Hierarchical clustering segments the data into groups based on a distance matrix (Jain and Dubes, 1988).

Conversely, non-hierarchical *k*-means clustering partitions the multidimensional data into similar groups based on the closeness of the group means. The *k*-means method reduces within-group variance and identifies a centroid of the clusters to produce groups of similar items (MacQueen, 1967). Clustering is conducted on sets of specific physical atmospheric variables (e.g., CAPE, 300 hPa shear, pressure, and wind speed) and social variables (e.g., SVI, total impacted population, and number of mobile homes) to develop categorizations of derecho impact. As an alternative method, self-organizing maps (SOMs) are also employed to group the derechos into statistically similar categories by simplifying the multi-dimensional data into distinct nodes (Kohonen, 1982; Kohonen, 1998 Agarwal and Skupin, 2008).

As stated earlier, Kocin and Uccellini's (2004) NESIS equation is used as a basis for quantifying the impact of derechos in the Northern Tier. Derecho impacts are quantified by calculating a DEWARS value using the following equation modeled on the NESIS:

$$\text{DEWARS value} = \sum_{n}^{X} [n(\frac{A_n}{A_{\text{mean}}} + \frac{P_n}{P_{\text{mean}}})].$$

In this equation, *n* represents derecho wind speed. Four categories of wind speed are used to represent the frequency distribution of SPC high-wind reports; $n = 1$, $n = 4$, $n = 6$, and $n = 9$, which are calculated based on the frequency distribution of SPC high-wind reports for the derechos in this research. Following Kocin and Uccellini (2014), A_n is the area of high-wind reports that exceeds the minimum wind speed represented by *n*. A_{mean} is the average area covered by high-wind reports in category *n* in the sample of derechos. P_n is the population that lives within A_n and P_{mean} is the average population affected by high winds in category *n* calculated from the derechos in this study. Wind speed, derecho

spatial extent, duration, and impacted population comprise the variables that are used to calculate the DEWARS values for the 56 Northern Tier derecho events. DEWARS values are analyzed statistically and qualitatively to determine how well the derechos were ranked by their DEWARS value.

DEWARS values are then categorized using clustering and natural breaks to create the DEWARS impact scale. Jenks natural breaks and *k*-means clustering sort the derecho events into categories by optimization (natural breaks) and machine learning following techniques investigated by research that classifies convective weather events. Clusters can describe their similarities in intensity of derecho events (Gong and Richman, 1995; Tudurí and Ramis, 1997). To maintain similarity to other impact scales while accounting for the fact that only 56 events are available to be categorized, four and five categories of derecho events were tested to analyze which produced an impact scale comparable to NESIS categories 1 – 5, EF0 – EF5 tornadoes, and category 1 – 5 hurricanes. The classifications derived through natural breaks and clustering were correlated with FEMA PA grant award amounts to recommend the most appropriate impact categories for derechos that are statistically similar and relevant to emergency management-based impact scales.

Results and Discussion

Simple linear, multiple, and random forest regressions run on physical atmospheric derecho data (e.g., CAPE, 300 hPa shear, pressure) and affected population data did not yield statistically significant results that could be used to group derecho events according to their impacts. Although some individual attributes are found to be

significantly related to derecho intensity (e.g., a positive correlation exists between CAPE and derecho maximum wind speeds implying high winds are related to high instability), the correlations do not adequately describe the impact of the derechos. No combination of physical and social variables used in the simple linear and multiple regressions yields $R^2 > 0.4$. Similarly, using random forest regressions to find non-linear relationships among physical and social variables and derecho intensity yielded no statistically significant associations. Models have an error rate consistently over 50% and most combinations of variables are associated with a model error rate of greater than 65%. These results show that there is no direct linear relationship between derecho physical atmospheric variables (e.g., CAPE, temperature, pressure) and social variables (e.g., population, SVI, number of mobile homes) as measured by size of the derecho, associated wind speed, rain rates, major axis, minor axis, or direction. Although these relationships are not evident in this dataset, it is possible that more finely resolved spatial and temporal physical atmospheric and derecho intensity data may yield stronger relationships through regression modeling. Meteorological case studies of derechos may reveal what data are most important to analyze and at what scale. In addition, reducing the generalization of the physical atmospheric and social data, which is introduced when aggregating the information by Census tract, may reduce the model error. These recommendations are made for possible future study with additional and more finely resolved derecho-specific data and collaboration among sociologists and meteorologists. The results from the regression analyses conducted herein produce some isolated significant results, but have accompanying errors too high to be statistically significant.

Likewise, assembling derechos into groups of similar impact using clustering is not successful in fully describing the differences in their impacts. Three, four, and five clusters of derechos based on their impacts are created using hierarchical clustering and *k*-means clustering designed to groups items together, in this case derechos. Comparing the clusters to the derecho intensity metrics of major axis length, minor axis length, wind speed, associated rain totals, and direction (the intensity metrics used in Chapter 2) revealed no statistically significant, consistent relationships among the clusters in terms of derecho impacts. Although the clustering methods were qualitatively more successful than the regression techniques, in other words they successfully grouped particularly large and damaging (high-impact) derechos together, the clusters did not distinguish between moderate- and low-impact derechos (which would have progressively lesser impacts). Another drawback of the clustering results was that clusters often contained a similar number of derechos, which is undesirable because it does not follow the Magnitude-Frequency relationship. Thus, clustering the events statistically does not generate a derecho impact scale that adequately described the events' impacts as an expected negative relationship.

The SOMs analysis grouped derecho impacts into four categories, but similar to the clustering methods, these categories did not adequately arrange the derechos based on their impacts. Using SOMs, high-impact derechos were again classified into their own group, but low-impact derechos were classified as a small group, which violates the Magnitude-Frequency relationship, and moderate-impact derechos were sorted into two large groups whose impacts were difficult to distinguish. Statistical relationships of derecho impacts with associated physical atmospheric attributes and population

characteristics were not statistically significant using either clustering or SOMs. These techniques could be further explored with additional cases as the record is extended forward in time such that each classification will contain 30 or more events. Additional events would likely improve the cluster and SOM results because variation in the derechos would increase between the classes but decrease within the classes, which is the ultimate objective of a successful classification system.

Despite the foregoing results, it is still important to categorize the impacts of derechos to aid decision-makers using an impact scale that can be compared to other meteorological impact scales with which emergency managers are familiar (Blong, 2003; Baumgart *et al.*, 2006). Accordingly, it is also important to relate the derecho impact categories to an emergency management metric such as FEMA PA grant awards. DEWARS values were calculated for the 56 Northern Tier derechos in the 2000-2014 study period (Table 4-1). Table 4-2 shows the events organized by descending DEWARS value. Qualitatively, the DEWARS impact values adequately identify derecho impact because they agree with NOAA SPC's list of "Noteworthy" Derechos in which particularly damaging derechos are indicated. Of the derechos studied herein, the SPC identifies 19 of them to be "Noteworthy" Derechos, and these are noted by an asterisk in Table 4-2. As indicated by the † in Table 4-2, 15 (79%) of these events have DEWARS values that are in the top half of the 56 Northern Tier derechos studied. As indicated by the ‡ in Table 4-2, 8 (42%) of the noteworthy events have DEWARS values that are in the top third of the 56 Northern Tier derechos. In particular, the June 29, 2012 derecho (derecho number 48) is often used as an example of an extraordinary derecho that impacted a large population and caused significant damage. This derecho has the highest

DEWARS value, indicating it had the greatest impact of the 56 events analyzed. Derechos having high DEWARS values tend to also have long major axes (> 1,000 km), affect a large population (20 – 40 million), and have high-wind reports associated with strong winds (> 39 m/s). Derechos that have moderate DEWARS values either have moderate major axis lengths (~ 900 km) affect medium-sized populations (tens of millions), and have associated moderate wind speeds (37 – 39 m/s), or are accompanied by high values of one or two of these factors and a very low value of the other(s). Last, derechos with low DEWARS values have associated shorter major axis lengths (<800 km), lower affected populations (< 10 million), and lower wind speeds (~ 37 m/s). Thus, the categories of DEWARS values seem to accurately separate large or intense events from those that may not be very large but track through major urban areas with high population densities or that are very large but that do not impact many people.

The Jenks natural breaks and *k*-means clustering approaches split the derecho event DEWARS values into categories that represent derecho impacts similar to those suggested by the NESIS, the tornado EF Scale, and the hurricane Saffir-Simpson scale. Tables 4-3a and 4-3b show the distribution of derechos across impact categories generated by splitting the events into four and also five categories using the natural breaks and clustering approaches. The final row of Tables 4-3a and 4-3b show Pearson's correlation coefficients of the DEWARS values with FEMA PA grant award amounts and their respective p-values. Each of these correlations is statistically significant for the four impact scales considered and is highest for the clustered derecho impact categories. The positive relationship between the PA grant award amounts and the DEWARS values of the derecho impact scales confirm that the scales accurately represent derecho impact.

Although each impact scale tested shows statistically significant correlation with PA grant award amounts, only one scale—the best performing—should be chosen for use by emergency managers. The distribution of derechos across the four categories generated using *k*-means clustering shows that the two lowest-impact derecho categories contain the same number of derechos. Thus, the four-category cluster-based scale does not demonstrate that lowest-intensity meteorological disasters tend to occur most frequently. However, the four-category classification scheme driven by Jenks natural breaks shows the more expected distribution of derecho events across impact categories, but also has the lowest correlation with FEMA PA grant award amounts. Using the four-category Jenks natural breaks scale may be less useful in an emergency management setting because it is less comparable to the five-category impact scales that emergency managers are familiar with using for tornadoes and hurricanes. While the EF scale has one additional category, five categories of derecho impact are closer to six categories than are four. Categorizing the derechos into five natural-break categories creates a reasonable distribution of a small number of highly impactful events to a large number of less impactful events across impact categories, however, there are still more events in Category 2 than Category 1. Although categorizing the events using clustering creates five categories of events that are evenly distributed in the two middle-impact categories (2 and 3), this categorization produces a decreasing number of derechos across the categories overall. In addition, the cluster-based categorization has a stronger correlation to FEMA PA grant award amounts relative to the impact scale produced using the natural breaks method. Thus, it is recommended to categorize derechos into five categories based on the *k*-means clustering of the 56 Northern Tier derechos. Each of the other methods

(i.e., four-category clustering and natural breaks and five-category natural breaks) could also be used, but the five-category clustering categorization is likely the best impact scale for emergency managers because it adequately distributes decreasing derechos across increasing intensities, it is significantly correlated with FEMA PA grant award amounts, and it is comparable to other meteorological impact scales.

Of the tests used to separate the 56 derechos into distinct impact categories, the five categories generated from *k*-means classification appears to be optimal. Table 4-4 lists the derecho impact scale category and DEWARS value for each derecho event. Table 4-5 shows color-coded impact categories along with descending DEWARS values for the derechos to help illustrate the categorization scheme. The categories are also shown in Figure 4-1 with five circles representing the 5 categories and the numbers representing the derecho events as numbered in Table 4-1. The range of DEWARS values associated with each category is shown in Table 4-6. A derecho ranked in DEWARS Category 1 is "low" impact, is small and affects small populations. DEWARS categories 2 and 3 derechos have "low-moderate" and "moderate" impacts. These events tend to be physically large, but affect low-population areas, or are small but affect more densely populated places. DEWARS Category 4—"severe"—derechos tend to be large events that affect a large number of people. DEWARS Category 5 derechos have the highest impact, and are considered "crippling" because they affect a very large number of people and are the largest. These DEWARS designations are similar to those used for the tornado EF Scale, hurricane Saffir-Simpson scale, and NESIS.

Calculating a DEWARS value for each future derecho event as it occurs would be ideal. However, it is a computationally cumbersome and time-consuming venture

because it requires pre-processing of social vulnerability, area of interest, and emergency management data, data collection of wind reports, and extended computing time. In an emergency response situation, it is important to have information as soon as possible. Thus, averages of potentially storm-relevant physical and social variables are given for each DEWARS impact scale category (Table 4-7) to serve as a guide for classifying derechos quickly, as is typically required in emergency response operations. Table 4-7 shows that major axis length and number of people impacted by the derecho increase positively with increasing DEWARS impact scale categorization. However, wind speed is not directly related to increasing DEWARS impact scale category. Although there is an overall upward trend in wind speed as derecho impact increases, the wind in a Category 4 derecho is only marginally higher than that in a Category 1 event. This lack of linearity is likely due to problems with SPC high-wind reports data such as over-reporting or overestimating high-wind occurrences (Trapp *et al.*, 2006). Overall, the five-category clustering derecho impact scale, derived from calculation of the associations among derecho area, societal, and wind impacts using the NESIS equation, can be used as a quick yet reliable guide to classifying derecho events in the field and improving emergency response.

Categorizing meteorological disasters can also help improve the climatological analysis of severe weather events. These storm climatologies can help emergency managers anticipate the impacts of a potential severe weather event, and are easily displayed on maps. To this end, Figure 4-2 maps the average tracks of derechos in each DEWARS impact scale category for the full 56 events. Category 1 derechos tend to be the shortest and track through the central Midwest. Category 2 derechos track slightly

north of Category 1 events and may impact Chicago, a densely populated city with pockets of populations that have high social vulnerability scores. Category 3 derechos average a longer track than Category 1 and 2 events. Category 4 derechos average a track farther south of categories 1, 2, and 3, and the path is longer. Finally, Category 5 derechos track over long distances and are more likely to impact the major population centers of Chicago and Washington than events in categories 1-4. Mapping derecho categories is useful for emergency management because it shows where impacts may occur and why an event may be more or less impactful (i.e., whether it affects major urban areas or if it has a long track).

GIS Tool Development And Application To A Derecho

Access to emergency management resources including, but not limited to hospitals, police stations, and disaster recovery centers, is critical for a community's recovery from a disaster. Integrating social vulnerability and physical attributes in a GIS can create a mapping product that aids emergency managers in decision-making when responding to a severe weather event. Accordingly, in addition to calculating a derecho impact scale to aid emergency management, a preliminary GIS tool is developed to visualize accessibility of emergency management resources. The DSS proposed here is intended to assist senior leaders in deciding where to site additional disaster recovery resources, such as mobile communications centers, to best suit the community based on the type and severity of a disaster and social vulnerability markers of the community (Figure 4-3). The physical impacts of a disaster such as potential flooding and wind-borne debris are analyzed in a GIS within context of the social vulnerability metrics

socioeconomic status and mobility, to create a map that identifies areas with adequate versus inadequate access to emergency management resources.

The development of a GIS tool, or utility that produces an analytical output such as a map, aid emergency managers in making decisions that are specific to the disaster they are addressing. Figure 4-4 shows a conceptual design for the tool. It incorporates physical variables such as the storm area of interest (AOI), defined as a previously identified area or a SPC-issued polygon, and storm type and impact scale category. During response operations FEMA runs dynamical models that generate areas impacted by the disaster every 12 hours that could be used as AOIs. Using this 12-hour AOI would allow the tool to model changes in access to emergency response resources such as disaster recovery centers over time. Storm type is also be an input to this tool; hazards vary with storm type and incorporation of the storm type should enable optimal analysis of hazards due to flooding, downed trees, bridge and dam breaks, and other disaster-specific hazards. These hazards can be portrayed in a land surface properties layers that includes terrain, soil types, and land-use/land-cover (LULC) showing vulnerability where the lowest elevations are in floods or where many trees could be blown down in a derecho. As emphasized in the Introduction to this chapter, storm impact scales often guide emergency management decisions because broad comparisons can be made to the impacts from past events. Thus, it is also important to include storm impact category in this tool. Social vulnerability is included through the CDC SVI and optional more specific metrics such as the number of mobile homes. Incorporating social vulnerability will improve understanding of the community's ability to respond to and recover from a disaster. The physical and social data are analyzed by the tool along with locations and

availability of emergency management resources such as disaster recovery centers and police stations where individuals can seek help and information in the wake of a disaster.

A workflow for the tool is presented in five steps (Figure 4-5). The tiered approach is important because it enables review of the data and outputs at the end of each step to ensure a logical, uncorrupted by user-error result, and it creates a standard for operating the tool to which an emergency manager with any level of experience can adhere because it is user-friendly and includes natural review points at each step. All data must be pre-processed in the tool to ensure appropriate map projection and registration of data layers. Next, emergency management resource coverage areas are identified by using a metric like walking distance. Often, in the wake of a disaster walking is the only means of transportation available to survivors. Social vulnerability is incorporated through the addition of a SVI and any relevant social vulnerability markers such as population below the poverty line and number of children and elderly. These data are related in a total vulnerability layer in the GIS tool to show areas of high-vulnerability and limited resource access grading through to areas that are less vulnerable and have easy access to emergency management resources. Finally, storm type, DEWARS impact scale category, and associated hazards are added to the tool to show how the storm could have affected emergency management resource access. Although the tool can be run successfully using the above steps, the workflow is a general guideline and can be altered to fit the needs of the specific disaster or the emergency manager running the tool. For example, a new AOI may be defined that is relevant to a specific region but that does not relate to the whole disaster. Similarly, specific vulnerability markers may be included or removed as desired. In addition, the tool is flexible such that while it is intended to be run

in a response operation (post-disaster), it could also be run prior to an event with estimated or anticipated values. Thus, the tool is versatile and able to be used in many situations and by many operators.

One of the main advantages of the tool is that it is simple and in a disaster response environment broad-scale, generalized analyses provide the best support to decision-makers. Simple DSSs are valued for their ability to aid senior leaders, who decide to deploy resources and allocate assistance, and in making educated decisions in an environment where an array of data and the luxury of time do not exist. Prioritizing efficiency and generalization of impact are important in the initial stages of disaster response. As communications are restored, additional information about the event can be incorporated into more complex decision support products including this flexible tool.

As proof-of-concept, the tool is run for a case study of a Category 5 derecho (Figure 4-6). The AOI (Philadelphia, PA) was used because the city has a high concentration of high-wind reports compared to others in the path of major Northern Tier derechos, it was impacted by the Category 5 29 June 2012 derecho, data are readily available, and the city has a diverse population that is well represented in a social vulnerability index. In addition, the tool could be used on another type of event in this area (e.g., flooding) to facilitate comparison of the outputs of the tool for different disasters. The map in Figure 4-6 shows areas having people who will have more difficulty reaching emergency management resources (dark red) versus those who have easier access (lighter red). Beige areas represent where data are not available for the analysis. The darkest red areas show locations with the highest socially vulnerable populations that are also likely to be impacted by derecho damage based on their LULC

type (i.e., downed trees and debris). With emergency management resources less accessible in the dark red areas, the people who live in these areas become more vulnerable and may have a more difficult time recovering from the derecho. An emergency manager may use this map to advise his or her decision to deploy mobile recovery or communications centers to areas that serve these isolated populations. In this situation, mobile assistance may be best deployed to the central part of the city where the darkest red is shown. The tool output improves community access to emergency management resources that enable their recovery. The development of this tool and its application support the goal of emergency management, and full recovery and improvement, by providing a link to isolated populations and those that may need more assistance faster, thereby bolstering their chances for a quicker recovery.

Summary and Conclusion

In this Chapter I investigate emergency management responses to derechos by developing a derecho impact scale similar to those used for other meteorological high impact events (e.g., tornados, snowstorms), and developed and applied a GIS tool that visualizes emergency management resource access for affected populations in a derecho event. Other meteorological disaster impact scales include the EF Scale, which ranks tornadoes EF0 – EF5 (i.e., 6 categories) based on the damage that correlates to increasing wind speeds. The Saffir-Simpson scale ranks hurricanes using a similar schema of five impact categories. These scales, however, have been criticized for not accounting for how the storms may impact people. Socioeconomic status, mobile homes residences, and population age are all social factors that influence the impact of a storm. Of all

meteorological impact scales used in the United States, only the NESIS attempts to incorporate storm intensity and a measure of human impact (i.e., the number of people in the impacted area). Therefore, the conceptual premise of the NESIS scale is used as a basis for the DEWARS derecho impact scale developed herein.

The DEWARS impact scale classifies derechos into five categories by calculating a value that takes into account storm size, wind speed, and total affected population. The five DEWARS categories range from "low"-impact events to those that are "crippling." Although developing the DEWARS impact scale is intended to improve emergency management of and response to derechos, it can be further refined as more events occur and are included in the database. Climatological analyses of DEWARS categories shows that higher-impact events (those that fall in the higher categories) have the longest tracks and track through major cities. These analyses also could be further clarified as additional events occur in the future. In addition, direct collaboration of geographer-climatologists with social scientists and meteorologists could lead to development of other derecho impact scales that are better suited to applications such as community outreach or for weather forecasters. Moreover, the DEWARS impact scale is ideal for emergency management use because it provides a general categorization that can be quickly referred to in the wake of a derecho. In addition, this research suggests that the impact scale be used in conjunction with the DSS GIS tool developed and applied herein that integrates the physical attributes of a storm (i.e., the meteorology) and social factors of the impacted population to aid decisions-makers who determine the allocation of resources and commodities when responding to disasters.

References

Agarwal P, Skupin A. (Eds.). 2008. *Self-organising maps: Applications in geographic information science*. John Wiley & Sons.

Baumgart L, Bass E, Philips B, Kloesel K. 2006. Emergency management decision-making during severe weather. *Proceedings of Human Factors and Ergonomics Society Annual Meeting,* **50**(3): 381-385.

Blong R. 2003. A review of damage intensity scales. *Natural hazards*, **29**(1): 57-76.

Breiman L. 2001. Random forests. *Machine learning*, **45**(1): 5-32.

Brooks HE. 2004. On the relationship of tornado path length and width to intensity. *Weather and Forecasting*, **19**(2): 310-319.

Brooks H, Doswell CA. 2001. Some aspects of the international climatology of tornadoes by damage classification. *Atmospheric Research*, **56**(1): 191-201.

Cerruti BJ, Decker SG. 2011. The local winter storm scale: A measure of the intrinsic ability of winter storms to disrupt society. *Bulletin of the American Meteorological Society*, **92**(6): 721-737.

Changnon S. 2003. Measures of economic impacts of weather extremes: Getting better but far from what is needed-a call for action. *Bulletin of the American Meteorological Society,* **84**(9): 1231-1235.

Choi O, Fisher A. 2003. The impacts of socioeconomic development and climate change on severe weather catastrophe losses: Mid-Atlantic Region (MAR) and the US. *Climatic Change,* **58**(1-2): 149-170.

Comfort L, Wisner B, Cutter S, Pulwarty R, Hewitt K, Oliver-Smith A, ... & Krimgold F. 1999. Reframing disaster policy: the global evolution of vulnerable communities. *Global Environmental Change Part B: Environmental Hazards*, **1**(1), 39-44.

Criminisi A, Shotton J, Konukoglu E. 2012. Decision forests: A unified framework for classification, regression, density estimation, manifold learning and semi-supervised learning. *Foundations and Trends® in Computer Graphics and Vision*, **7**(2–3): 81-227.

Cutter S, Boruff B, Shirley W. 2003. Social vulnerability to environmental hazards. *Social Science Quarterly,* **84**(2): 242-261.

Cutter S, Finch, C. 2008. Temporal and spatial changes in social vulnerability to natural hazards. *Proceedings of the National Academy of Sciences,* **105**(7): 2301-2306.

Demuth JE, Gruntfest DS, Morss RE Lazo J. 2007. WAS*IS: Building a community for integrating meteorology and social science. *Bulletin of the American Meteorological Society,* **88**(11): 1729.

Dolan R, Davis RE. 1992. An intensity scale for Atlantic coast northeast storms. *Journal of Coastal Research*, 840-853.

Doswell, CA. 2003. A guide to F-scale damage assessment. *US Dept. of Commerce, NOAA/NWS.*

Doswell CA, Brooks HE, Dotzek N. 2009. On the implementation of the enhanced Fujita scale in the USA. *Atmospheric Research*, **93**(1): 554-563.

Doswell CA, Burgess DW. 1988. On some issues of United States tornado climatology. *Monthly Weather Review*, **116**(2): 495-501.

Doswell CA, Edwards R, Thompson R, Hart J, Crosbie K. 2006. A simple and flexible method for ranking severe weather events, *Weather and forecasting,* **21**(6): 939-951.

Dotzek N, Grieser J, Brooks HE. 2003. Statistical modeling of tornado intensity distributions. *Atmospheric research*, **67**: 163-187.

Dvorak, VF. 1975. Tropical Cyclone Intensity Analysis and Forecasting from Satellite Imagery. *Monthly Weather Review,* **103**: 420-430.

Edwards R, LaDue JG, Ferree JT, Scharfenberg K, Maier C, Coulbourne WL. 2013. Tornado intensity estimation: Past, present, and future. *Bulletin of the American Meteorological Society*, **94**(5): 641-653.

Emanuel K. 2005. Increasing destructiveness of tropical cyclones over the past 30 years. *Nature*, **436**(7051): 686.

Fekete A, Damn M, Birkmann J. 2010. Scales as a challenge for vulnerability assessment. *Natural Hazards,* **55**(3): 729-747.

Feuerstein B, Dotzek N, Grieser J. 2005. Assessing a tornado climatology from global tornado intensity distributions. *Journal of Climate*, **18**(4): 585-596.

Flanagan BE, Gregory EW, Hallisey EJ, Heitgerd JL, Lewis B. 2011. A social vulnerability index for disaster management. *Journal of Homeland Security and Emergency Management*, **8**(1).

Forbes GS, Wakimoto RM. 1983. A concentrated outbreak of tornadoes, downbursts and microbursts, and implications regarding vortex classification. *Monthly Weather Review*, **111**(1): 220-236.

Fujita TT. 1971. Proposed characterization of tornadoes and hurricanes by area and intensity. *Satellite and Meteorology Research Paper 91, The University of Chicago*. Chicago, IL.

Fujita TT. 1973. Tornadoes around the world. *Weatherwise,* **26**(2): 56-83.

Golden J, Adams C. The tornado problem: Forecast, warning, and response. *Natural Hazards Review,* **1**(2): 107-118.

Greenough G, McGeehin M, Bernard S, Trtanj J, Riad J, Engelberg D. 2001. The potential impacts of climate variability and change on health impacts of extreme weather events in the United States. *Environmental health perspectives,* **109**(s2): 191.

Gong X, Richman MB. 1995. On the application of cluster analysis to growing season precipitation data in North America east of the Rockies. *Journal of climate*, **8**(4): 897-931.

Han Q, Liu Z. 2008. Goal programming model for emergency material dispatch problem. *Logistics at The Emerging Frontiers of Transportation and Development in China,* 1007-1013.

Hart RE, Grumm RH. 2001. Using normalized climatological anomalies to rank synoptic-scale events objectively. *Monthly weather review*, **129**(9): 2426-2442.

Hazen HA. 1890. *The Tornado*. Hodges.

Hinkel J. 2011. "Indicators of vulnerability and adaptive capacity": Towards a clarification of the science–policy interface. *Global Environmental Change*, **21**(1), 198-208.

IPCC 2013 Working Group I. 2013. Fifth Assessment Report of the Intergovernmental Panel on Climate Change. Cambridge University Press, Cambridge, United Kingdom.

Ho TK. 1998. The random subspace method for constructing decision forests. *IEEE transactions on pattern analysis and machine intelligence*, **20**(8): 832-844.

Irish JL, Resio DT. 2010. A hydrodynamics-based surge scale for hurricanes. *Ocean Engineering*, **37**(1): 69-81.

Irish JL, Resio DT, Ratcliff JJ. 2008. The influence of storm size on hurricane surge. *Journal of Physical Oceanography*, **38**(9): 2003-2013.

Jain AK, Dubes RC. 1988. *Algorithms for clustering data*. Prentice-Hall, Inc.

Jordan MR, Clayson CA. 2008. Evaluating the usefulness of a new set of hurricane classification indices. *Monthly Weather Review*, **136**(12): 5234-5238.

Kantha L. 2006. Time to replace the Saffir-Simpson hurricane scale?. *Eos, Transactions American Geophysical Union*, **87**(1): 3-6.

Kapucu N. 2008. Collaborative emergency management: better community organising, better public preparedness and response. *Disasters,* **32**(2): 239-262.

Kocin PJ, Uccellini LW. 2004. A snowfall impact scale derived from Northeast storm snowfall distributions. *Bulletin of the American Meteorological Society*, **85**(2): 177-194.

Kohonen T. 1982. Self-organized formation of topologically correct feature maps. *Biological cybernetics*, **43**(1): 59-69.

Kohonen T. 1998. The self-organizing map. *Neurocomputing*, **21**(1): 1-6.

Kunkel K, Pielke Jr. R, Changnon S. 1999. Temporal fluctuations in weather and climate extremes that cause economic and human health impacts: A review. *Bulletin of the American Meteorological Society,* **80**(6): 1077.

Li L, Jin M. 2010. Sheltering planning and management for natural disasters. In *THC-IT 2010 Conference & Exhibition*.

Liaw A, Wiener M. 2002. Classification and regression by randomForest. *R news*, **2**(3): 18-22.

Liu S, Quenemoen L, Malilay J, Noji E, Sinks T, Mendlein J. 1996. Assessment of a severe- weather warning system and disaster preparedness, Calhoun County, Alabama, 1994. *American journal of public health,* **86**(1): 87-89.

MacQueen J. 1967. Some methods for classification and analysis of multivariate observations. In *Proceedings of the fifth Berkeley symposium on mathematical statistics and probability,* **1**(14): 281-297.

Mahendran, M. 1998. Cyclone Intensity Categories. *Weather and Forecasting,* **13**(3): 878-883.

Mayes Boustead BE, Hilberg SD, Shulski MD, Hubbard KG. 2015. The accumulated winter season severity index (AWSSI). *Journal of Applied Meteorology and Climatology*, **54**(8): 1693-1712.

McLaughlin P, Dietz T. 2008. Structure, agency and environment: Toward an integrated perspective on vulnerability. *Global Environmental Change,* **18**(1): 99-111.

Meade C, Abbott M. 2003. Assessing federal research and development for hazard loss reduction, Rand Corporation.

Meaden GT. 1975. Tornadoes in Britain. *Physics Bulletin*, **26**(10): 429.

Meaden GT, Kochev S, Kolendowicz L, Kosa-Kiss A, Marcinoniene I, Sioutas M, ... & Tyrrell J. 2007. Comparing the theoretical versions of the Beaufort scale, the T-Scale and the Fujita scale. *Atmospheric research*, **83**(2): 446-449.

Mesinger F, DiMego G, Kalnay E, Mitchell K, Shafran PC, Ebisuzaki W, ... & Ek MB. 2006. North American regional reanalysis. *Bulletin of the American Meteorological Society*, **87**(3): 343-360.

Morrow B. 1999. Identifying and mapping community vulnerability. *Disasters,* **23**(1): 1-18.

Morss R, Lazo J, Brown B, Brooks H, Ganderton P, Mills B. 2008. Societal and economic research and applications for weather forecasts in decision support systems. *Bulletin of the American Meteorological Society,* **89**(3): 335.

Morss R, and Ralph, F. 2007. Use of information by National Weather Service forecasters and emergency managers during CALJET and PACJET-2001. *Weather and forecasting,* **22**(3): 539-555.

Morss RE, Wilhelmi OV, Meehl GA, Dilling L. 2011. Improving societal outcomes of extreme weather in a changing climate: an integrated perspective. *Annual Review of Environment and Resources*, **36**.

Penning-Roswell E, Wilson T. 2006. Gauging the impact of natural hazards: the pattern and cost of emergency response during flood events. *Transactions of the Institute of British Geographers,* **31**(2): 99-115.

Pielke Jr R, Carbone R. 2002. Weather impacts, forecasts, and policy: An integrated perspective. *Bulletin of the American Meteorological Society,* **83**(3): 393.

Potter S. 2007. Fine-Tuning Fujita: After 35 years, a new scale for rating tornadoes takes effect. *Weatherwise*, **60**(2): 64-71.

Powell MD, Reinhold TA. 2007. Tropical cyclone destructive potential by integrated kinetic energy. *Bulletin of the American Meteorological Society*, **88**(4): 513-526.

Riad J, Norris F, Ruback, R. 1999. Predicting evacuation in two major disasters: risk perception, social influence, and access to Resources. *Journal of Applied Social Psychology,* **29**(5): 918-934.

Riebsame W, Price M, Diaz H, Moses T. 1986. The social burden of weather and climate hazards. *Bulletin of the American Meteorological Society,* **67**(11): 1378-1388.

Saffir H. 1977. Design and Construction Requirements for Hurricane-Resistant Construction. American Society of Civil Engineers.

Sallenger Jr AH. 2000. Storm impact scale for barrier islands. *Journal of Coastal Research*, 890-895.

Senkbeil JC, Sheridan SC. 2006. A postlandfall hurricane classification system for the United States. *Journal of Coastal Research*, 1025-1034.

Simpson RH, Saffir H. 1974. The hurricane disaster potential scale. *Weatherwise*, **27**(8): 169.

Smit B, Wandel J. 2006. Adaptation, adaptive capacity and vulnerability. *Global Environmental Change,* **16**(3): 282-292.

Squires MF, Lawrimore JH. 2006. 5.9 Development of an Operational Northeast Snowfall Impact Scale.

Squires MF, Lawrimore JH, Heim Jr RR, Robinson DA, Gerbush MR, Estilow TW. 2014. The regional snowfall index. *Bulletin of the American Meteorological Society*, **95**(12): 1835-1848.

Subramaniam C, Kerpedjiev S. 1998. Dissemination of weather information to emergency managers: a decision support tool. *IEEE Transactions on Engineering Management,* **45**(2): 106-114.

Tate E, Cutter SL, Berry M. 2010. Integrated multihazard mapping. *Environment and Planning B: Planning and Design*, **37**(4): 646-663.

Trapp RJ, Wheatley DM, Atkins NT, Przybylinski RW, Wolf R. 2006. Buyer beware: Some words of caution on the use of severe wind reports in postevent assessment and research. *Weather and forecasting*, **21**(3): 408-415.

Tudurí E, Ramis C. 1997. The environments of significant convective events in the western Mediterranean. *Weather and Forecasting*, **12**(2): 294-306.

Webster PJ, Holland GJ, Curry JA, Chang HR. 2005. Changes in tropical cyclone number, duration, and intensity in a warming environment. *Science*, **309**(5742): 1844-1846.

White C, Turoff M. 2012. Factors that influence crisis managers and their decision-making ability during extreme events. *Managing Crises and Disasters with Emerging Technologies: Advancements,* 161.

Xu L, Brown RE. 2008. A hurricane simulation method for Florida utility damage and risk assessment. In *Power and Energy Society General Meeting-Conversion and Delivery of Electrical Energy in the 21st Century,* 1-7.

Zhao D, Zhao Y, Li Z, Chen J. 2009. Multi-objective emergency facility location problem based on genetic algorithm. *Computational Intelligence and Intelligent Systems,* 97-103.

Zielinski GA. 2002. A classification scheme for winter storms in the eastern and central United States with an emphasis on nor'easters. *Bulletin of the American Meteorological Society*, **83**(1): 37-51.

Tables and Figures

Table 4-1. Chronological listing of derecho events with derecho date and DEWARS value.

Event Number	Derecho Date	DEWARS Value
1	01 Jun 2000	30.1
2	25 Jun 2000	23.7
3	06 Aug 2000	40.2
4	09 Aug 2000 A	9.8
5	09 Aug 2000 B	40.3
6	11 Jun 2001	46.1
7	08 Jul 2001	52.4
8	09 Aug 2001	4.1
9	11 Jun 2002	5.3
10	27 Jul 2002	3.1
11	02 Jul 2003	17.6
12	04 Jul 2003	57.6
13	07 Jul 2003	37.2
14	26 Aug 2003	22.9
15	14 Jun 2004	42.9
16	13 Jul 2004	37.5
17	03 Aug 2004	51
18	08 Jun 2005	28.7
19	20 Jun 2005	40.8
20	23 Jul 2005	13.4
21	25 Jul 2005	13.7
22	13 Jul 2006	20.2
23	21 Jul 2006	58.6
24	09 Aug 2007	15
25	11 Aug 2007	10
26	12 Aug 2007	7.1
27	03 Jun 2008	28.7
28	04 Jun 2008	34.9
29	08 Jun 2008	33.5
30	20 Jul 2008	26.5
31	27 Jul 2008	11.4
32	31 Jul 2008	14.1
33	04 Aug 2008	29.4
34	18 Jun 2009	37
35	19 Jun 2009	32.9
36	04 Aug 2009	72.8
37	01 Jun 2010	12
38	18 Jun 2010	66.3
39	19 Jun 2010	18.6
40	23 Jun 2010	60.8
41	04 Aug 2010	55.5
42	18 Jun 2011	25.6
43	26 Jun 2011	80.5
44	10 Jul 2011	21.1
45	11 Jul 2011	107.3
46	30 Jul 2011	17
47	19 Aug 2011	17
48	29 Jun 2012	142.4
49	24 Jul 2012	42
50	26 Jul 2012	22.4
51	04 Aug 2012	27.1
52	13 Aug 2012	14
53	13 Jun 2013 A	44.8

54	13 Jun 2013 B	27.5
55	24 Jun 2013	35.7
56	30 Jun 2014	50.6

Table 4-2. Derecho events sorted by descending DEWARS Value. * represents a derecho listed in the SPC-designated list of "Noteworthy" derechos. † identifies a SPC "Noteworthy" derecho that is ranked within the top half of derechos based on DEWARS values. ‡ denotes a SPC "Noteworthy" derecho that is ranked within the top third of derechos based on DEWARS values.

Event Number	Derecho Date	DEWARS Value
48	*†‡ 29 Jun 2012	142.4
45	*†‡ 11 Jul 2011	107.3
43	26 Jun 2011	80.5
36	04 Aug 2009	72.8
38	*†‡ 18 Jun 2010	66.3
40	*†‡ 23 Jun 2010	60.8
23	*† 21 Jul 2006	58.6
12	04 Jul 2003	57.6
41	04 Aug 2010	55.5
7	08 Jul 2001	52.4
17	03 Aug 2004	51
56	*†‡ 30 Jun 2014	50.6
6	*†‡ 11 Jun 2001	46.1
53	*†‡ 13 Jun 2013 A	44.8
15	14 Jun 2004	42.9
49	24 Jul 2012	42
19	20 Jun 2005	40.8
5	*†‡ 09 Aug 2000 B	40.3
3	06 Aug 2000	40.2
16	*† 13 Jul 2004	37.5
13	07 Jul 2003	37.2
34	*† 18 Jun 2009	37
55	*† 24 Jun 2013	35.7
28	*† 04 Jun 2008	34.9
29	08 Jun 2008	33.5
35	*† 19 Jun 2009	32.9
1	01 Jun 2000	30.1
33	*† 04 Aug 2008	29.4
18	08 Jun 2005	28.7
27	03 Jun 2008	28.7
54	* 13 Jun 2013 B	27.5
51	04 Aug 2012	27.1
30	* 20 Jul 2008	26.5
42	18 Jun 2011	25.6
2	25 Jun 2000	23.7

14	26 Aug 2003	22.9
50	26 Jul 2012	22.4
44	* 10 Jul 2011	21.1
22	13 Jul 2006	20.2
39	19 Jun 2010	18.6
11	02 Jul 2003	17.6
46	30 Jul 2011	17
47	19 Aug 2011	17
24	09 Aug 2007	15
32	31 Jul 2008	14.1
52	13 Aug 2012	14
21	25 Jul 2005	13.7
20	23 Jul 2005	13.4
37	01 Jun 2010	12
31	27 Jul 2008	11.4
25	11 Aug 2007	10
4	* 09 Aug 2000 A	9.8
26	12 Aug 2007	7.1
9	11 Jun 2002	5.3
8	09 Aug 2001	4.1
10	27 Jul 2002	3.1

Table 4-3a. Number of derechos (and percent) in each category of a potential four-category impact scale categorized using Jenks natural breaks and clustering. Bottom row shows Pearson's correlation coefficient for correlation of categories and FEMA PA grant award amounts and p-value in parentheses.

DEWARS Impact Scale Category	Jenks Natural Breaks	Clustering
1	32 (57.1%)	22 (39.3%)
2	21 (37.5%)	22 (39.3%)
3	2 (3.6%)	10 (17.9%)
4	1 (1.8%)	2 (3.6%)
Correlation with FEMA PA grant award amounts	**0.27 (0.04)**	**0.44 (0.0006)**

Table 4-3b. Number of derechos (and percent) in each category of a potential five-category impact scale categorized using Jenks natural breaks and clustering. Bottom row shows Pearson's correlation coefficient for correlation of categories and FEMA PA grant award amounts with p-value given in parentheses. Highlighted text designates the recommended categorizations for the DEWARS impact scale.

DEWARS Impact Scale Category	Jenks Natural Breaks	Clustering
1	21 (37.5%)	17 (30.4%)
2	22 (39.3%)	15 (26.8%)
3	10 (17.9%)	15 (26.8%)
4	2 (3.6%)	7 (12.5%)
5	1 (1.8%)	2 (3.6%)
Correlation with FEMA PA grant award amounts	**0.35 (0.007)**	**0.42 (0.001)**

Table 4-4. Derechos listed as in Table 4-1 with additional column indicating DEWARS impact scale category.

Event Number	Derecho Date	DEWARS Value	DEWARS Impact Scale Category
1	01 Jun 2000	30.1	**2**
2	25 Jun 2000	23.7	**2**
3	06 Aug 2000	40.2	**3**
4	09 Aug 2000 A	9.8	**1**
5	09 Aug 2000 B	40.3	**3**
6	11 Jun 2001	46.1	**3**
7	08 Jul 2001	52.4	**3**
8	09 Aug 2001	4.1	**1**
9	11 Jun 2002	5.3	**1**
10	27 Jul 2002	3.1	**1**
11	02 Jul 2003	17.6	**1**
12	04 Jul 2003	57.6	**4**
13	07 Jul 2003	37.2	**3**
14	26 Aug 2003	22.9	**2**
15	14 Jun 2004	42.9	**3**
16	13 Jul 2004	37.5	**3**
17	03 Aug 2004	51	**3**
18	08 Jun 2005	28.7	**2**
19	20 Jun 2005	40.8	**3**
20	23 Jul 2005	13.4	**1**
21	25 Jul 2005	13.7	**1**
22	13 Jul 2006	20.2	**2**
23	21 Jul 2006	58.6	**4**
24	09 Aug 2007	15	**1**
25	11 Aug 2007	10	**1**
26	12 Aug 2007	7.1	**1**
27	03 Jun 2008	28.7	**2**
28	04 Jun 2008	34.9	**3**
29	08 Jun 2008	33.5	**2**
30	20 Jul 2008	26.5	**2**
31	27 Jul 2008	11.4	**1**
32	31 Jul 2008	14.1	**1**
33	04 Aug 2008	29.4	**2**
34	18 Jun 2009	37	**3**
35	19 Jun 2009	32.9	**2**
36	04 Aug 2009	72.8	**4**
37	01 Jun 2010	12	**1**
38	18 Jun 2010	66.3	**4**
39	19 Jun 2010	18.6	**1**
40	23 Jun 2010	60.8	**4**
41	04 Aug 2010	55.5	**4**
42	18 Jun 2011	25.6	**2**
43	26 Jun 2011	80.5	**4**
44	10 Jul 2011	21.1	**2**
45	11 Jul 2011	107.3	**5**
46	30 Jul 2011	17	**1**
47	19 Aug 2011	17	**1**
48	29 Jun 2012	142.4	**5**
49	24 Jul 2012	42	**3**
50	26 Jul 2012	22.4	**2**
51	04 Aug 2012	27.1	**2**
52	13 Aug 2012	14	**1**
53	13 Jun 2013 A	44.8	**3**
54	13 Jun 2013 B	27.5	**2**
55	24 Jun 2013	35.7	**3**
56	30 Jun 2014	50.6	**3**

Table 4-5. Table 4-2 with descending DEWARS impact scale categories identified by lightening the greyscale.

Event Number	Derecho Date	DEWARS Value
48	***29 Jun 2012	142.4
45	***11 Jul 2011	107.3
43	26 Jun 2011	80.5
36	04 Aug 2009	72.8
38	***18 Jun 2010	66.3
40	***23 Jun 2010	60.8
23	**21 Jul 2006	58.6
12	04 Jul 2003	57.6
41	04 Aug 2010	55.5
7	08 Jul 2001	52.4
17	03 Aug 2004	51
56	***30 Jun 2014	50.6
6	***11 Jun 2001	46.1
53	***13 Jun 2013 A	44.8
15	14 Jun 2004	42.9
49	24 Jul 2012	42
19	20 Jun 2005	40.8
5	***09 Aug 2000 B	40.3
3	06 Aug 2000	40.2
16	**13 Jul 2004	37.5
13	07 Jul 2003	37.2
34	**18 Jun 2009	37
55	**24 Jun 2013	35.7
28	**04 Jun 2008	34.9
29	08 Jun 2008	33.5
35	**19 Jun 2009	32.9
1	01 Jun 2000	30.1
33	**04 Aug 2008	29.4
18	08 Jun 2005	28.7
27	03 Jun 2008	28.7
54	*13 Jun 2013 B	27.5
51	04 Aug 2012	27.1
30	*20 Jul 2008	26.5
42	18 Jun 2011	25.6
2	25 Jun 2000	23.7
14	26 Aug 2003	22.9
50	26 Jul 2012	22.4
44	*10 Jul 2011	21.1
22	13 Jul 2006	20.2
39	19 Jun 2010	18.6
11	02 Jul 2003	17.6
46	30 Jul 2011	17
47	19 Aug 2011	17
24	09 Aug 2007	15
32	31 Jul 2008	14.1
52	13 Aug 2012	14
21	25 Jul 2005	13.7
20	23 Jul 2005	13.4
37	01 Jun 2010	12
31	27 Jul 2008	11.4
25	11 Aug 2007	10
4	*09 Aug 2000 A	9.8
26	12 Aug 2007	7.1
9	11 Jun 2002	5.3
8	09 Aug 2001	4.1
10	27 Jul 2002	3.1

Table 4-6. DEWARS impact scale categories and associated DEWARS values and impact descriptions.

DEWARS Impact Scale Category	DEWARS Values	Impact Description
1	0 – 19.99	"Low"
2	20 – 33.99	"Low-Moderate"
3	34 – 53.99	"Moderate"
4	54 – 99.99	"Severe"
5	≥ 100	"Crippling"

Table 4-7. Averages of DEWARS values, event rank, major axis length, wind speed, and impacted populations associated with derechos in each DEWARS impact scale category.

DEWARS Impact Scale Category	DEWARS Value	DEWARS Relative Rank	Major Axis Length in km	Wind Speed in m/s	Impacted Population in millions
1	13.8	46	783.8	36.8	8.0
2	34	24.5	945.5	39.1	18.4
3	57.2	8.5	954.4	40.2	19.6
4	93.9	2.5	1190.2	36.9	20.4
5	142.4	1	1371.6	41.6	41.3

Figure 4-1. Derecho categories identified by *k*-means clustering. Derecho numbers (as in Table 4-1) are in grey. DEWARS impact scale categories are identified in the blue ellipses.

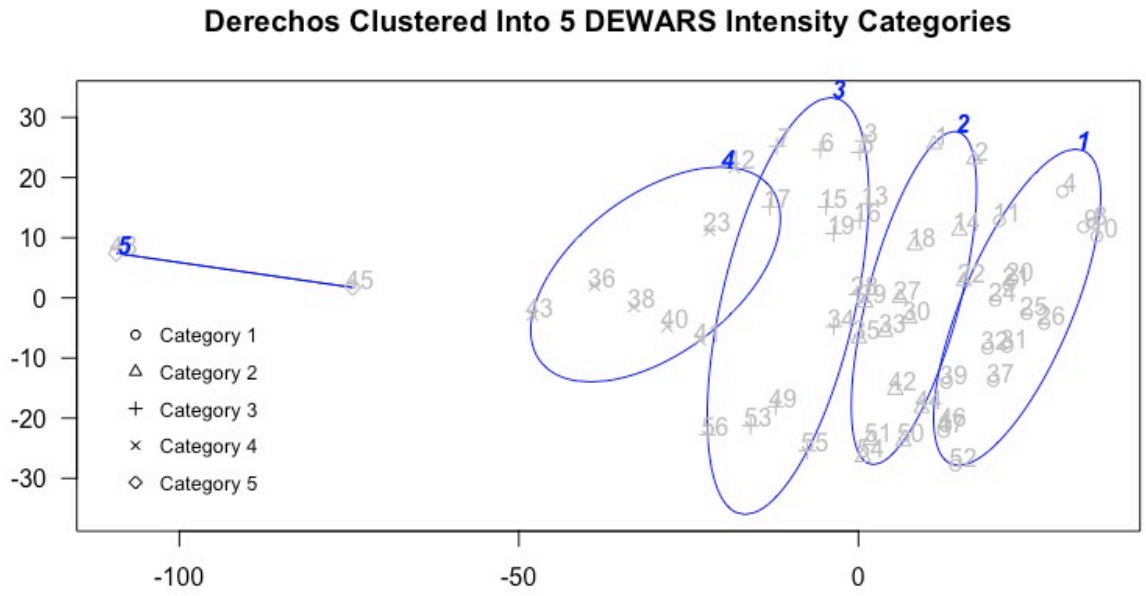

Figure 4-2. Composite tracks of Northern Tier derechos by DEWARS Category.

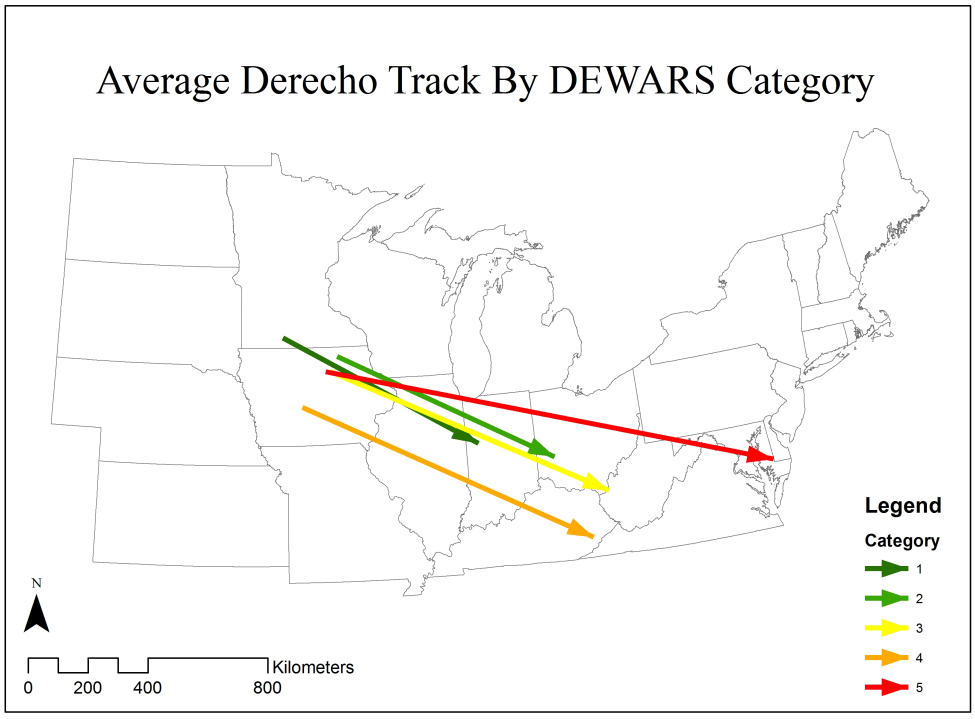

Figure 4-3. Representation of the emergency management GIS tool developed and applied herein. Inputs of AOI (such as storm warning polygon or previously identified area), storm impact category, and social vulnerability are analyzed together to create an output map of access to emergency management resources such as disaster recovery centers (refer text).

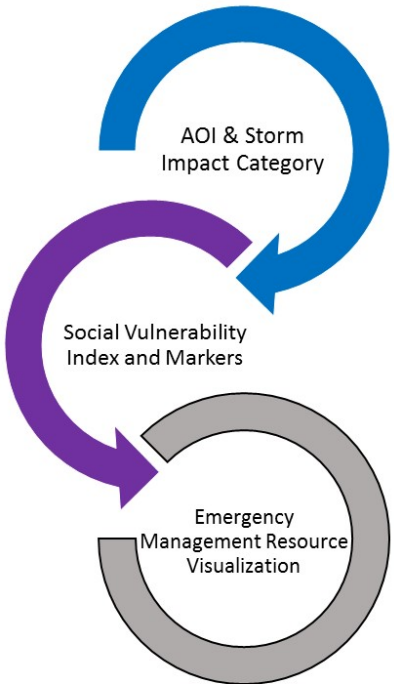

Figure 4-4. Framework for the emergency management GIS tool showing integration of physical variables (blue and green), social variables (purple), and emergency management context (yellow) with the output (grey box) being a map showing resource access (refer text).

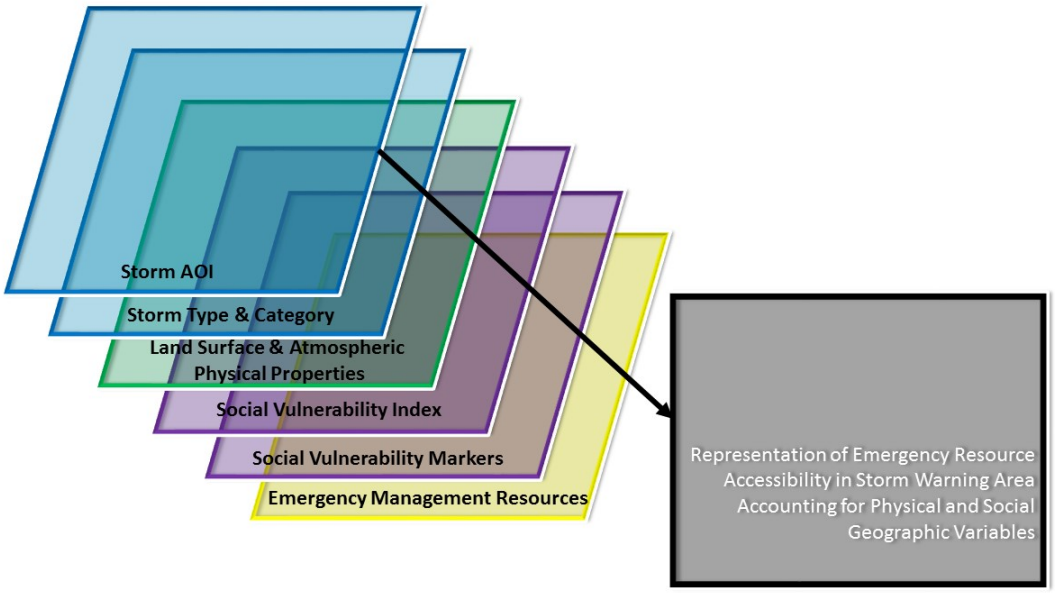

Figure 4-5. A sample GIS workflow for the tool that maps resource access to follow (refer text).

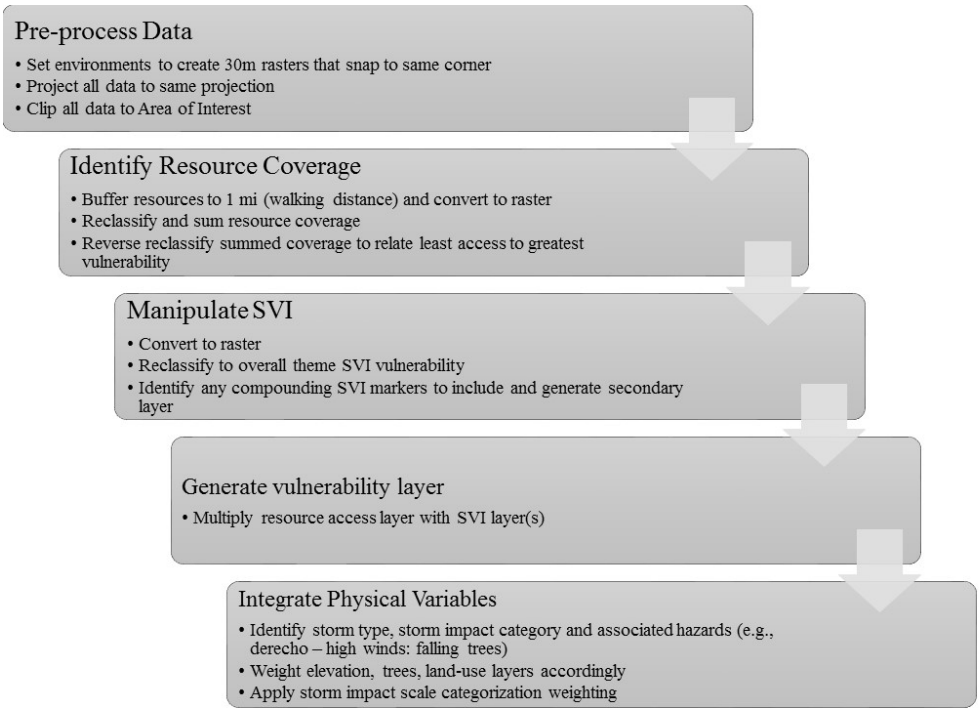

Figure 4-6. Example tool output that shows resource access in the wake of a derecho in AOI (Philadelphia, PA). Darker red areas have less access to emergency management resources that could help them in the wake of a damaging derecho.

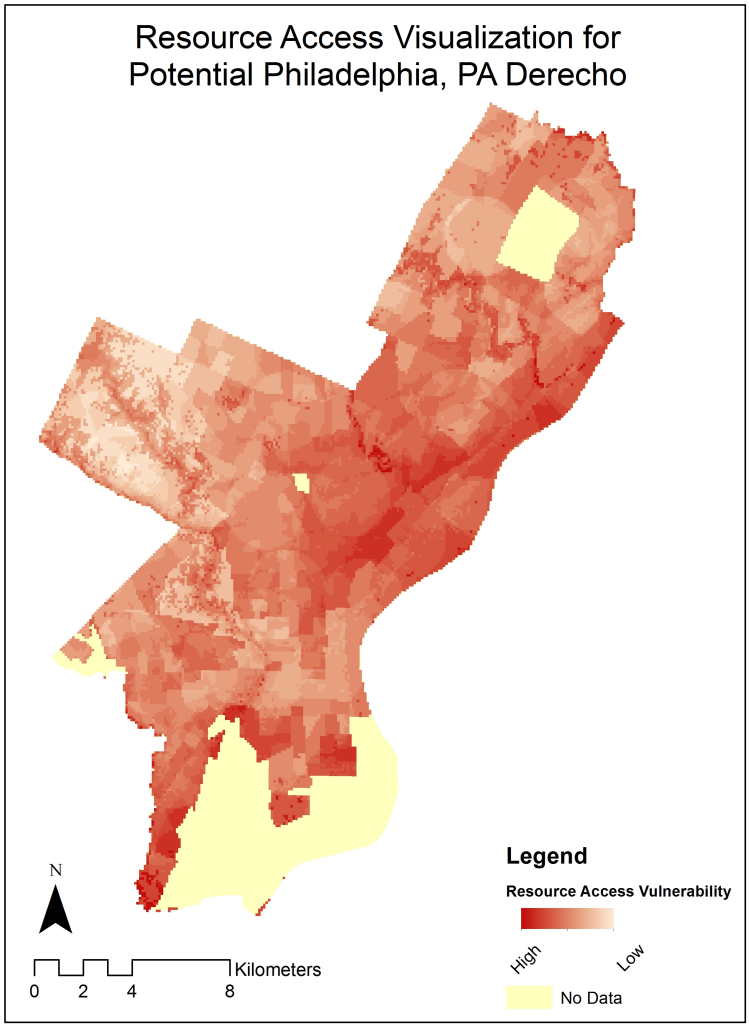

CHAPTER 5

CONCLUSION

This dissertation investigates derecho intensity and impacts. Intensities are defined in terms of storm direction, associated rain totals, maximum wind speed, and major and minor axis lengths. These storm attributes are tested for associations with physical atmospheric and land surface features that could magnify or reduce their intensity. Impact is then considered in terms of FEMA PA grant awards through examining the social characteristics that are related to response and recovery grant amounts awarded in the wake of derechos. Finally, a meteorological impact scale for derechos is developed and applied to the 56 Northern Tier derechos investigated herein. In addition, an emergency management response GIS tool is developed and applied to a derecho scenario.

The intent of these chapters is to investigate and describe derecho intensity and impacts in order to improve response to and recovery from these storms. The work directly applies to emergency management operations, and specifically can be used by FEMA to improve their response to derechos. Although FEMA conducts cost analysis for other disaster types (e.g., hurricanes, floods), derechos hitherto have not been analyzed in this way. The spatial component investigated in this dissertation adds to regression and correlation tests to show where certain meteorological, climatic, and social variables influence derecho impact.

The objectives of this study laid out in the Introduction are to identify atmospheric and land surface variables that are associated with differences in derecho intensity, to describe the relationships of variables that influence the cost of FEMA

response to and recovery from derechos, and to develop a derecho meteorological impact scale and GIS tool for emergency managers. Each of these objectives moves toward the larger aim of improving emergency management of derecho events. The goals were met through statistical and geospatial analysis of modeled, observed, and remotely sensed data on 56 summer 2000 – 2014 Northern Tier derecho events.

Chapter 2 classified derechos by intensity based on storm direction, associated rain totals, maximum wind speed, and major and minor axis lengths. High- and low-intensity subsets are mapped to display how the tracks differed for higher versus lower intensity derechos. Results show that direction of movement and minor axis length are not statistically significantly related to any atmospheric or land surface variables tested. Rain totals, however, are higher in events with lower 500 hPa geopotential mean height. Maximum wind speeds are higher in events with the presence of an upper-tropospheric jet streak and dissipate farther north. A longer major axis length is associated with storms coming from a more westerly direction, higher CAPE, tracking over a dry-to-wet land use boundary, and higher specific humidity at 925 hPa, the latter being related to the presence of a LLJ. This relationship is further investigated to show that 925 hPa specific humidity, CAPE, and time of event can successfully predict derecho major axis length in the Northern Tier, however these variables' influence varies across the study region.

Chapter 3 relates FEMA PA grant award amounts to physical and social properties of derechos and the populations they impact. Multiple and geographically weighted regressions show that the number of counties impacted and the social vulnerability of the impacted populations, successfully predict the amount of FEMA PA grants awarded for response and recovery efforts. A Varimax-rotated PCA finds that five

components explain the variance of the data and further clarifies the results shown in the regressions. Temperature, living conditions, storm size, exposure, and socioeconomics are the five components that describe the variation in FEMA PA grant awards, showing that both physical and social variables play an important role in determining the value of PA grants awarded.

Chapter 4 describes meteorological impact scales (e.g., EF scale, Saffir-Simpson scale, NESIS) and how they are used in emergency management situations, and develops a derecho-specific impact scale. The DEWARS impact scale is derived from an equation used to calculate winter snow storm impacts (NESIS) that takes into account storm size, wind speed, and the impacted population. DEWARS values are calculated for each derecho using this equation. Categorizations are then made using *k*-means clustering of the events to create a five-category impact scale. The DEWARS values are correlated with FEMA PA grant award amounts to ensure that the calculated impact scale is a reasonable representation of the effects of derechos, and that emergency managers could use the scale logically to improve operations. An emergency management GIS tool that maps resource access of communities is also developed. It is applied to an AOI (Philadelphia) in the wake of a derecho event as proof-of-concept.

The work presented in this dissertation is important for research linking climatology, hazards, and emergency management. The Northern Tier derecho climatology is updated and further described in terms of intensity. Economic losses from hazards are investigated using a geographic approach that shows the importance of spatial variation and population characteristics in awarding emergency management grants. Emergency management operations are improved through development and application

of a derecho meteorological impact scale and GIS tool. Future research adding derecho events as the data extend forward in time can build on these results and applications. The GIS tool can be applied and adjusted to suit other storm types and can be tested in both pre- and post- storm operations. Future research in these areas will also directly improve emergency management operations, and thus enhance life-saving and community-stabilizing abilities.

The research comprising this cohesive dissertation meets the objectives of classifying derecho intensity, describing FEMA PA grant awards, and improving emergency management of derechos. The work thoroughly analyzes derecho intensity and impact, and develops a scale and tool based on findings to help guide emergency management. The results and products of this study have immediate and important broader impacts on the emergency management of derechos.

VITA

Adrienne Katherine Kramer

Ph.D. Geography, The Pennsylvania State University [May 2018]

Adviser: Andrew Carleton

Dissertation Title: Defining Derecho Intensity And Impacts Through Physical Properties, FEMA Assistance, And An Emergency Management Impact Scale And GIS Response Tool

M.Sc. Geography, The Pennsylvania State University [May 2015]

Adviser: Andrew Carleton

Master's Thesis Title: Role of Soil Moisture Gradients and Land-Use/Land-Cover Boundaries in U.S. Northern Tier Derecho Initiation and Intensification

B.A. Geography, SUNY Geneseo [May 2013]

Selected Funding and Awards

2nd Place Penn State Ph.D. Proposal E. Willard Miller Award in Geography [2016]

2nd Place Penn State M.S. Paper E. Willard Miller Award in Geography [2015]

NASA PA Space Grant Consortium Fellowship [2013 – 2015]

PSU College of Earth and Mineral Sciences Centennial Research Travel Award [2015]

Affiliations

American Association of Geographers, American Meteorological Society, Phi Beta Kappa, Gamma Theta Upsilon Geography Honor Society